LEABHARLANN CHOLÁISTE NA TRÍONÓIDE, BAILE ÁTHA CLIATH | TRINITY COLLEGE LIBRARY DUBLIN
Ollscoil Átha Cliath | The University of Dublin

Terms and Conditions of Use of Digitised Theses from Trinity College Library Dublin

Copyright statement

All material supplied by Trinity College Library is protected by copyright (under the Copyright and Related Rights Act, 2000 as amended) and other relevant Intellectual Property Rights. By accessing and using a Digitised Thesis from Trinity College Library you acknowledge that all Intellectual Property Rights in any Works supplied are the sole and exclusive property of the copyright and/or other IPR holder. Specific copyright holders may not be explicitly identified. Use of materials from other sources within a thesis should not be construed as a claim over them.

A non-exclusive, non-transferable licence is hereby granted to those using or reproducing, in whole or in part, the material for valid purposes, providing the copyright owners are acknowledged using the normal conventions. Where specific permission to use material is required, this is identified and such permission must be sought from the copyright holder or agency cited.

Liability statement

By using a Digitised Thesis, I accept that Trinity College Dublin bears no legal responsibility for the accuracy, legality or comprehensiveness of materials contained within the thesis, and that Trinity College Dublin accepts no liability for indirect, consequential, or incidental, damages or losses arising from use of the thesis for whatever reason. Information located in a thesis may be subject to specific use constraints, details of which may not be explicitly described. It is the responsibility of potential and actual users to be aware of such constraints and to abide by them. By making use of material from a digitised thesis, you accept these copyright and disclaimer provisions. Where it is brought to the attention of Trinity College Library that there may be a breach of copyright or other restraint, it is the policy to withdraw or take down access to a thesis while the issue is being resolved.

Access Agreement

By using a Digitised Thesis from Trinity College Library you are bound by the following Terms & Conditions. Please read them carefully.

I have read and I understand the following statement: All material supplied via a Digitised Thesis from Trinity College Library is protected by copyright and other intellectual property rights, and duplication or sale of all or part of any of a thesis is not permitted, except that material may be duplicated by you for your research use or for educational purposes in electronic or print form providing the copyright owners are acknowledged using the normal conventions. You must obtain permission for any other use. Electronic or print copies may not be offered, whether for sale or otherwise to anyone. This copy has been supplied on the understanding that it is copyright material and that no quotation from the thesis may be published without proper acknowledgement.

Preparation of uniform ZnO microparticles by hydrothermal methods; Conventional *vs.* microwave heating

By

Ruth A. Mc Bride

A thesis submitted to the University of Dublin for the degree of Doctor of Philosophy

Trinity College
Dublin

October 2000

TRINITY COLLEGE
24 JAN 2001
LIBRARY DUBLIN
Thesis
6159

DECLARATION

This thesis has not been submitted as an exercise for a degree at any other university. Except where otherwise stated, the work described herein has been carried out by the author alone.

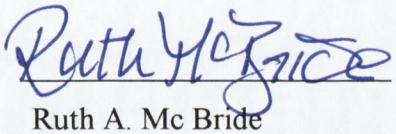

Ruth A. Mc Bride

October 2000

DECLARATION

I give permission for the Library to lend or copy this thesis upon request.

Signed: Ruth McGrice

SUMMARY

Uniform particles of ZnO and $Zn(OH)_2$ have been prepared in the micron size range, using a number of hydrothermal methods. In a forced hydrolysis procedure, when aqueous zinc nitrate solutions are reacted with sodium hydroxide, precipitation of either zinc oxide or zinc hydroxide can take place. At temperatures above 55 °C, ZnO star-like particles precipitate from solution and grow to a size of approximately 6.5 μm, with a distribution of 4.0 to 10.0 μm after five hours ageing at reflux temperature. Alternatively, precipitation at room temperature gives $Zn(OH)_2$ rhombic particles. Thermal decomposition of this $Zn(OH)_2$ in the reaction suspension, results in the formation of needle-like ZnO particles with average dimensions of 4.5 μm (L) x 1.0 μm (W) and a length distribution of 2.5 to 7.5 μm. Variations in reactant concentrations, ageing times, zinc salt counter-ion and pre-stirring times have been carried out to examine the effect of each parameter on the particles formed.

The growth mechanisms for the formation of star-like ZnO, rhombic $Zn(OH)_2$ and needle-like ZnO have been investigated using SEM, XRD and EDTA titration. It has been found that star-like ZnO grows by a diffusional growth mechanism with multiple nucleation events. The star-like morphology is believed to be a result of twinning along the $(11\bar{2}2)$ plane of the hexagonal lattice. Rhombic $Zn(OH)_2$ also grows by diffusion with multiple nucleations; however, unlike star-like ZnO, a self-sharpening step appears to takes place. Needle-like ZnO results from the thermal decomposition of $Zn(OH)_2$, by loss of H_2O from the lattice. Evidence suggests that this takes place by a solid phase transformation, without dissolution of $Zn(OH)_2$ and subsequent re-precipitation of ZnO. The uniformity of the needle-like ZnO sample is dependent upon the uniform nature of the $Zn(OH)_2$ particles.

Using the same reactions, ZnO particles have been produced using microwave oven heating. Both morphologies (star-like and needle-like) were seen to grow by the same

mechanism as those formed under conventional heating methods. However, in each case, enhanced growth rates were observed. Star-like particles of an equivalent size and distribution can be produced over 80 times faster and needle-like particles form with at least a 20-fold decrease in reaction time. Nonetheless, control over the $Zn(OH)_2$ decomposition reaction is lost and the speed at which the conversion from hydroxide to oxide occurs results in a highly disperse sample of needle-like ZnO. The operating power of the microwave oven was found to have only a kinetic effect on the reactions performed, with faster precipitation and growth taking place at higher power settings.

Preparation of uniform ZnO particles has also been carried out using the urea hydrolysis method. Decomposition of urea in the presence of zinc sulphate results in the formation of rod-like ZnO particles. By increasing ageing times, the dimensions of the rod-like particles can be influenced; for example, (3.0 ± 0.9) x (1.4 ± 0.5) μm after one hour at 95 °C and (5.0 ± 2.5) x (1.3 ± 0.5) μm after three hours at 95 °C. The importance of control over ageing temperatures has also been demonstrated, as a drop in temperature during the ageing process results in the formation of a side product of amorphous zinc basic carbonate.

Decomposition of a Zn-HMT complex has also been used to produce uniform ZnO particles. Growth of these particles occurs by directional aggregation along the c-axis of the ZnO lattice. By carrying out this reaction using a microwave heat source, an enhanced rate of growth is observed, approximately three times faster when compared to conventional heating.

Finally, particle coating using electroless deposition has been investigated. Tin, palladium and silica coated ZnO needle-like and star-like particles have been prepared. Non-uniform coatings of copper, nickel and silver coating have also been produced.

"I would remind you then that when we want to find out anything that we do not know, there are two ways of proceeding. We may either ask somebody else who does know, or read what the most learned men have written about it, which is a very good plan if anyone happens to be able to answer our question; or else we may adopt another plan, and by arranging an experiment, try for ourselves."

C.V. Boys

Soap bubbles and the forces which mould them.

(A Science Study Series Book).

ACKNOWLEDGEMENTS

The hard bit.....

First and foremost, I'd like to thank my two supervisors, Prof. John M. Kelly, TCD and Dr. Declan E. Mc Cormack, DIT. I know that over the four years I probably tried their patience and they mine, but I really did appreciate all their help and no doubt wouldn't have reached this stage without them. To John, for taking on a plucky student he didn't know and trusting she could do the job and to Declan, for committing himself to more years of dealing with me after surviving the first four! Your confidence in me was much appreciated.

Financially, Enterprise Ireland (in two of their many incarnations), have contributed considerably to my research and should be thanked. From an academic point of view, I know I'll probably leave someone out, but here are some of the people who deserve acknowledgement. The staff of the Electron Microscope Unit for all their help, in particular Neil and Neal, whose assistance was greatly appreciated. Dr. Tia Keyes of DIT, for her help with Raman spectroscopy and Dr. Paul Lyons of Enterprise Ireland for his assistance with light scattering measurements.

From when I first started in Trinity as a scared young DIT graduate, the staff and students have made me feel very welcome and at home. I would like to show my appreciation to each and every one of them but the acknowledgements would be longer than the thesis. Therefore, to the special ones..... The Kelly groupers, from day one Clare, Richie, Mark, Emmanuel (a.k.a. Frenchie) and of course himself, and more recently, Michael, Karen, Sarah, Carlos and Suresh. To Dr. Dorothy Donnelly, a great friend to all the Kelly group, full of advice and Crosaire explanations! To the 'Hotel California' resident, Dr. Martin Feeney and his partner in crime Brendan Mulvaney. To all the other technical staff, especially Fred and Patsy and to the academics of both TCD and DIT who were always available for consultations should the need arise.

Without the help and support of my family and friends, I know I wouldn't be here now. A very special thanks is most certainly due to my Dad and Mam, who both worked hard so I could remain in study for this long. I think they both went a bit weak when I suggested returning to college for another four years after my degree but to their credit supported me (emotionally and financially) every step of the way. A debt that can never be repaid. To my siblings, (especially Stuart, for all his help on 'V-Day' i.e. the day my computer got the virus!), I'm no longer a waster student; I'm going to get a real job now!!! Of all the friends I've made over the years, none are more special than Rita and Emer. They helped me through my degree by going through it with me and they helped me through my Ph.D. by taking me away from it all regularly and talking about things other than Chemistry!

My final and most difficult thanks to express are those directed towards Dan. He hates soppy tripe so I'll just say that I'm glad I came to Trinity. For the proof reading, for regularly putting things in perspective for me, for being my shoulder to cry on and my cohort with whom to enjoy life, Ta Love.

Thanks everyone,

Ruth

TABLE OF CONTENTS

LIST OF ABBREVIATIONS

A	Absorption.
A_0	Zero absorption.
A_S	Sample absorption.
A_T	Total absorption.
ACA	Anisotropically conductive adhesive.
C	Concentration.
C_s	Solubility concentration.
CBD	Chemical bath deposition.
CDJP	Controlled double jet precipitation.
DMO	Domestic microwave oven.
DSC	Differential scanning calorimetry.
EDTA	Ethylenediaminetetraacetic acid.
en	Ethylendiamine.
HAp	Hydroxyapatite.
HMT	Hexamethylenetetraamine.
L	Length.
ppt	precipitate / precipitation.
®	Registered trademark.
R_n	Rate of nucleation.
SEM	Scanning electron microscope / microscopy.
TEA	Triethanolamine.
TEM	Transmission electron microscope / microscopy.
TEOS	Tetraethylene orthosilicate.
UV/vis.	Ultra-violet / visible.
vs.	Versus.
W	Width.
XRD	X-ray diffraction.
XRF	X-ray fluorescence.

LIST OF FIGURES AND TABLES

Chapter 1

Introduction.

1.1 INTRODUCTION

This thesis is concerned with the hydrothermal preparation of uniform ZnO microparticles and a comparison between conventional heating and microwave oven alternatives.

Monodisperse systems have many applications, several of them theoretical but they have also found numerous uses in industry. It is now widely recognised that a uniform size and shape can increase the effectiveness of metal oxides and sulphides in various industries; for example catalysis, pigments, non-linear optics, antireflection surfaces, pharmaceutics, conducting adhesives and semiconductor technologies.[1-3] The last two applications mentioned will be discussed in more detail in section 1.2 below. The production of uniform cubic PbS particles was previously achieved in our laboratories.[4] By metal plating the PbS cubes, their conductivity was enhanced and in tests, they out-performed gold-coated polystyrene beads, the current industrial standard for conducting adhesive technology. Following this success, interest was expressed in developing similar systems with different morphologies. Due to their needle / rod-like morphology, uniform particles of ZnO in the micron size range were investigated.

Controlled growth of metal hydrous oxides, to produce monodisperse particles, has been studied extensively over the last twenty years.[5] Several preparation methods have been developed and the effect of reaction parameters for many metal oxide and sulphide systems has been well documented.[e.g. 6, 7] Although a number of growth mechanisms have been proposed for uniform particle formation it is not possible to generalise and each system must be studied in its own right.

This report will focus on the preparation of ZnO microparticles, by four different procedures, in an attempt to produce particles of a uniform size distribution. Initially a urea hydrolysis method was studied, the results for which are reported in Chapter 5. However, difficultly was encountered with this method due to unwanted side products.

For this reason, a forced hydrolysis procedure was considered. Using a hydroxide ion forced hydrolysis method, the pattern of ZnO particle growth will be examined in an attempt to gain an understanding of the formation mechanism for various morphologies. Conventional heating methods are compared to microwave alternatives, with the aim of enhancing growth rates and also to determine the effect, if any, of microwave heating on the ZnO systems. To date, controlled particle growth using microwave heating techniques has not received any attention in the literature. Finally, particle modification will be investigated using electroless metal plating techniques, to enhance electrical properties and hence improve microparticle applications.

In this introduction chapter, the methods and mechanisms for uniform microparticle growth will be considered, with emphasis on the ZnO systems studied to date. The use of microwave ovens for chemical synthesis will also be discussed.

1.2 MICROPARTICLE APPLICATIONS

As was mentioned above, microparticles can have a number of different applications, most depending on their individual properties e.g. conductivity or refractive index and there are some uses for which a uniform sample of microparticles could be advantageous. With ZnO particles particularly in mind, two of these uses will be discussed.

1.2.1 Varistor technology.

A varistor is an electronic component that protects circuitry against power surges. The main component of these varistors is doped ZnO particles.[8 - 10] Figure 1.1 shows a schematic diagram of a varistor. The doped ZnO particles are mounted between two electrodes and the current passes through them. The amount of grain boundaries through which the current passes determines the cut-off voltage, above which the circuit will be protected by the varistor.

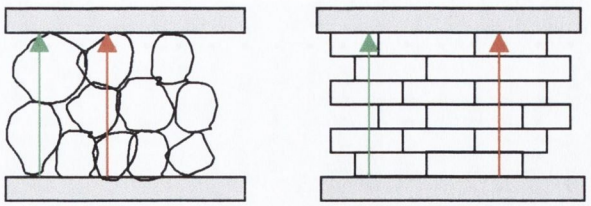

Figure 1.1 Schematic of varistor (A) with non-uniform particles and (B) with uniform particles.

In Figure 1.1 A, the varistor is made from non-uniform ZnO particles. The two arrows indicate two alternative pathways the current can take from one electrode to the other. The first must pass through two particles, whereas the second passes through three. This means that the current control is not exact. On the other hand, when uniform rod-like particles are used, as is illustrated in Figure 1.1 B, the packing is more efficient and the current passes through the same number of grain boundaries in all cases.

Uniform particles when used in varistors, may offer better control over the amount of current that can pass through the component. Also, by growing the particle to specific dimensions, the amount of ZnO particles that fill the cavity between the two electrodes can be altered. Therefore, a possible application of uniform ZnO could lie in the formation of better-controlled power surge components.

1.2.2 Anisotropically Conducting Adhesives.

It is the aim of the electronics industry to constantly reduce the size of the circuitry they can produce. Limitations are imposed primarily by component size but restrictions are also present by the use of solder. Solder is undesirable, not only because it is environmentally unfriendly by the use of lead but also because the proximity of the lines of solder laid down on a circuit board can result in 'bridges' between the two lines. In this way, current can flow where it is not intended. A solder alternative, which

conducts in only one direction, is therefore an area that attracts much attention. Anisotropically conducting adhesives (ACA's) are that alternative.[11, 12]

These ACA's are composed of conducting microparticles aligned in an adhesive matrix. Conduction takes place in only one direction and hence lines running along side each other cannot have current flow between them. Conduction in these ACA's relies on good contact between the microparticles within the adhesive matrix. At present, metal-coated spherical polystyrene is the most common microparticle used for these applications. Maximum contact between spheres can only be a point contact. However, if inorganic microparticles were used, such as rod-like ZnO, a more efficient contact between particles could be made. As was previously discussed, preliminary tests using gold-coated PbS cubes have already shown enhanced properties when compared to gold-coated polystyrene spheres.[4]

Uniform microparticulate inorganics may present a good alternative to polystyrene beads. However, in order to use the microparticles in this way, their conductivity must be enhanced by metal coating.

1.3 ZINC OXIDE AND ZINC HYDROXIDE

In this thesis, the growth of ZnO is reported, using a number of different methods. ZnO was chosen for many reasons. Firstly, ZnO is known to form with a number of interesting morphologies from spherical to rod-like particles (see Table 1.1). Secondly, ZnO is used in many industries including pharmaceutics, ceramics, vulcanization of rubber and varistor and semiconductor technologies.[13] A uniform morphology could, in theory, improve the efficiency of the ZnO in some of these industries. Also, ZnO is a semiconductor and so novel samples with a well-defined morphology could present the opportunity of new applications for ZnO or modified ZnO, e.g. varistors or conducting adhesives.

Perhaps the most important reason for studying ZnO however, is the fact that although the effect of reaction parameters has been studied for the system, the fundamental growth pattern of the particles has been neglected. Only one report exists where the growth of the ZnO particles by hydrothermal methods is outlined.[14] As there are a large number of hydrothermal precipitation methods for ZnO, an understanding of another method and of how particular morphologies are produced would be desirable.

1.3.1 Zinc oxide properties.[15]

Zinc oxide (ZnO) is a semiconductor with a band gap of approximately 3.4 eV. It is a white powder that can exist in three different crystalline structures. The hexagonal close packed structure (zincite), with an *a:c* axial ratio of 1:1.6, is similar to wurtzite and can be seen in Figure 1.2. It is the naturally occurring form and by far the most common. The other two forms of ZnO are cubic. When the hexagonal lattice is compressed to pressures of 100 bar or over, a new more dense structure results (similar to NaCl). The second is a face centred cubic structure, which is only known to form when zinc, deposited on copper wire, is oxidized.[16]

Zincite has its c-axis of the hexagonal structure lying along the z-axis of the lattice. From the diagram below, it can be seen that cut-planes along both the x- and y- axis contain an equal number of Zn^{2+} and O^{2-} ions (in an infinite lattice). A plane cut perpendicular to the z- axis however contains only Zn^{2+} or O^{2-}. This causes a net polarity through the lattice in the c-axis direction.

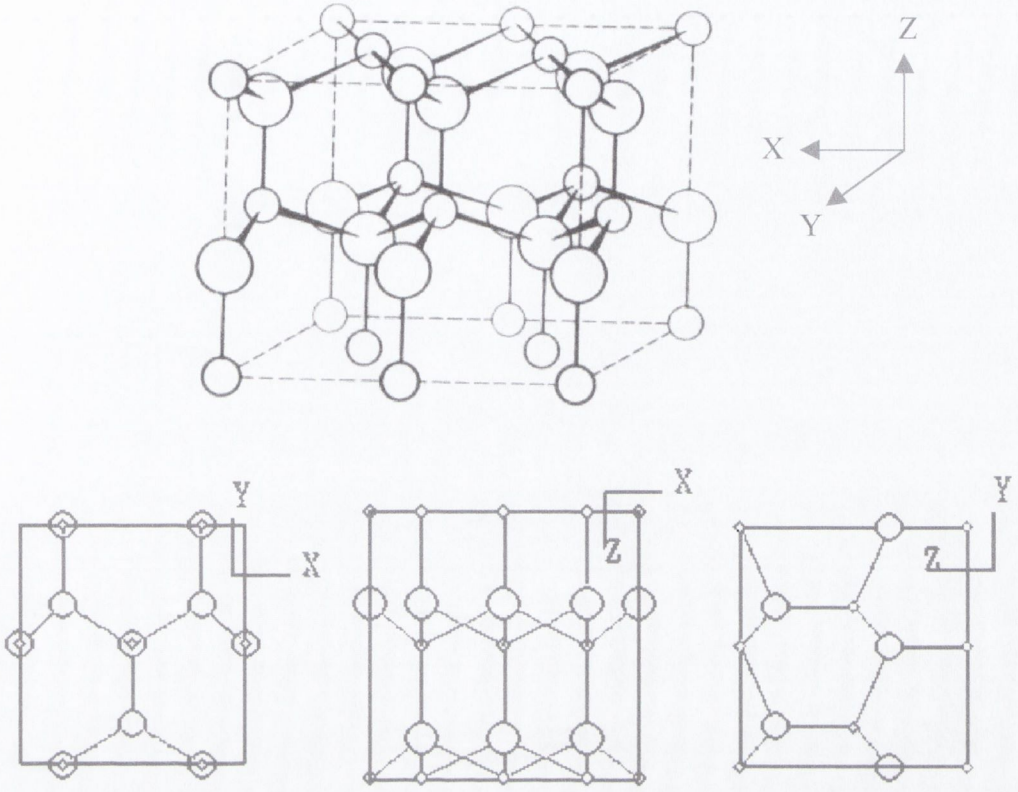

Figure 1.2 Zincite structure,[17] including cut-planes along each axis.[18]
(Large spheres - O^{2-}, smaller spheres - Zn^{2+}).

Although zinc oxide is found naturally occurring in a crude form, commercially it is produced by two different methods. The 'French' process involves vaporizing the pure metal and burning it in air. In the direct or 'American' process, zinc ore and coke are heated in air and the resultant vapour is oxidized *in situ*. In the laboratory, very pure ZnO is prepared by thermal decomposition of zinc carbonate, hydroxide and oxalate or hydrothermally from alkaline solutions. It is an amphotheric solid, dissolving readily in concentrated acids and bases to produce Zn^{2+} salts and zincates respectively.

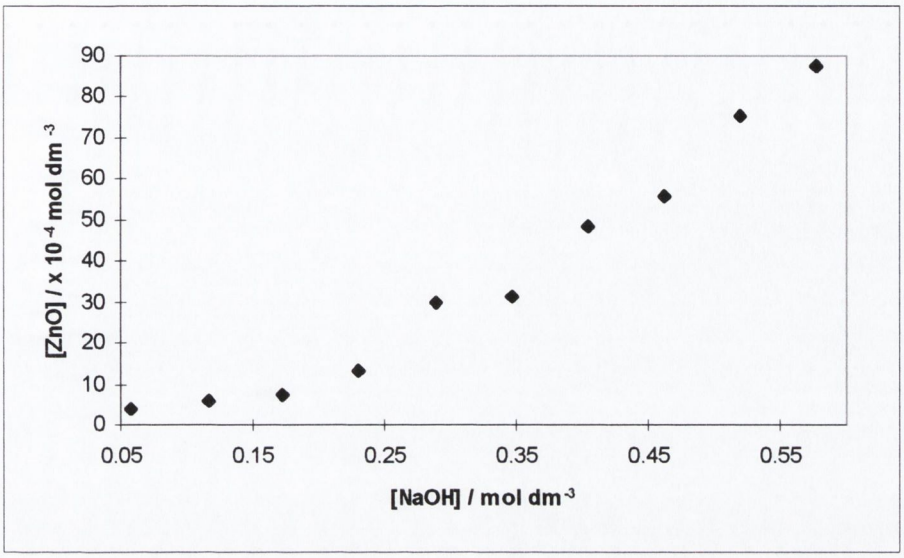

Figure 1.3 Solubility data for ZnO in NaOH at 298 K.[19]

The solubility of ZnO in NaOH can be seen in Figure 1.3. Although ZnO dissolves readily in concentrated bases, its solubility in weak base solution is quite low. Reported values for the water solubility of ZnO vary somewhat but generally range from 3 to 5 x 10^{-4} g in 100g H_2O at 298 K.

1.3.2 Zinc hydroxide properties.[15]

Zinc hydroxide is also a white solid with six different forms recorded; α, β_1, β_2, γ, δ, and ε. The latter is the only form that is stable in water below 39°C. α-$Zn(OH)_2$ has a hexagonal lattice but can only exist in the presence of certain anions such as carbonate or silicate. The two β forms and γ are layered structures similar to brucite, $Mg(OH)_2$. The δ form rapidly transforms into ε-$Zn(OH)_2$ and they are therefore assumed to have similar structures. The ε form has an orthorhombic structure and is the only one for which structural data is complete. It is also similar to the brucite structure which can be seen in Figure 1.4 below. As this is the only form which shall be discussed, it will be referred to only as $Zn(OH)_2$ for the purposes of this study.

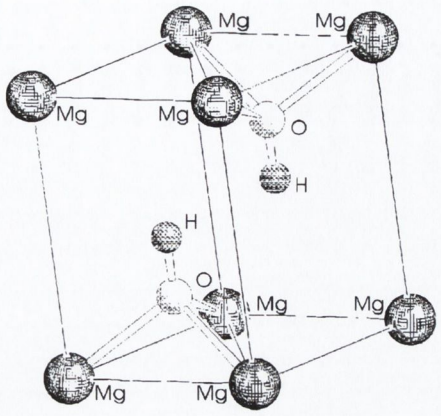

Figure 1.4 $Mg(OH)_2$, brucite structure.[20]

$Zn(OH)_2$ can be prepared by adding hydroxide ions to a zinc salt solution or by adding hydroxide to a suspension of ZnO in water followed by boiling. Above 120 °C, $Zn(OH)_2$ loses water at an appreciable rate; however, for complete conversion to ZnO temperatures of approximately 900 °C are required. This suggests that migration of H_2O through the $Zn(OH)_2$ lattice is a difficult process.

Widely different solubility values for $Zn(OH)_2$ have been reported[21] and even accounting for different polymorphs, the values still seem inconsistent. In general, it is found that solubility increases with increased pH, with values of 5×10^{-4} M to 5×10^{-2} M for 0.1 M and 1 M NaOH solutions at 298 K respectively.[15] Solubility data for $Zn(OH)_2$ in NaOH at 298 K can be seen below in Figure 1.5.

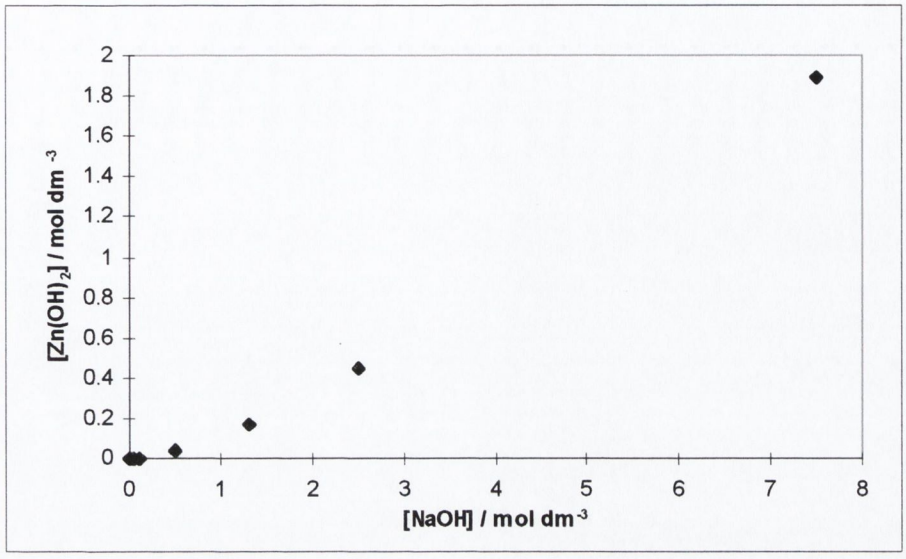

Figure 1.5 Solubility data for $Zn(OH)_2$ in NaOH at 298 K.[22]

Similar to ZnO, $Zn(OH)_2$ readily dissolves in concentrated base. However, in more dilute base it has a slightly higher solubility; 1 x 10^{-3} M in 0.05 M NaOH at 298 K,[22] compared to approximately 4 x 10^{-4} M for ZnO.[19]

1.4 CONTROLLED PARTICLE GROWTH

Controlled growth of particles in the micron size range can be achieved by a number of different methods. There has been much success for AgX systems, due to their importance in the photography industry.[23, 24] However, the least success was achieved for metal oxide / oxyhydroxide systems, until the 1970's, when Matijevic and co-workers[5] prepared a number of different metal hydrous oxides of uniform size and shape. Since then, much work has been done in this area.

Hydrothermal methods are by far the most widely studied for metal oxide, hydroxide and sulphide systems.

1.4.1 Hydrothermal methods for metal hydrous oxide formation.

Hydrothermal growth involves precipitation of particles from solution at elevated temperatures or pressures. In order to control the growth of the particles and produce a monodisperse sample, the release of one of the reactants into solution must be controlled. Simply adding hydroxide ions to a metal salt solution makes the system difficult if not impossible to control. The kinetics of hydrolysis of the metal cation must be managed. There are three well documented methods to achieve this control; forced hydrolysis, controlled release of hydroxide ions and decomposition of organometallics. Each of these methods will be discussed with respect to specific systems in section 1.4.3.

1.4.1.1 Forced hydrolysis. In this procedure aqueous metal salt solutions are reacted at elevated temperatures (usually 80 to 100°C) for given times, a process usually referred to as ageing. Ageing temperatures and times depend on the hydrolyzability of the metal cation in question. During the course of the reaction the pH drops due to the deprotonation of the hydrated cation, eventually leading to the precipitation of a solid hydrous oxide.

$$[M(H_2O)_x]^{w+} \xrightarrow{\Delta H} [M(H_2O)_{x-1}(OH)]^{(z-1)+} \rightarrow\rightarrow M(OH)_w \text{ or } MO_y \qquad \text{equation 1.1}$$

For cations that are less easily hydrolysed, e.g. Zn^{2+}, it is sometimes necessary to add a weak base to promote deprotonation. The final morphology and composition of the crystals formed are found to be reliant upon the nature of the base used. The mechanisms by which the particles form can also vary depending on the base employed. When using an inorganic base, such as NaOH or KOH, the reaction shown above will be followed. The hydrated cations will slowly deprotonate, then depending on the ageing temperature and the solvent used, either the solid oxide or hydroxide will form.

However, often an organic base will be used, usually a complex amine, such as TEA, EDTA, en or HMT and many articles have been written reporting the effect of different bases on various systems,[e.g. 7] for example morphology and size changes. When an organic base is used, it not only increases the pH to promote deprotonation but it also can form a complex with the metal ion. As the temperature is raised to that of ageing, the metal-amine complex slowly decomposes, releasing the metal cation into solution. In this way, the amine acts as a reservoir for the metal, allowing the concentration to stay below that of the critical concentration. This has the result of only one nucleation event taking place (as described by LaMer, section 1.5.1) and so the particles can grow in a slow and controlled manner.

This reservoir effect can also be seen if a metal hydroxide is precipitated first. The more stable phase in contact with the media will be precipitated. If this is the metal hydroxide, alterations in the temperature or pH can result in the formation of the oxide. The oxide can either form as a result of a dissolving-reprecipitation process or from a phase transformation. Dissolving the hydroxide may act as a reservoir for the release of metal ions into the solution. However, a lattice rearrangement is a little more complicated. Depending on the degree of rearrangement involved, the hydroxide may act as a reservoir or alternatively, the uniformity of the hydroxide may be a key factor as to whether or not the resultant oxide forms uniform particles.

With the forced hydrolysis method, crystals of different morphology but of the same composition can often be formed. This is because the growth of such particles is strongly dominated by the reaction conditions, such as temperature, pressure and reactant concentrations.

1.4.1.2 Controlled release of hydroxide ions. Instead of a slow deprotonation of the metal ion as described above, the hydroxide ion can be slowly released into the solution. This is usually achieved by the decomposition of certain organic compounds such as urea or formamide. The decomposition pathway of urea can be seen below;

$$CO(NH_2)_2 + 3\,H_2O \rightarrow 2\,NH_4^+ + 2\,OH^- + CO_2 \qquad \text{equation 1.2}$$

This thermal decomposition of urea (or formamide) results in a slow release of hydroxide ions, which react with the free metal ions in solution to produce the metal hydrous oxide. In the case of urea, an additional reaction can take place.

$$CO(NH_2)_2 + OH^- + H_2O \rightarrow CO_3^{2-} + NH_3 + NH_4^+ \qquad \text{equation 1.3}$$

The urea can react with some of the released hydroxide to produce the carbonate ion. This carbonate, accompanied by an increase in pH, often leads to the precipitation of a basic metal carbonate. This can then be thermally decomposed to form the metal oxide. If the heating is carried out extremely carefully, the morphology of the particles can be retained. In the case of some metals, for example zinc, the temperature at which the solution is aged can determine whether the hydrous oxide or the carbonate is precipitated. There can often be a very small difference between the temperature at which the oxide is the stable phase and that at which the carbonate is more stable. Therefore, when using this method, precise control over the ageing temperature is necessary.

1.4.1.3 Decomposition of metal organics. The most common metal organics used in the preparation of metal hydrous oxides are alkoxides, as they readily hydrolyse at low temperatures in the presence of water. The properties of the final particles formed can be controlled by the concentration of alcoholic alkoxide solution and the amount of water added. Under properly controlled conditions these solutions yield spherical particles. Haile and Johnson,[25] in their work on ZnO systems, have proposed a mechanism for the formation of this spherical morphology. As the oxide particle forms, the surface-active organics hold a shell of alcohol around the growing oxide. As all surfaces of the particles are equally affected, the growth kinetics at each face are essentially 'evened out'. For this reason a spherical particle results. In a similar method,

the organometallic can be decomposed in aqueous alkaline solution to produce uniform metal oxide particles.

1.4.2 Alternative methods for metal hydrous oxide production.

Controlled double-jet precipitation (CDJP) is a variation on a hydrothermal method and has primarily been employed for the photographic industry.[26] Recently however, it has also been extended to metal oxides.[27] This method involves continuously pumping reactants into the reaction vessel, in order to exercise slow and controlled growth. Zhong and Matijevic[27] report the production of ZnO by CDJP. Zinc nitrate and TEA are pumped into preheated water at a constant flow rate to produce uniform ZnO particles.

Also, chemical bath deposition (CBD) has been used for ZnO and ZnS production.[28, 29] In this case however, thin films are prepared rather than discrete particles. The method involves growth of films onto a glass substrate, suspended in the reaction mixture e.g. zinc acetate and ethane-1,2-diamine.[30]

There are also non-hydrothermal methods available for the production of uniform microparticles an example of which is vapour phase growth. This is carried out in a furnace with particle formation taking place onto a ceramic substrate. Noritake *et al*[31] grew c-axis orientated ZnO onto a polished ZnO ceramic between 600 and 950°C.

1.4.3 Previous work on controlled particle growth.

The formation of particles of a uniform size and shape is an area that has attracted much attention. For a number of years, monodisperse sols, such as gold, silica and polymer latex have been known to form. Recently however, much of the work in this field has centred on metal hydrous oxides, with the first comprehensive study published by Matejivic[5] in the late 1970's. Since that time several reviews have been

published,[1, 32, 33] covering a number of different metals and the effects of added base, counter-ion, concentration and ageing time. However, by far the most work done in this area can be attributed to Matijevic and co-workers.

1.4.3.1 Matijevic and co-workers. In 1969, Demchak and Matijevic[34] first published the preparation of monodisperse metal hydrous oxides, in this case studying chromium systems. A subsequent review article[5] details the formation of ferric and aluminium hydrous oxides. Work on ferric systems[6, 35, 36] showed that by ageing ferric perchlorate with perchloric acid, both bipyramidal-type and ellipsoidal Fe_2O_3 were formed. These morphologies could be obtained by varying both the concentrations of the acid and of the ferric salt. By then changing the counter-ions of both the salt and the acid, (chlorides instead of perchlorates), needle-like particles of FeOOH are formed. This indicates that different anions in the growth media influenced both the morphology and the size of the particulates produced under otherwise identical conditions.

Studies of zinc sulphide systems[37] show that spherical particles with a radius in the range 0.15 to 0.3 μm could be formed. The sols were produced by ageing zinc salt solutions with thioacetamide as the source of sulphide ions. Colloidal particles of cadmium carbonate, oxide and oxychloride,[38] were all produced using a urea hydrolysis method. By altering the salt used, different morphologies and compositions were produced. Cadmium chloride resulted in the formation of rod-like Cd(OH)Cl, whereas cadmium nitrate gave cubic cadmium carbonate. Thermal decomposition of the carbonate resulted in the formation of CdO, with retention of the cubic morphology.

Urea hydrolysis of copper salts[39] results in bipyramidal and needle-like particles from copper chloride and copper sulphate respectively. Using the same method, Matijevic showed that by sealing reaction tubes, increased pressure also affected the morphology of particles. When lanthanum nitrate[39] is heated in the presence of urea, small spheres are formed in sealed tubes, whereas needle-like particles result from the

open stirred vessels. Yttrium chloride[39] solutions aged with urea give spherical $Y(OH)CO_3.H_2O$ particles. By increasing the ageing temperature and time and the concentration of the reactant, $Y_2(NH_3)(CO_3)_3.3H_2O$ was formed with a needle-like morphology.

This is by no means a complete review of the work carried out by Matijevic and co-workers, however, it does summarize some of the main results obtained. Matijevic has also carried out a number of studies on the ZnO system, which will be discussed in more detail in section 1.4.4.

1.4.3.2 Some other controlled growth systems. As controlled growth is such a broad area, only a small number of systems will be discussed in this section. Preparation of cubic lead sulphide has been extensively studied and there have been a number of different methods investigated. Meehan[40] first reported bubbling H_2S through a solution of EDTA-Pb complex. However, it was later determined[41] that a better way to produce a monodisperse sample was to use decomposition of thioacetamide as a reservoir for the release of sulphide ions into the solution. Our laboratory[4] has recently produced monodisperse PbS particles in the micron size range using this thioacetamide decomposition method.

$$CH_3CSNH_2 + 2\,H_2O \rightarrow CH_3COOH + H_2S + NH_3 \qquad \text{equation 1.4}$$

In a similar preparation method to that used for PbS, zinc sulphide has been prepared by thermal decomposition of thioacetamide in the presence of zinc salts and various organic bases.[7] Although the particle morphologies were not very well defined in alkaline media, at pH 6 and 60°C spherical particles resulted. The effect of altering the base was not marked in this case. Haruta and Delmon[32] reported the synthesis of spherical molybdenum sulphide, again by the decomposition of thioacetamide.

α-Hydroxides of nickel and cobalt were prepared by Dixit *et al*[42] by urea hydrolysis. The nickel hydroxide showed a fibrous morphology, however, the cobalt hydroxide was produced as well-defined needle-like particles. Musić *et al*[43] showed the influence of experimental conditions on the size and morphology of iron oxides. By decomposing urea in the presence of $FeCl_3$, β-FeOOH needles formed up to pH 9. At higher pH's unstable amorphous $Fe(OH)_3$ also formed which readily decomposed to produce α-FeOOH and/or α-Fe_2O_3. Although the needle-like morphology was retained, it was not as well defined.

1.4.4 Controlled growth of ZnO.

Of the controlled particle growth methods discussed earlier (section 1.4.1), forced hydrolysis and urea hydrolysis are the hydrothermal methods that have been studied in depth for ZnO. Table 1.1 outlines the ZnO morphologies that have been prepared to date. Using the urea hydrolysis and forced hydrolysis methods, needle, rod, star-like, ellipsoidal and spherical ZnO have been formed. Also included on the table are two references to ball milling.[7, 25] This method involves growth of ZnO particles by hydrothermal methods, with one of the alternative morphologies, then milling the sample to form approximately spherical uniform particles.

The forced hydrolysis method, when applied to Zn^{2+}, requires the addition of a base to increase the pH and promote deprotonation. To achieve this both inorganic bases (hydroxides) and organic bases (amines) have been investigated. With the exception of the spherical morphology, all shapes have been produced using hydroxide ions. NaOH is seen to produce needle-like particles. When an organic base (TEA) is also added, the rod-like particles can be achieved. The absence of the hydroxide can also have a marked effect. Matijevic[33] showed how zinc nitrate in the presence of NaOH and TEA gave rod-like particles, whereas O'Brien and co-workers[7] showed that zinc nitrate and TEA, with no NaOH, gave needle-like particles. KOH on the other hand, in the absence of an

amine, results in the rod-like morphology. Finally, ammonium hydroxide can give either the ellipsoidal or star-like morphology.

Table 1.1 Morphologies of ZnO produced by hydrothermal methods.

ZnO morphology	Preparation	Reference
Rod	Zinc nitrate + HMT	14
	Zinc sulphate + urea	44, 45
	Zinc nitrate + KOH	46
	Zinc nitrate + en	7
	Zinc nitrate + TEA + NaOH	33
Needle	Zinc chloride + HMT	14
	Zinc nitrate + urea	44, 45
	Zinc nitrate + NaOH	7
	Na_2Zn-EDTA	47
Sphere	Zinc nitrate + TEA	27, 33
	Zinc acetate + ethan-1,2-diol	48
	Ball milling	7, 25
Star-like	Zinc nitrate + HMT	14
	Zinc nitrate + en	7, 46
	Zinc nitrate + NH_4OH	33
Ellipsoidal	Zinc nitrate + NH_4OH	33, 46

In the case of organic bases, ethylendiamine (en), triethanolamine (TEA) and hexamethylenetetraamine (HMT) have been investigated. HMT can produce rod, needle and star-like particles, whereas en and TEA do not result in the needle-like particles. Rods, stars and spheres can be produced in these cases. Decomposition of a disodium-zinc-EDTA complex was shown by Nishizawa *et al*[47] to also give a needle-like morphology. Collins and Spencer[48] showed that by using an alcoholic rather than an aqueous medium, spherical ZnO could be produced.

The effect of zinc salt can also be analysed. Andres-Verges *et al*[14] showed how under the same experimental conditions, zinc nitrate and zinc chloride resulted in rod-like and needle-like particles respectively. In the urea hydrolysis method, Tsuchida and Kitajima[44, 45] showed that a change from zinc sulphate to zinc nitrate, gave needle-like instead of rod-like particles.

Other than hydrothermal methods and ball-milling as mentioned above, thermal decomposition methods for the production of ZnO have been investigated. Urea hydrolysis can be used to produce uniform zinc basic carbonate, by ageing at a temperature that favours precipitation of zinc basic carbonate. By decomposing the zinc basic carbonate at a slow rate, the morphology and hence the uniformity of the sample can be maintained. Klissurski *et al*[49] used this method but did not attempt to produce a uniform sample. Castellano and Matijevic[50] on the other hand, produced highly uniform ZnO rods from zinc nitrate solutions. Auffrédic *et al*[51] decomposed zinc oxalate to produce ZnO. The uniformity of these samples was not reported. Although it is well known that thermal decomposition of $Zn(OH)_2$ results in ZnO, this method has not yet been studied in any detail as a route to the formation of uniform ZnO particles.

1.5 CRYSTAL GROWTH MECHANISMS

There are a number of different mechanisms proposed for the growth of crystals from solution. Each of the mechanisms has aspects that apply to the growth of some particles, but no one mechanism can describe the growth of all crystals from solution. Therefore, it is best to consider aspects from each mechanism when examining the growth of a particular substance.

1.5.1 LaMer Growth Theory.[52]

LaMer's theory was devised to account for the growth of sulphur spheres from solution. LaMer observed that in order to produce particles that were monodisperse,

nucleation must take place only once. The concentration of the solution was low enough such that the critical concentration was only reached once.

Figure 1.6 shows the three distinct stages to the growth process. Stage I involves an increase in the concentration of the reactant(s) until critical concentration, $C_{Rn\to\infty}$, is reached. Critical concentration is achieved when supersaturation is attained. This is obtained by either increasing the concentration of reactants in solution or by reducing the solubility. This can be done using chemical potential, temperature, pH or solvent. At the critical point, one burst of nucleation takes place. The appearance of the nuclei in stage II partially relieves supersaturation, i.e. the rate of nucleation (R_n) falls to almost zero. By controlling the initial concentrations of reactants, the period in which repetitive nucleation can occur is made so short that a monodisperse colloid results by the subsequent growth of the existing nuclei, (stage III).

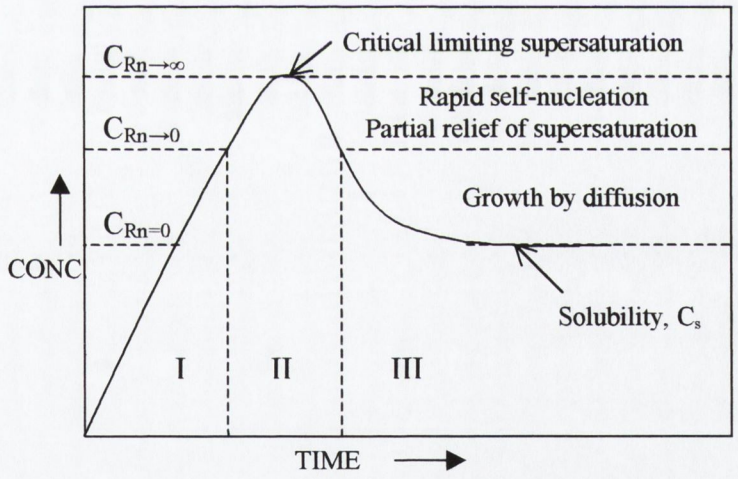

Figure 1.6 LaMer diagram.[52]

If the initial concentrations are not dilute, the rate of nucleation by chemical reaction will become so rapid that the concentration of dissolved species will continuously exceed the concentration at which the rate of nucleation is approximately zero, $R_n \sim 0$. A continuous cascading of nuclei, in addition to growth, then ensues. Therefore, the size

of particles will depend on when they are formed. Non-uniform growth is the result in this case. At concentrations below critical, a small number of particles capable of scattering light should be seen. The solution will appear very slightly turbid. At critical particle formation, R_n increases rapidly and turbidity will increase rapidly.

1.5.2 Aggregation Growth Theories.

It is not always the case that only one burst of nucleation takes place. Although LaMer theory was widely accepted for many years, it does not hold for many particle growth reactions, in particular those of metal oxides and hydroxides. With the advent of electron microscopy, the progress of particle growth can be more clearly studied. If an aggregation process is responsible for the growth of the particles, separation of nucleation and growth steps is not always needed. Figure 1.7 outlines a simplified schematic of the aggregation process.

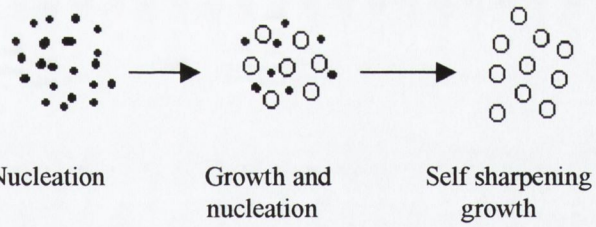

Figure 1.7 Aggregation growth process.

At the start of the particle growth, there is a broad size distribution, therefore a number of nucleations have taken place. Uniformity in this case, is achieved by self-sharpening, i.e. smaller particles grow more rapidly than larger ones. Murphy *et al*[53] were first to report growth by aggregation of sub-units, 0.1μm rods of akageneite, α-FeOOH, from 30Å spheres.

Aggregation growth theory can further be divided into non-directional and directional aggregation processes. When non-directional growth occurs, the primary particles form, aggregate and an internal cementation takes place. This type of aggregation always results in spherical particles, examples of which are TiO_2,[54] SnO_2[55] and SiO_2.[56]

In the case of goethite $Fe(OH)_2$, however, directional aggregation takes place.[53] The primary particles precipitate as spheres, approximately 3 nm in diameter. Aggregation then results in the formation of rod-like particles with an average length of 100 nm. This directional aggregation also occurs in many other systems, including ZnO formation.[14] Almost spherical particles are seen to aggregate in the c-axis direction to form rod-like ZnO. It is thought that this directional aggregation is a result of the net polarization in the c-axis direction through the ZnO lattice (section 1.3.1).

1.5.3 Template growth.

Template growth is seen when the primary particles formed, instead of aggregating, act as a template onto which the final particles grow. In the case of the formation of ellipsoidal hematite (α-Fe_2O_3)[57] from an iron (III) nitrate solution, the powder formed was found to have approximately 10% goethite, $Fe(OH)_2$. Rather than the goethite precipitating first, then recrystallizing to form hematite, it was proposed that the goethite forms a template onto which the hematite grows. Figure 1.8 shows the mechanism for growth similar to that of this system.

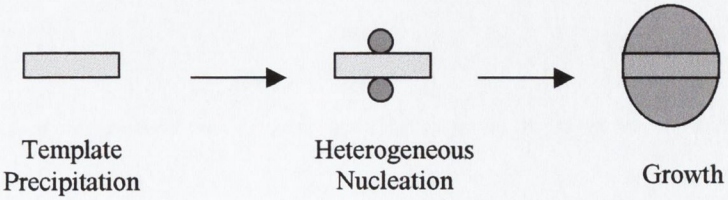

Figure 1.8 Schematic representation of template growth mechanism.

Electron diffraction patterns can be used to show core particles existing in the centre of particles grown by this mechanism. The final particles can either retain the template shape or can adopt a new morphology. In the case reported above, the hematite had an ellipsoidal morphology grown on platelets of goethite. Magnetite (Fe_3O_4) however, grown on the same hexagonal platelets of $Fe(OH)_2$, yield particles which retain the platelet-like morphology of the template. Template growth can also be achieved by the addition of an organic template e.g. malonic acid or carboxylate monolayers[58] to the reaction to act as a substrate for the growth of the inorganic material.

1.5.4 Role of the counter-ion.

For many systems studied, it can be seen that the counter-ion used in the reaction can have a discernible effect on the morphology of the final particles. It is assumed that an interaction takes place between the growing surface and the agent (counter-ion or added impurity). This interaction can control the primary particle formation and / or the aggregation process. The agent can function in a number of different ways. It could adsorb efficiently, competing with growth units for surface sites, blocking growth in some directions. On the other hand, it may also disturb the potential field around the particle and create sites where favourable interactions could take place between growing particles, i.e. act as an aggregation agent.

The agent should also have a disruptive effect on aggregation however, so that it stops functioning at a certain size. At initial growth, nanoparticulate nuclei form, which have a huge surface to volume ratio. When two of these nanoparticles come into contact a highly reactive grain boundary is formed where surface diffusion and even nucleation at the junction is favourable. This reduction of surface area of the particle can eventually favour desorption of the impurity and hence aggregation of the particles takes place. These impurities can then be recycled in the system. The aggregation process further reduces the surface area, which affects the solubility of the particle. The surface would reach an energy minimum and aggregation would no longer be favoured.

This surface adsorption effect can be seen for many systems. In the case of hematite formation from iron chloride solutions, when KH_2PO_4 is added, the phosphate ions are seen to have an effect on the final hematite morphology.[59] There is approximately one phosphate ion added for every fifty iron cations. By addition of this small amount of phosphate to the system, ellipsoidal particles rather than spheres are seen to form. Figure 1.9 shows the proposed mechanism for this growth.[60]

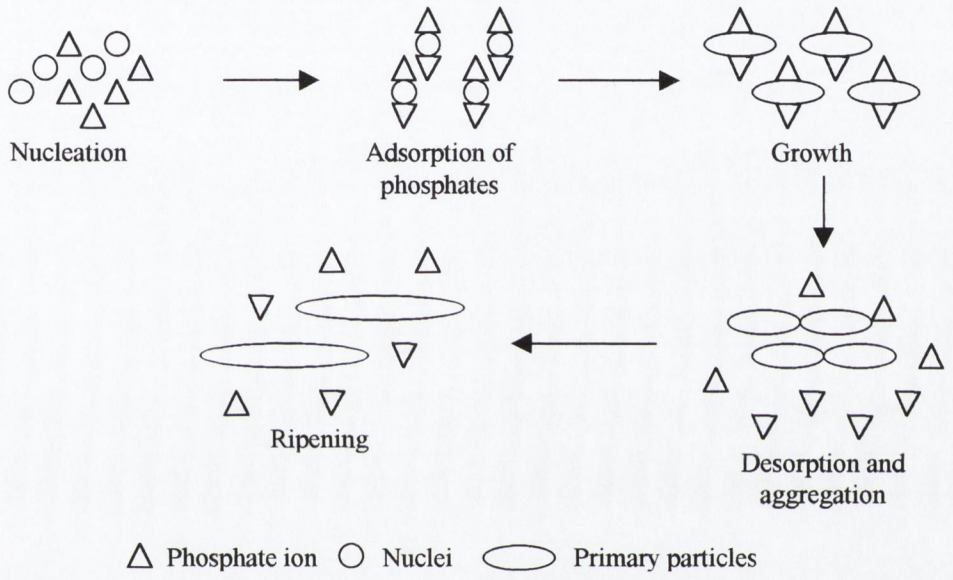

Figure 1.9 Simplistic schematic representation of the formation mechanism of Fe_2O_3 from $FeCl_3$ in the presence of phosphate ions.[60]

The phosphate ions are found to adsorb parallel to the c-axis. This could be accounted for by the fact that the magnetic moment of the Fe_2O_3 particles lie along this c-axis and adsorption of the phosphate ions is occurring parallel to this magnetic moment.

1.5.5 Crystal twinning.[61]

While an ideal crystal is an infinite lattice of atoms or ions arranged in repeating patterns in three dimensions, in reality, a crystal is finite and contains defects. One of the most common defects that can occur when a crystal is growing is twinning.

A twinned crystal is one in which a twin plane defect has occurred. A twin plane is described as a sheet defect. If during or after growth a crystal is strained, it may be energetically favourable for the atoms to adopt an alternative position, resulting in a break in the order of the crystal lattice. The external shape of the crystal may be altered.

If the horizontal atom planes (right of diagram, Figure 1.10) are parallel to a singular face (atomically smooth face), AB creates corners on the external face. Re-entrant corners (such as that at A) may be easy sites for deposition of atoms and hence rapid growth. This is called dendritic growth.

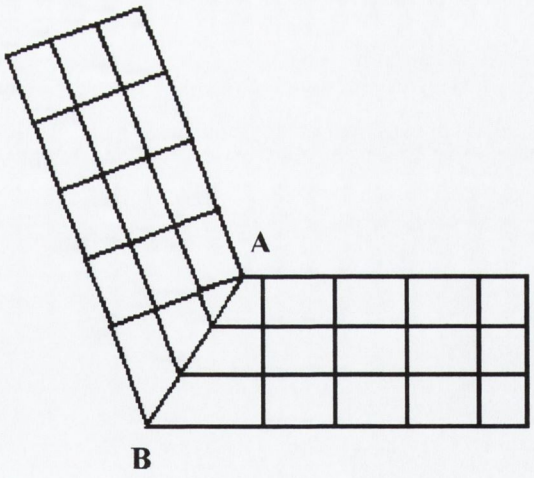

Figure 1.10 A twin plane in a crystal.[61]

By optically examining crystals a lot can be inferred about the crystal structure. Flat faces are singular, a line across a face is usually a twin plane and pits or hillocks are

usually signs of terminations of dislocations or stacking faults.[61] When crystals are grown freely, the absence of a face normally found suggests a twin.

1.6 MICROWAVE HEATING

Microwave oven heating is a form of radiative heating. Thermal motion results in a random orientation of molecules in a solution. When placed in an external electric field, the molecules will align with the field, if they have a permanent dipole. When the frequency of the field is equal to the relaxation time of the molecule, microwave energy is converted into kinetic energy. The efficiency of this conversion is referred to as the loss tangent of the material. A substance with a high loss tangent will be heated efficiently in the microwave oven.

A domestic microwave oven (DMO) operates at a frequency of 2450 MHz, a wavelength of 12.2 cm. Contrary to common belief, this is not the wavelength at which water molecules absorb most strongly.[62] If that were the case, a high heating rate would be confined to the surface of the object being heated, as surface water would absorb all the radiation. To ensure uniformity of heating, the optimum frequency would be one whose wavelength is approximately the length of the object to be heated. This would allow the entire object to be penetrated and hence heating would take place throughout the whole object. The selected frequency for a commercial microwave oven is in fact considerably lower than peak absorption of the water molecule.

Most polar organic molecules have a sufficiently high loss tangent at 2450 MHz that they can be efficiently heated in a domestic microwave oven. This is the reason that microwave technology has been extensively applied to organic synthesis.[63] On the other hand, as solid substances have no rotational relaxation process, they are transparent to microwaves. However, in semiconductors and ion conductors, the movement of electrons or ions, associated with their conduction, can result in their coupling strongly in the microwave region. As the temperature increases, so too does their conduction and

hence also their loss tangent. Consequently, thermal runaway can be a problem in inorganic solids. However, due to the mode of interaction of the microwaves with the materials, when the source is switched off, the sample cools very rapidly.

1.6.1 Microwave heating of inorganics.

Baghurst and Mingos[64] applied microwave heating to inorganic solid state synthesis. They discovered that many inorganic oxides efficiently couple with microwaves and that their heating rate is extremely fast. Samples of 1 to 5 grams of V_2O_5 and WO_3 reached temperatures in excess of 700°C within one minute at 500 W. The same quantities of CuO reached in excess of 550°C and 5 to 10 gram samples of ZnO and MnO_2 reached over 800°C under the same conditions.

A recent comprehensive review[65] of the application of microwave synthesis to inorganic solids, outlines all aspects of inorganic solid and solution state chemistry which has been carried out using a microwave oven heat source, up to 1999. The majority of solution phase microwave work has been concentrated on the synthesis of hydroxyapatite. HAp is the bioceramic substance that makes up the skeletal structure in living creatures. The synthesis of such a compound is of particular interest to those working in the area of dentistry and prosthesis. Much success has been reported in improving the time scale of this originally slow and tedious synthesis.[66]

The slow ageing times required for controlled synthesis and decomposition, to form uniform particles could perhaps benefit from the use of a microwave heat source. However, as yet no controlled crystal growth studies have been carried out using a microwave oven.

1.7 SUMMARY

The production of particles of a monodisperse nature has been studied extensively for many years. There have been a number of particle growth theories proposed, with the aggregation theory being favoured over the LaMer theory for many systems. But in truth, each system must be investigated individually and the growth pattern usually incorporates aspects from both growth mechanisms. Metal hydrous oxide preparation appears to largely rely on the aggregation theory. From the studies of the metal oxides carried out to date, the effect of the counter-ion and of the base used in the hydrolysis reaction can be clearly seen.

For ZnO, many studies have been carried out to examine the effect of various reaction parameters. The temperature of hydrolysis, the hydrolysis method used (base or urea hydrolysis) and the reactant concentrations are all seen to have an effect on the morphology of the particles produced. The growth of ZnO particles by hydrothermal methods has been examined in only one study, that by HMT hydrolysis of zinc nitrate. Growth by hydroxide ion hydrolysis and urea hydrolysis are still unexplored. It is therefore clear, that there is still an enormous amount of work to be carried out in this area.

1.8 THESIS GUIDE

- Chapter 2 will report the preparation of ZnO microparticles by a forced hydrolysis method, using hydroxide ions to promote deprotonation of the hydrated zinc cation. Two ZnO morphologies, needle-like and star-like particles are prepared and the mechanism by which these morphologies grow will be discussed. The effect of ageing times, pre-stirring conditions, reactant concentrations and zinc salt counter-ion on the particles formed will also be determined.

- Chapter 3 will again report ZnO production by hydroxide ion hydrolysis; however, in this case a microwave heat source will be employed. The growth of both needle-like and star-like particles will be considered and the effect of microwave oven heating established, at a number microwave operating power levels.

- In Chapter 4, two alternative hydrothermal procedures are discussed. Preparation of ZnO rod-like particles by urea hydrolysis is reviewed and the effect of ageing time and temperature ascertained. ZnO needle-like particles are also grown by a forced hydrolysis method using an organic base, that being hexamethylenetetraamine. The mechanism by which these particle form has been previously reported[14] and so the effect of microwave heating will be determined.

- Modification of needle-like and star-like ZnO particles by electroless plating techniques is discussed in Chapter 5. Tin and palladium coatings are deposited, for activation of the particle surface and coating with copper, nickel, silver and gold are attempted.

- Chapter 6 outlines the materials and methods used throughout these studies and Chapter 7 concludes this dissertation and discusses any area covered in the thesis that merits further work.

1.9 REFERENCES

1. E. Matijevic, *Langmuir*, 1986, **2**, 12-20
2. E. Matijevic, *Acc. Chem. Res.*, 1981, **14**, 22-29
3. J.Th.G. Overbeek, *Chem. Austrailia*, 1981, **48**, 419-426
4. M. Armstrong, *Ph.D. Thesis*, Dublin, 1998
5. E. Matijevic, *Pure & Appl. Chem.*, 1978, **50**, 1193-1210
6. E. Matijevic, P. Schneiner, *J. Colloid Interface Sci.*, 1978, **63**, 509-524

7. T. Trindade, J.D. Pedrosa de Jesus, P. O'Brien, *J. Mater. Chem.*, 1994, **4**, 1611-1617
8. O. Milošević, D. Uskoković, L.J. Karanović, M. Tomšević-Čanović, M. Trontelj, *J. Mater. Sci.*, 1993, **28**, 5211-5217
9. G. Westin, Å. Ekstrand, M. Nygren, R. Österlund, P. Merkelbach, *J. Mater. Chem.*, 1994, **4**, 615-621
10. T.K. Gupta, *J. Am. Ceram. Soc.*, 1990, **73**, 1817-1840
11. D.D. Chang, P.A. Crawford, J.A. Fulton, R. McBride, M.B. Schmidt, R.E. Sinitski, C.P. Wong, *IEEE Trans. on CHMT*, 1993, **16**, 828-835
12. A.O. Ogunjimi, O. Boyle, D.C. Whalley, D.J. Williams, *J. Electronics Manuf.*, 1992, **2**, 109-118
13. A. Perl, *Amer. Ceram. Soc. Bull.*, 1997, **76**, 140-143
14. M. Andres-Verges, A. Mifsud, C.J. Serna, *J. Chem. Soc. Faraday Trans.*, 1990, **86,** 959
15. *Comprehensive Inorganic Chemistry Vol. 3,* Ed J.C. Bailar, H.J. Emeléus, R. Nyholm, A.F. Trotman-Dickenson, Pergamon Press, 1975
16. W.L. Bragg, J.A. Darbyshire, *Trans Faraday Soc.*, 1932, **28**, 522
17. J.D. Lee, *Concise Inorganic Chemistry 4th Ed.,* Chapman and Hall, London, 1992
18. http--cst-www.nrl.navy.mil-lattice-struk.picts-b4.s.png.url
19. T.P. Dirske, C. Postmus, R. Vandenbosch, *J. Am. Chem. Soc.*, 1954, **76**, 6022-6024
20. http://www.cryst.bbk.ac.uk/PPS2/projects/loesel/chap04.htm, Zigan, Rothbauer 1967
21. *IUPAC Solubility Data Series Vol. 23*, Pergamon Press, 1986, 156-269
22. J. Moir, *Proc. Chem. Soc.*, 1905, **21**, 310-311
23. R. Jagannathan, V.V. Gokhale, *J. Imaging Sci.*, 1991, **35**, 113-118
24. W.A. Schimdt, H.J. Metz, *J. Inform. Rec. Mater.*, 1993, **20**, 375-281
25. S.M. Haile, D.W. Johnson, *J. Am. Ceram. Soc.*, 1989, **72**, 2004-2008
26. C.R. Berry, in *The Theory of the Photographic Process 4th Ed.*, ed. T.H. James, Macmillan, New York, 1977

27. Q. Zhong, E. Matijevic, *J. Mater. Chem.*, 1996, **6**, 443-447
28. J. McAleese, P. O'Brien, *Mat. Res. Soc. Symp. Proc.*, 1998, **485**, 255-260
29. P. O'Brien, J. McAleese, *J. Mater. Chem.*, 1998, **8**, 2309-2314
30. P.O'Brien, T. Saeed, J. Knowles, *J. Mater. Chem.*, 1996, **6**, 1135-1139
31. F. Noritake, N. Yamamoto, Y. Horiguchi, *J. Am. Ceram. Soc.*, 1991, **74**, 232-233
32. M. Haruta, B. Delmon, *J. Chim. Phys.*, 1986, **83**, 859-868
33. E. Matijevic, *Chem. Mater.*, 1993, **5**, 412-426
34. R. Demchak, E. Matijevic, *J. Colloid Interface Sci.*, 1969, **31**, 273
35. T. Sugimoto, E. Matijevic, *J. Colloid Interface Sci.*, 1980, **74**, 227-243
36. R.S. Sapiesko, E. Matijevic, *J. Colloid Interface Sci.*, 1980, **74,** 405-422
37. D. Murphy Wilhelmy, E. Matijevic, *J. Chem. Soc. Faraday Trans.*, 1984, **80**, 563-570
38. A. Janekovic, E. Matijevic, *J. Colloid Interface Sci.*, 1985, **103**, 436-447
39. E. Matijevic, *Pure & Appl. Chem.*, 1988, **60**, 1479-1491
40. E.J. Meehan, *J. Colloid Interface Sci.*, 1975, **49**, 160
41. T. Sugimoto, *Adv. Colloid Interface Sci.*, 1987, **28**, 65-108
42. M. Dixit, G.N. Subbanna, P.V. Kamath, *J. Mater. Chem.*, 1996, **6**, 1429-1432
43. S. Musić, M. Maljković, S. Popović, *Models in Chemistry*, 1999, **136**, 299-316
44. T. Tsuchida, S. Kitajima, *J. Mater. Sci.*, 1992, **27**, 2713-2718
45. T. Tsuchida, S. Kitajima, *Chem. Lett.*, 1990, 1769-1772
46. E. Matijevic, *Faraday Discuss.*, 1991, **92**, 229-239
47. H. Nishizawa, T. Tani, K. Matsuoka, *Comm. Am. Ceram. Soc.*, 1984, C98-100
48. I.R. Collins, S.E. Spencer, *J. Mater. Chem.*, 1992, **2**, 1277-1281
49. D. Klissurski, I. Uzunov, K. Kumbilieva, *Thermochimica Acta*, 1985, **93**, 485-488
50. M. Castellano, E. Matijevic, *Chem. Mater.*, 1989, **1**, 78-82
51. J.P. Auffrédic, A. Boultif, J.I. Langford, D. Louër, *J. Am. Ceram. Soc.*, 1995, **78**, 323-328
52. V. LaMer, R.H. Dinegar, *J. Am. Chem. Soc.*, 1950, **72**, 4847-4854
53. P.J. Murphy, A.M. Posner, J.P. Quirk, *J. Colloid Interface Sci.*, 1976, **56**, 284

54. G.H. Bogush, C.F. Zukoski, *Ultrastructure Processing of Advanced Ceramics,* Wiley, New York, 1988, p. 477
55. L.H. Edelson, A.M. Glaeser, *J.Am. Ceram. Soc.,* 1988, **71**, 225
56. M. Ocaña, E. Matijevic, *J. Mater. Res.,* 1990, **5**, 1083
57. E. Matijevic, P. Scheiner, *J. Colloid Interface Sci.,* 1978, **63**, 509
58. B.R. Heywood, S. Mann, *Adv. Mater.*, 1994, **6**, 9-20
59. M.P. Morales, T. González-Carreño, C.J. Serna, *J. Mater. Res.,* 1992, **7**, 2538
60. M. Ocaña, R. Rodriguez-Clemente, C.J. Serna, *Adv. Mater.,* 1995, **7**, 212-216
61. J.C. Brice, *Crystal Growth Processes*, J.Wiley & Sons, Blackie & Son, Glasgow, 1986
62. C.F. Bohren, *Am. J. Phys.*, 1997, **65**, 12
63. R.A. Abramovitch, D.A. Abramovitch, K. Iyanar, K. Tamareselvy, *Tet. Lett.*, 1991, **32**, 5251-5254
64. D.R. Baghurst, D.M. Mingos, *J. Chem. Soc. Chem. Comm.*, 1988, 829-830
65. K.J. Rao, B. Vaidhyanathan, M. Ganguli, P.A. Ramakrishnan, *Chem. Mater.*, 1999, **11**, 882-895
66. A.L. Macipe, J.G. Morales, R.R. Clemente, *Adv. Mater.*, 1998, **10**, 49

Chapter 2

Growth of ZnO and $Zn(OH)_2$ microparticles by forced hydrolysis; conventional heating.

2.1 INTRODUCTION

Controlled growth of microparticulate metal oxides, by hydrothermal methods, has been studied in great detail.[e.g. 1] Nevertheless, the mechanisms by which these particles form are poorly understood. A number of theories for particle growth have been proposed and are discussed in Chapter 1 (section 1.5). It has been observed however, that most systems contain elements of all the growth theories and for this reason, each system must be studied separately.

This chapter will deal with the growth of ZnO and $Zn(OH)_2$ microparticles by forced hydrolysis using hydroxide ions. Although this method has been used previously for ZnO formation,[2-4] the effect of the various reaction parameters has not been studied, in particular, the effect of precipitation temperature. More importantly however, no mechanism for ZnO growth by hydroxide ion forced hydrolysis has been proposed.

2.1.1 Forced hydrolysis of metal salts.

A well-reported method for the production of metal oxide particles is that of forced hydrolysis.[1, 5] The reaction below shows how a hydrated metal salt is gradually deprotonated, by an increase in temperature, to form a metal hydrous oxide. In the case of metal ions that are not easily hydrolysed, a base may be added to increase the pH and hence encourage deprotonation.

$$[M(H_2O)_x]^{w+} \xrightarrow{\Delta H} [M(H_2O)_{x-1}(OH)]^{(w-1)+} \rightarrow\rightarrow M(OH)_w \text{ or } MO_y \quad \text{equation 2.1}$$

The base used for this reaction can be either organic or inorganic. In the case of organic bases, those commonly used are amines, such as triethanolamine (TEA), ethylenediaminetetraacetic acid (EDTA) or ethylenediamine (en). For inorganic base hydrolysis, sodium or potassium hydroxides are those most widely used. When organic bases are employed, as well as increasing the pH, they may also form complexes with

the metal ion, which decompose on heating, resulting in a slow release of metal ions into solution.

2.1.2 Forced hydrolysis of zinc salts using sodium hydroxide.

As was outlined in Chapter 1 (section 1.4.1.1), forced hydrolysis is a method commonly used for ZnO synthesis and can result in the formation of a number of different morphologies. Chittofrati and Matijevic[2] were the first to study NaOH hydrolysis of zinc salts. NaOH was added in sufficiently high concentrations to yield zinc nitrate solutions of pH $\geq$ 12. These solutions were then aged at 150 or 250 °C to precipitate ZnO (zincite) with an intertwined needle-like morphology. By adding a fluorinated surfactant to the solution, the twinning was reduced and discrete needle-like particles were formed. Matijevic[3] also found that by adding TEA to the NaOH / zinc nitrate solution, rod-like particles, rather than needles, formed.

O'Brien and co-workers[4] also studied NaOH / zinc nitrate systems. They found that ageing at 100°C gave needle-like particles and in agreement with Matijevic[3], that the addition of TEA gave rod-like particles. They attributed this morphology change to the fact that addition of the organic ligand inhibits the formation of zinc hydroxide.

2.1.3 Growth of ZnO particles.

The growth pattern of ZnO particles by hydrothermal methods is an area that has not received much attention. To date only one report exists outlining the growth mechanism of ZnO by hydrothermal forced hydrolysis. This was carried out by Andres-Verges *et al*,[6] who studied the growth of ZnO using HMT. By adding HMT to an aqueous zinc nitrate solution, then ageing in sealed tubes at 100°C, the growth of rod-like ZnO was followed. They found that rod-like ZnO formed from an aggregation of smaller spherical particles.

Although ZnO particles have been synthesised by hydroxide ion forced hydrolysis[2 - 4] (section 2.1.2), the mechanism of particle growth has not yet been investigated.

2.1.4 Aims.

In this chapter, the growth of ZnO and $Zn(OH)_2$ microparticles by NaOH hydrolysis of zinc salts will be examined. The effect of the reaction parameters will be investigated, by altering zinc salt concentrations, hydroxide ion concentration, ageing times, pre-stirring times and also the zinc salt counter-ion. The effect of these parameters on particle composition, size and morphology will be assessed. The growth pattern of these particles will also be studied and compared to the LaMer and aggregation growth theories.

2.2 PRELIMINARY RESULTS

The term ageing will be used throughout this report and is defined as follows; heating to boiling temperature (101°C) and holding the temperature constant. Therefore an experiment described as having been aged for two hours, refers to heating to reflux (approx. 20 minutes) and holding the temperature constant for the remainder of the time (approx. 100 minutes).

By carrying out forced hydrolysis of zinc nitrate (0.04 M, 250 ml) using NaOH (1 M, 150 ml), a number of different ZnO morphologies were produced. The flow chart below (Figure 2.1) outlines the experiment procedures that will be discussed in this report. Zinc nitrate (0.04 M) and sodium hydroxide (1 M) solutions were mixed together. After addition of a small amount of base, an initial precipitate forms, which dissolves as the remaining base is added. The reaction solution was then treated in two separate ways.

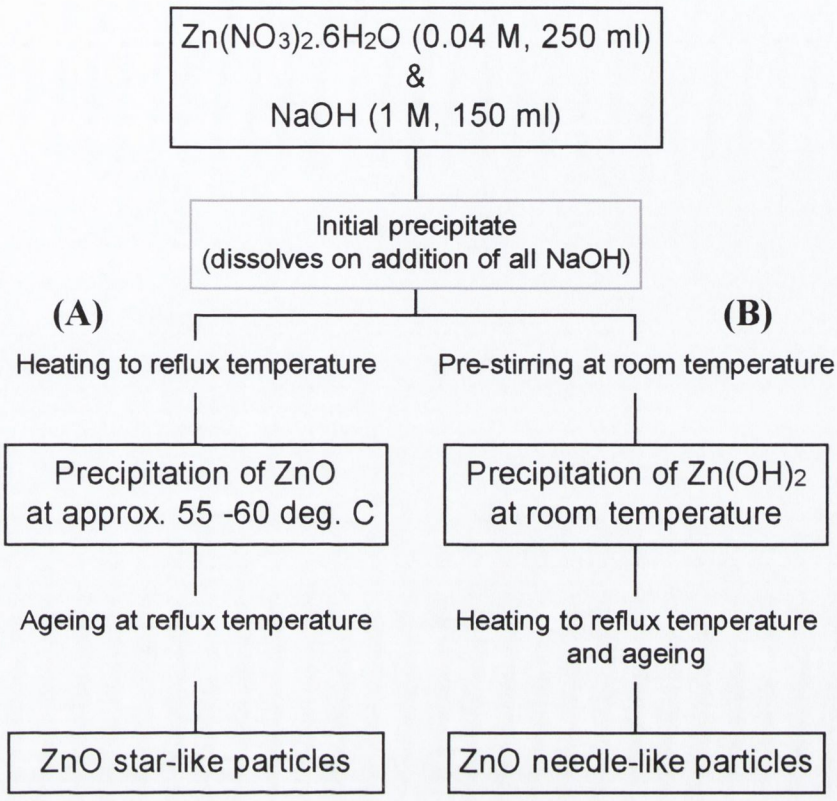

Figure 2.1 Flow chart of experimental procedure for the production of ZnO particles of two morphologies.

Path (A) involves directly heating the reaction solution after mixing. ZnO precipitates at approximately 55 – 60 °C and the dispersion is aged at reflux temperature. The end product of this pathway is star-like ZnO, the growth of which will be reported in Part 1 of this chapter, (sections 2.3 and 2.4). Path (B) involves a pre-stirring step, resulting in precipitation occurring at a different temperature and hence the formation of a different phase, i.e. $Zn(OH)_2$ with a rhombic morphology, as opposed to ZnO. The suspension is then heated to reflux and aged for given times. The final particles formed in this case are needle-like ZnO and their growth is outlined in Part 2 (sections 2.5 and 2.6).

An example of each of the particle morphologies, star-like ZnO, rhombic $Zn(OH)_2$ and needle-like ZnO, can be seen in Figure 2.2.

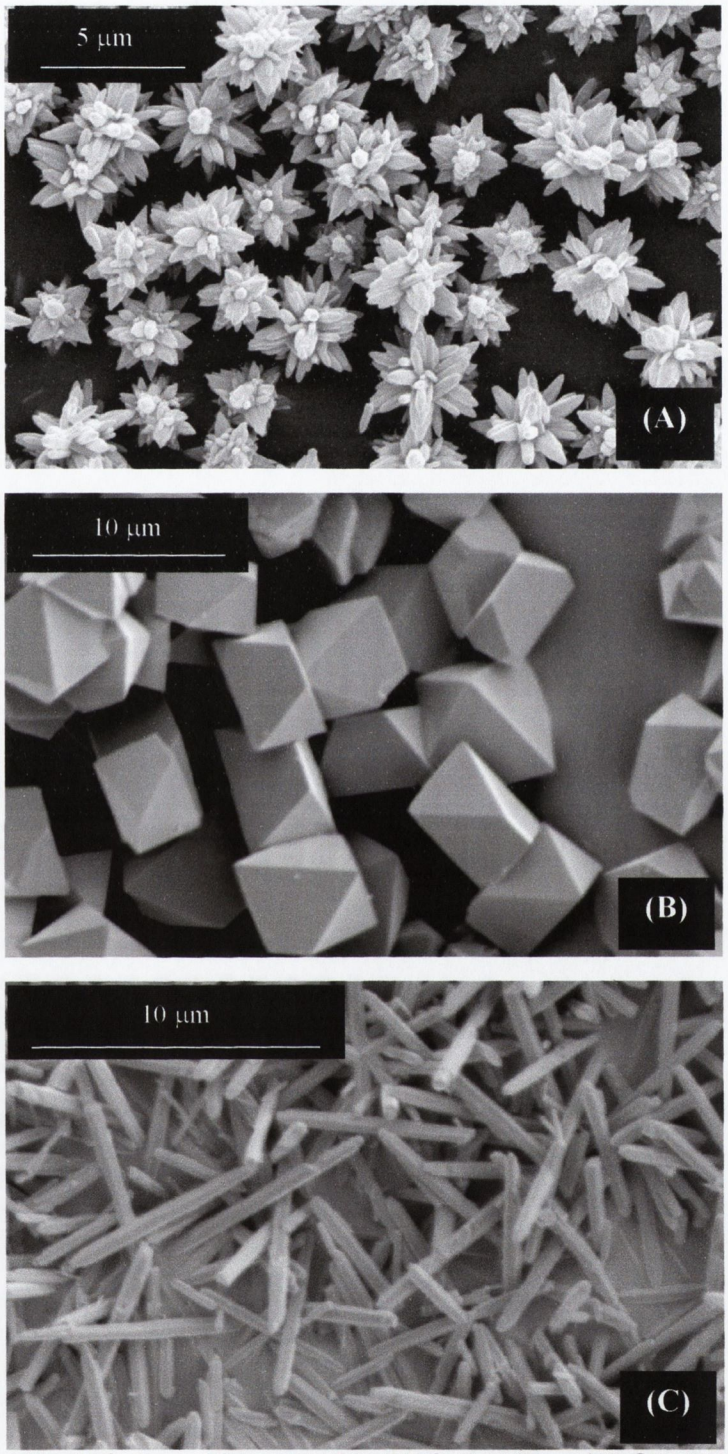

Figure 2.2 (A) Star-like ZnO, formed from $Zn(NO_3)_2.7H_2O$ (0.04 M) and NaOH (1 M) aged for 2 hours, (B) Rhombic $Zn(OH)_2$, formed from $Zn(NO_3)_2.6H_2O$ (0.04 M) and NaOH (1 M) stirred together for two hours at room temperature, (C) Needle-like ZnO, formed from $Zn(NO_3)_2.7H_2O$ (0.04 M) and NaOH (1 M) stirred together for two hours at room temperature followed by two hours ageing.

Ageing times, pre-stirring time, zinc counter-ion and reactant concentrations were altered independently of one another, in order to determine the effect of each on the particles formed.

2.2.1 Stability studies.

As was shown above, treating aqueous solutions of zinc nitrate hexahydrate with sodium hydroxide can result in the formation both zinc oxide and zinc hydroxide. The temperature at which precipitation takes place determines the phase that is formed. According to previous studies,[7] 39 °C is the temperature at which zinc oxide becomes the more stable phase in water with respect to $Zn(OH)_2$. However, in this study, a reaction solution of 0.375 M NaOH is used. Therefore, the stability of $Zn(OH)_2$ and ZnO with respect to each other in this solution needed to be determined. This was investigated by analysing the composition of the precipitate that formed at various temperatures. Both the zinc nitrate solution and the NaOH were heated to the required temperature, added together and the precipitate filtered approximately one minute after turbidity. The crystalline phase was determined by powder x-ray diffraction and matching their patterns to JCPDS diffraction data.[8] Table 2.1 shows the precipitated phase at various temperatures.

Table 2.1 Effect of precipitation temperature on crystalline phase.

Precipitation temperature	Crystalline phase
20 °C	$Zn(OH)_2$ (wulfingite)
30 °C	$Zn(OH)_2$ (wulfingite)
40 °C	$Zn(OH)_2$ (wulfingite)
50 °C	$Zn(OH)_2$ (wulfingite)
55 °C	ZnO (zincite)
60 °C	ZnO (zincite)
70 °C	ZnO (zincite)

It can be seen that between 50 and 55 °C, ZnO becomes the more stable phase in contact with the reaction solution with respect to $Zn(OH)_2$. Below 51°C, $Zn(OH)_2$ forms preferentially and above 55 °C the precipitate is found in all cases to be ZnO.

2.2.2 Initial precipitate.

When a small amount of NaOH (~20 ml, 1 M) is added to the zinc nitrate solution, an initial precipitate is formed. This precipitate was identified by XRD as ZnO (Figure 2.3). Therefore at room temperature and at the pH in question (approximately pH 12.9), ZnO is the more stable phase with respect to $Zn(OH)_2$.

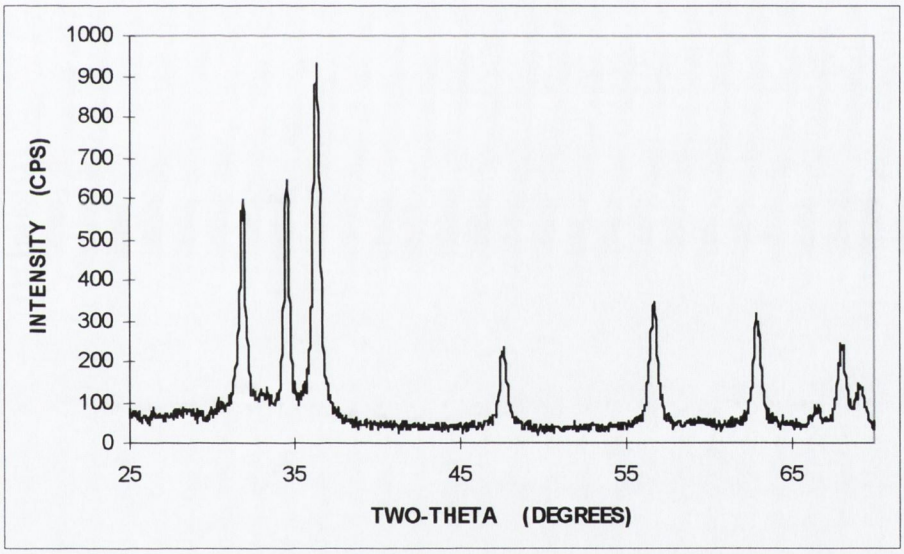

Figure 2.3 XRD of initial precipitate obtained when NaOH (1 M) is added to $Zn(NO_3)_2.6H_2O$ (0.04 M).

From the SEM (Figure 2.4), it appears that the particles are aggregates of much smaller needle-like or platelet particles, (approximately 500 nm in length). With an increase of pH by addition of the remainder of the hydroxide, to achieve a theoretical pH of 13.57, the precipitate dissolves.

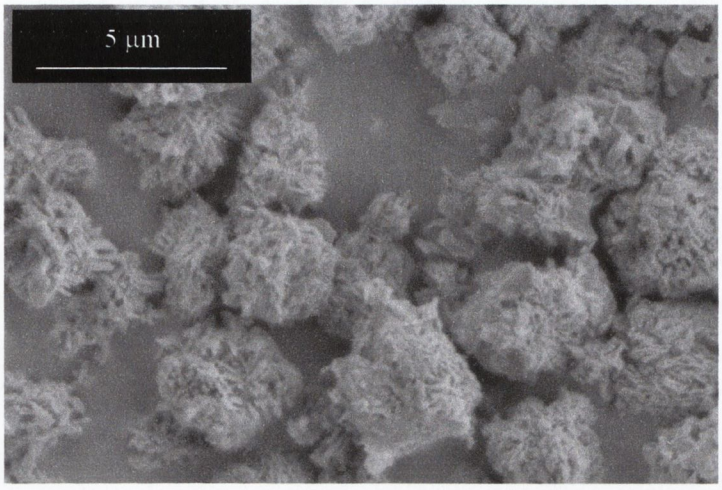

Figure 2.4 SEM of initial precipitate formed when NaOH (1 M) is added to $Zn(NO_3)_2.6H_2O$ (0.04 M).

Dirske[9] showed that at room temperature, an increase in pH results in an increase of the solubility of ZnO. As was observed in the stability studies, at room temperature $Zn(OH)_2$ is the more stable phase at the pH of the final reaction solution. Hence, as the NaOH is added and the pH is raised, the ZnO phase dissolves, giving way to the precipitation of the more stable $Zn(OH)_2$. O'Brien and co-workers[4] also reported the formation of this initial precipitate, finding that it dissolved at pH > 13.5. In that case however, the precipitate was very poorly defined and they were unable to obtain a diffraction pattern for it. By comparing IR spectra, they deduced that it was a hydrated ZnO.

PART 1 - GROWTH OF STAR-LIKE ZnO – (PATH A)

2.3 RESULTS

Zinc nitrate (0.04 M) and NaOH (1 M) were added together at room temperature and heated to reflux. Precipitation took place around 10 minutes after mixing and at approximately 55 – 60 °C. The white precipitate formed was identified as ZnO (zincite, see Appendix I) with a star-like morphology. Reflux temperature (101 °C) is reached after approximately 35 minutes, (i.e. 20 to 25 minutes after precipitation).

Samples were withdrawn from the mixture at regular intervals and the growth of these star-like ZnO particles was followed by XRD and microscopy. Figure 2.5 shows the XRD patterns of samples withdrawn at periods of 5 to 120 minutes after precipitation. All patterns are consistent with ZnO (zincite) and the sample crystallinity appears to increase as the heating time increases.

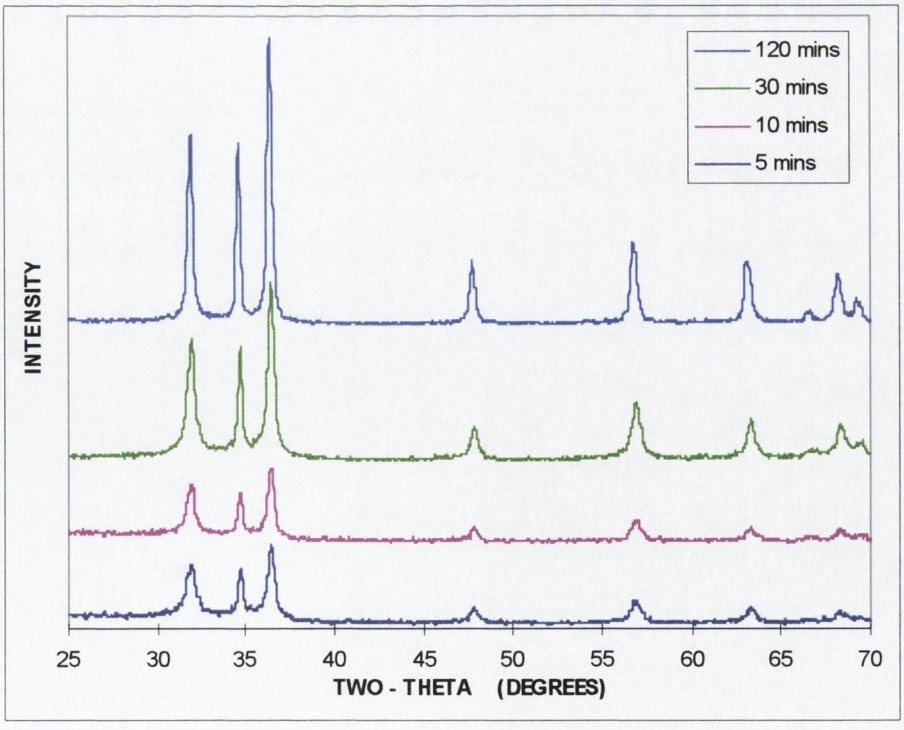

Figure 2.5 XRD patterns for ZnO star-like particle growth, 5, 10, 30 and 120 minutes after precipitation.

The star-like morphology is formed at precipitation and the particles increase in size during the ageing process from an average of 3.5 μm to 6.5 μm in diameter. Figure 2.6 follows the growth of the ZnO star-like particles using SEM. The large particles visible up to 10 minutes after precipitation are $Zn(OH)_2$ particles. These particles are no longer present in the sample after 15 minutes.

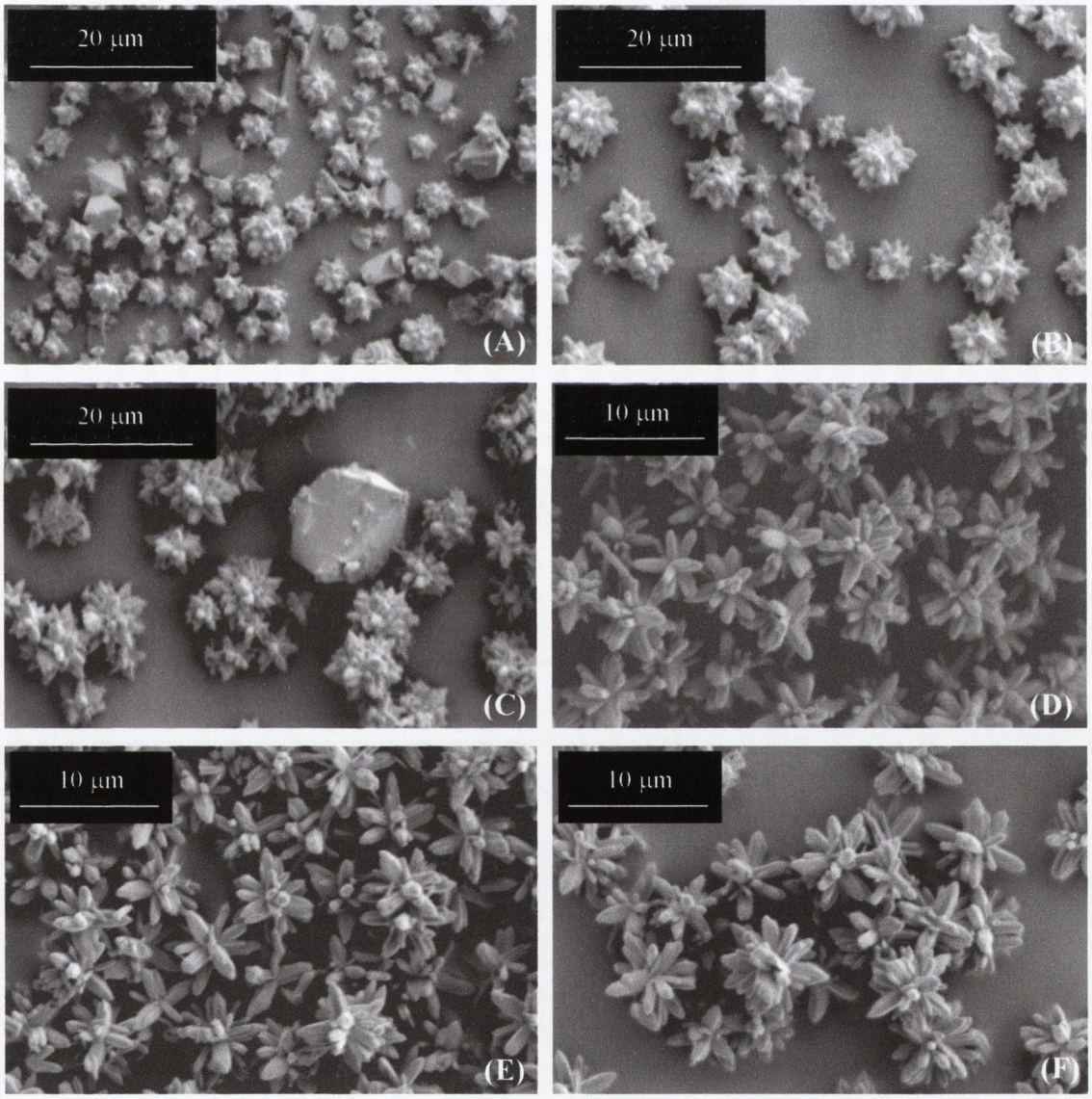

Figure 2.6 SEM of ZnO star-like particles prepared by ageing $Zn(NO_3)_2.6H_2O$ (0.04 M) with NaOH (1 M). SEM of particles after (A) precipitation, (B) 5 minutes, (C) 10 minutes, (D) 30 minutes, (E) 60 minutes and (F) 120 minutes after precipitation.

After samples were removed from the reaction mixture, the filtrate was retained and analysed by EDTA titration. Using an NH_3 / NH_4Cl buffer at pH 10 and solochrome black indicator, the concentration of Zn^{2+} ions remaining in solution was determined. Figure 2.7 shows the titration curve obtained for star-like ZnO growth.

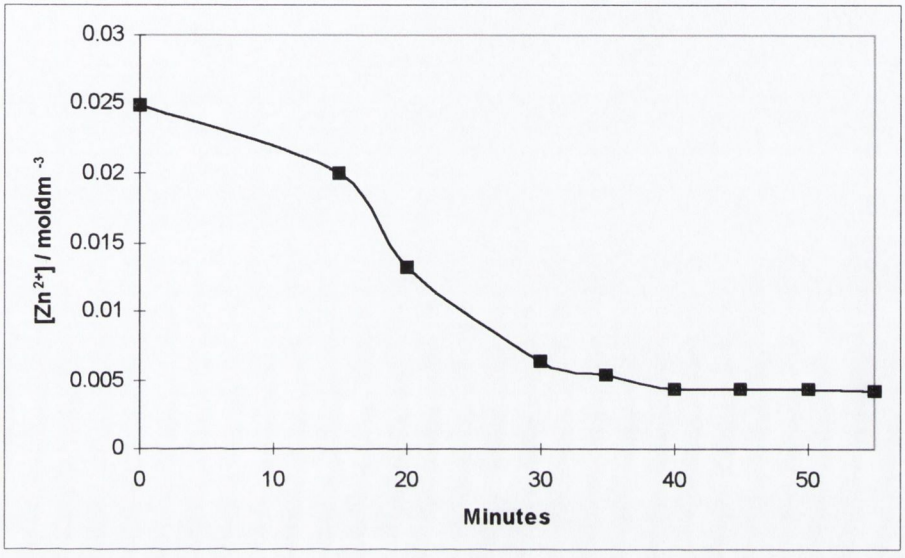

Figure 2.7 Profile of $[Zn^{2+}]$ in solution during star-like ZnO particle growth.

2.3.1 Effect of ageing times on star-like ZnO formation.

With no pre-stirring the precipitation takes place between 55 and 60 °C, then ageing for given times is carried out. The effect of this ageing time on the size of the final particles was examined. Table 2.2 shows how the average star diameter and the diameter distribution change with ageing time. Figure 2.8 shows the particle diameter distributions.

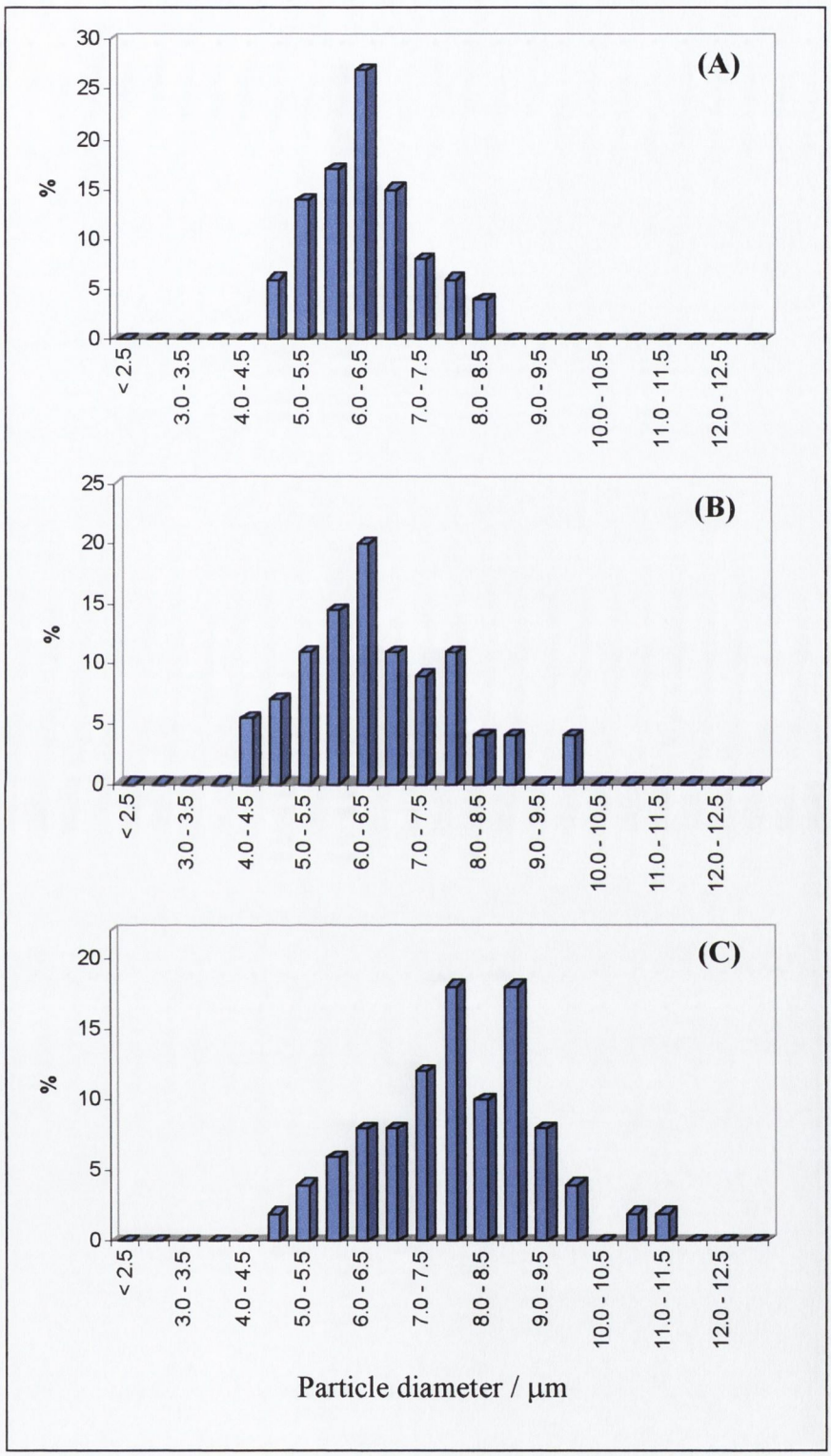

Figure 2.8 Star-like ZnO particle diameter after (A) 2 hours, (B) 5 hours and (C) 8 hour ageing.

Table 2.2 Effect of ageing time on ZnO star-like particle size.

Pre-stirring time (hours)	Ageing time (hours)	Average particle diameter (μm)	Particle diameter distribution (μm)	Yield (± 5%)
0	2	6.3	4.5 – 8.5	0.486 g / 60 %
0	5	6.5	4.0 – 10.0	0.633 g / 78 %
0	8	7.7	4.5 – 11.5	0.523 g / 64 %

2.3.2 Effect of reactant concentrations on ZnO star-like particles.

The concentrations of zinc nitrate and NaOH were varied to examine the effect of each on the system. Table 2.3 outlines the concentration changes and the resultant morphologies. All samples showed XRD patterns consistent with the ZnO (zincite) structure.

Table 2.3 Effects of concentration changes on the ZnO morphology produced when $Zn(NO_3)_2.6H_2O$ and NaOH are aged for 5 hours.

$[Zn(NO_3)_2.6H_2O]$ mol dm^{-3}	[NaOH] mol dm^{-3}	Morphology	Yield
0.02	1	----	----
0.04	1	Star-like	0.691 g / 84 %
0.08	1	Spherical, filled star-like	1.59 g / 98 %
0.04	0.5	Spherical, platelet aggregations	0.794 g / 98 %
0.04	2	----	----

--- indicates no precipitate formed.

Examples of the two spherical type structures reported in Table 2.3 can be seen in Figure 2.9. (A) and (B) represent samples formed when the zinc nitrate concentration is doubled (0.08 M) and (C) and (D) show particles prepared when the sodium hydroxide concentration is halved (0.5 M).

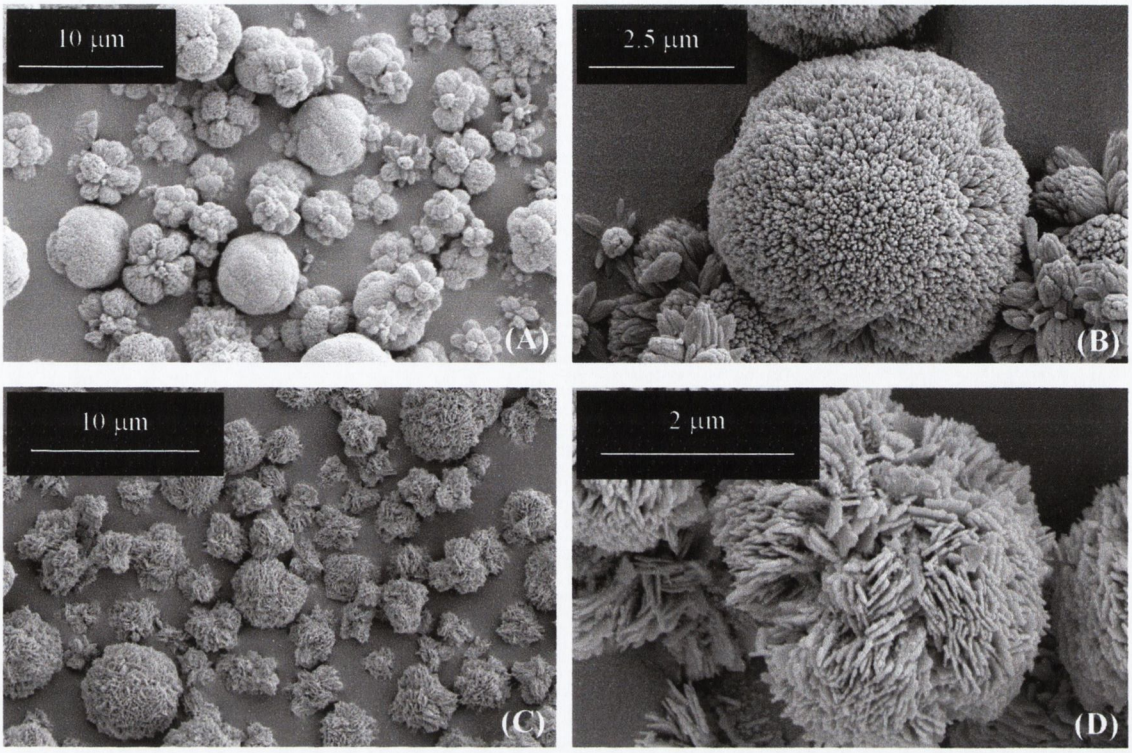

Figure 2.9 SEM images of ZnO particles formed from (A) & (B) 0.08 M $Zn(NO_3)_2.6H_2O$ and 1 M NaOH and (C) & (D) 0.04 M $Zn(NO_3)_2.6H_2O$ and 0.5 M NaOH, aged for 5 hours.

In an attempt to further fill the spherical type particles shown in Figure 2.9 A & B and form solid spheres, the concentration of the zinc salt was again increased to 0.1 M. This resulted in particles similar to those formed when 0.08 M zinc nitrate was used. Therefore, a further experiment was carried out where excess zinc nitrate was added to the solution after the formation of the filled star-like particles. It was hoped that this extra Zn^{2+} in solution would result in further growth rather than more nucleation. Zinc nitrate (0.08 M) was mixed with NaOH (1 M) and aged for two hours. After two hours, enough solid $Zn(NO_3)_2.6H_2O$ was added to double the remnant concentration of Zn^{2+} in the solution. A sample of the powder after 2 hours, i.e. before addition of the extra $Zn(NO_3)_2.6H_2O$ and also after 5 hours ageing can be seen in Figure 2.10. It is observed that rather than forming completed spheres, the addition of extra Zn^{2+} to the system results in the aggregation of the filled star-like particles.

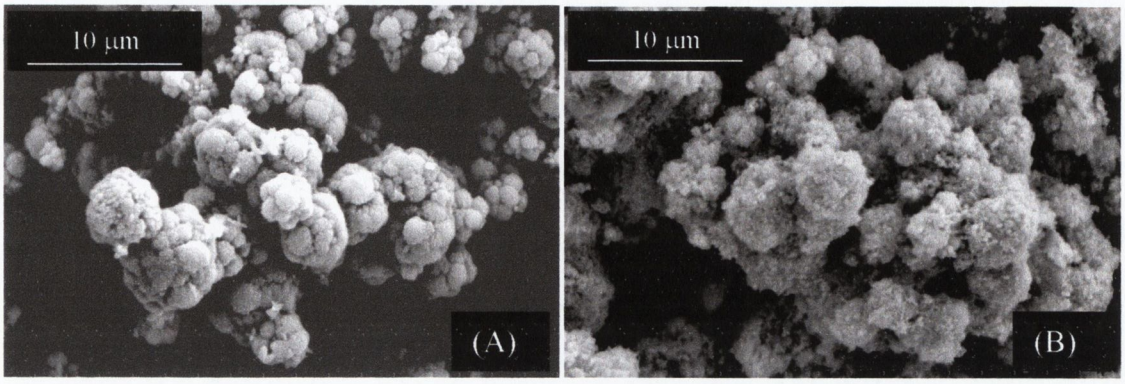

Figure 2.10 SEM images of ZnO formed when $Zn(NO_3)_2.6H_2O$ (0.08 M) and NaOH (1 M) are added together and (A) aged for two hours and (B) aged for a further 3 hours after the addition of solid $Zn(NO_3)_2.6H_2O$.

2.3.3 Effect of zinc salt counter-ion on ZnO star-like particles.

In order to determine the influence, if any, of the zinc counter-ion on the formation of the star-like morphology, the zinc salt used was altered. Zinc nitrate was substituted by the chloride and sulphate under identical reaction conditions. Table 2.4 outlines the morphology and composition of the samples obtained for each salt. The crystallinity of the uniform needle-like particles prepared from zinc nitrate is higher than those of the non-uniform zinc sulphate and chloride products.

Table 2.4 Morphology and composition of samples obtained when different zinc salt solutions (0.04 M) are aged with NaOH (1 M) for five hours.

Zinc salt	Morphology	Composition
Nitrate	Star-like	ZnO, zincite
Sulphate	Non-uniform	ZnO, zincite
Chloride	Non-uniform	ZnO, zincite

Figure 2.11 shows the SEM images of the particles obtained when zinc chloride and zinc sulphate was used in place of the nitrate salt.

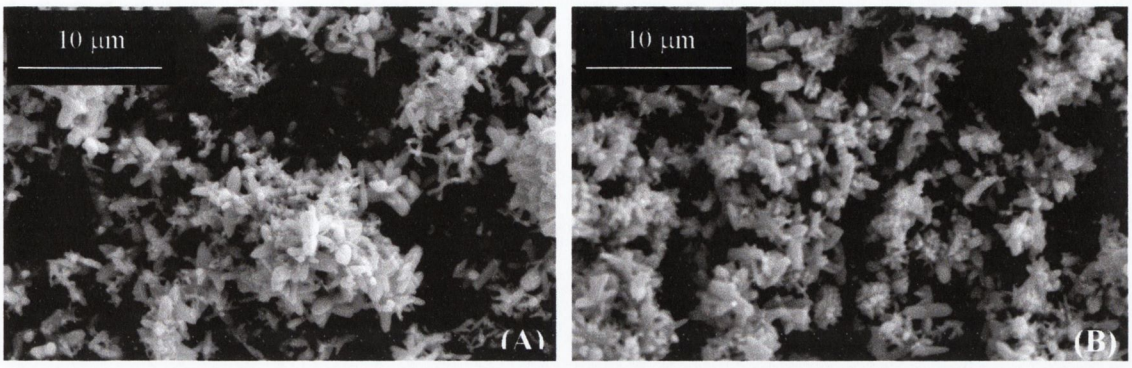

Figure 2.11 SEM of ZnO particles formed from (A) zinc sulphate (0.04 M) and (B) zinc chloride (0.04 M) aged with NaOH (1 M) for 5 hours.

2.4 DISCUSSION

When the zinc nitrate and sodium hydroxide solutions were added together and heated to reflux, turbidity was observed after approximately 10 – 15 minutes. As the temperature of precipitation was at least 55°C, the crystalline structure of the particles formed was expected to be ZnO and was found to be so, consistent with the JCPDS[8] library data for hexagonal ZnO, zincite (see Appendix I).

SEM was used to follow the growth of these particles over two hours ageing in the solution. As can be seen from Figure 2.6, the particles precipitate with a diameter of approximately 3.5 μm (those removed at turbidity). At precipitation and up to ten minutes after precipitation, some rhombic $Zn(OH)_2$ particles can be seen, however these particles are very scarce and have disappeared from the sample after 15 minutes of heating, as the temperature increases above 70 °C. Figure 2.6 B shows the particles five minutes after precipitation. The size distribution has now increased, with particles of approximately 3.5 to 8 μm in diameter present. The average particle diameter is in the order of 6 μm. It is clear therefore that particles present in solution are beginning to grow but also that nucleation is still taking place. As none of the components of the

reaction are being slowly released into solution by means of a reservoir, it is expected that several nucleation events will take place.

After 10 minutes (Figure 2.6 C), the largest particles observed have an average diameter of 8 μm and there are also smaller particles present, with diameters of less than 4 μm. After 30 minutes, the average particle diameter is still approximately 6 μm, however, the distribution of particle diameters has decreased slightly, with the smallest particles now being 4 μm. As the particles grow, XRD shows an increase in crystallinity of the sample up to 30 minutes (Figure 2.5). From 30 to 120 minutes, no notable change in the average particle size or in sample crystallinity is observed. At 2 hours ageing, the dimensions of the particles are now 4.5 – 8.5 μm in diameter, with an average size of 6.3 μm.

These observations, that precipitation sized particles (~ 3.5 μm) are in existence for heating times less than 30 minutes, implies that nucleation is taking place up to that point. By not providing a reservoir for any component of the reaction, a number of nucleation events appear to occur. From 30 to 120 minutes the average particle size does not increase to any great extent, nor are any new particles seen to form.

By examining the titration curve (Figure 2.7), it is evident that the concentration of Zn^{2+} in solution decreases rapidly up to 30 minutes, from 0.025 M to 0.006 M. After that time, the drop in concentration is significantly lower and after 40 minutes heating, the concentration of Zn^{2+} in solution has levelled off at approximately 0.0044 M. This result concurs with what is seen with the particle sizes. While nucleation is taking place, the concentration of Zn^{2+} drops rapidly. However, when the particle growth has slowed considerably, the change in concentration is almost zero. The solubility of ZnO in a 0.375 M sodium hydroxide solution is 0.004 M at 25 °C[9]. The levelling off concentration that is observed in Figure 2.7 is slightly higher than this, as expected due to the higher temperature. That is, the samples are filtered hot and the reaction is

quenched therefore at approximately 70 to 80 °C. The levelling off of the Zn^{2+} concentration at approximately solubility, means that there is only a small amount of Zn^{2+} ions available for growth. Hence, for the particles to significantly increase in size, dissolution / re-precipitation must occur and consequently, a significant increase in particle size beyond 30 – 40 minutes heating is not observed.

It would appear that the growth of these star-like ZnO particles follows neither the LaMer[10] nor the aggregation growth[11] theories, as outlined in Chapter 1 (section 1.5). Instead, the growth proceeds by a modified LaMer mechanism. Rather than nucleation taking place only once, several nucleation events take place. After first nucleation, the particles begin to grow by diffusion of the reactants through the solution to the surface of the growing particles. While this is taking place, second and subsequent nucleations occur. However, when a level below critical concentration is achieved, nucleation no longer takes place and growth of the particles occurs only by diffusion.

When particles grow by this mechanism self-sharpening[12] can be observed, as proposed by Den Ouden and Thompson.[13] They reported that towards the end of the ageing process for spherical α-Fe_2O_3 production, the distribution of particle sizes narrows significantly. Following the growth of star-like ZnO particles in this study, shows that the size distributions broaden rather than narrow as the reaction time is increased. Therefore, self-sharpening is not occurring in this case.

2.4.1 Formation of the ZnO star-like morphology.

As ZnO has a hexagonal lattice, with an *a:c* axial ratio of 1:1.6,[14] the most common morphologies observed are either rod-like or needle-like crystals, elongated in the c-axis direction and with hexagonal prismatic faces. However, as was discussed in Chapter 1 (section 1.5.5), crystal twinning is common. Although many crystalline compounds exhibit twinning consisting of two lattices growing from a common junction, zinc oxide

is the only inorganic compound which readily forms fourlings. These fourlings consist of four acicular spines united at a common base and approximately tetrahedral to each other.[15] These star-like ZnO particles were previously observed using hydrothermal methods, forced hydrolysis of zinc nitrate using HMT,[6] en[4, 16] and NH_4OH[3] and also by the decomposition of hydrozincite.[17] However, no reports to date have shown the formation of these particles using NaOH as the base in the hydrolysis system.

The star-like particles were also observed in ZnO smoke[18] and their morphology was studied in detail by Fuller,[19] using electron microscopy. He deduced that the ZnO particles twinned along the $(11\bar{2}2)$ planes to produce these so called fourlings. A simplified version of this twinning can be seen in Figure 2.12. Two hexagonal lattices (extended in the c-axis direction) are represented twinned along their $(11\bar{2}2)$ planes. A further two ZnO crystals would produce the fourling.

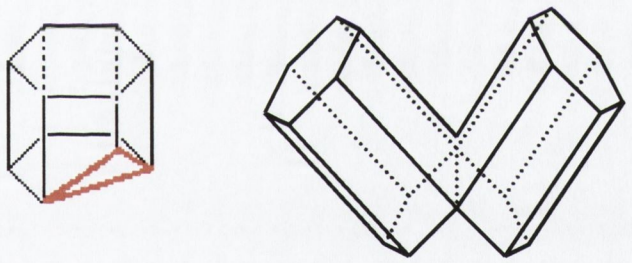

(A) **(B)**

Figure 2.12 Twinning of a hexagonal lattice along the $(11\bar{2}2)$ plane; (A) hexagonal lattice with $(11\bar{2}2)$ plane marked in red and (B) twinning of two hexagonal lattices along their $(11\bar{2}2)$ planes.

Each spine of the fourling is a ZnO crystal, elongated along the c-axis. Thin sheets (approximately 50 to 500 Å) can form between spines, with each sheet lying in the plane of two spines, similar to webbing. These sheets can then act as nuclei for further spines to grow. Fourlings can also grow together, binding along two spines and hence ideally having seven spines. An example of this structure can be seen in Figure 2.13.

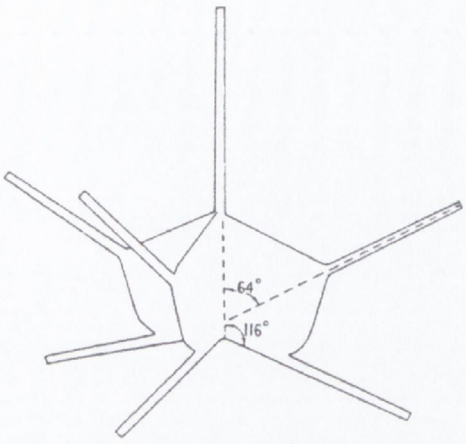

Figure 2.13 Idealized group of three sheets and seven spines, related by $(11\bar{2}2)$ twinning.[18]

However, many deviations from this ideal structure can occur. For example, only one sheet may be well developed resulting in missing spines or others can have a large portion of complex groups, resulting in many spines and sheets radiating from a central nucleus. It would appear from the results obtained that the latter case is evident in this study.

2.4.2 Effect of ageing time on star-like particles.

As was discussed earlier, after 2 hours ageing the star-like particles have an average diameter of 6.3 μm and range from approximately 4.5 – 8.5 μm in length. A study of prolonged ageing showed that after 5 hours ageing the average particle size, now 6.5 μm, had not increased significantly. The size distribution also increased only slightly to 4.0 –10.0 μm. After 8 hours, the average size increased to 7.7 μm and the size distribution had further increased, with the largest particles now 12.0 μm in diameter. It can therefore be concluded, that prolonged heating results in dissolution / re-precipitation taking place, accounting for the increase in particle sizes. No significant trend is observed in the yields obtained after different ageing times.

2.4.3 Effect of reactant concentrations on star-like ZnO particles.

Variations in the concentrations of the zinc nitrate and of the sodium hydroxide appear to have a marked effect on the particle morphology produced. By halving the zinc salt concentration or doubling the hydroxide concentration, no precipitate formed. This would suggest that the molar ratio of Zn^{2+} to OH^- in solution could be important, as well as the pH of the system. Table 2.5 outlines the changes in pH, molar ratio and particle morphology.

Table 2.5 Effect of reactant molar ratios on the formation of ZnO star-like particles.

[NaOH] mol dm^{-3}	[$Zn(NO_3)_2.6H_2O$] mol dm^{-3}	Moles OH^- in 150 ml	Moles Zn^{2+} in 250 ml	Molar ratio OH^- : Zn^{2+}	Calculated pH	ZnO Particle morphology
0.5	0.04	0.075	0.01	7.5 : 1	13.27	Spherical platelet aggregates
1	0.04	0.15	0.01	15 : 1	13.57	Star-like
2	0.04	0.3	0.01	30 : 1	13.87	----
1	0.08	0.15	0.02	7.5 : 1	13.57	Spherical filled stars
1	0.02	0.15	0.005	30 : 1	13.57	----

When a 1 M NaOH stock solution is used, it is diluted to 0.375 M by addition to the $Zn(NO_3)_2.6H_2O$ solution. This would theoretically result in a reaction mixture of pH 13.57. By altering the zinc concentration the following effects are observed; 0.04 M gives star-like particles, 0.08 M gives spherical filled star-like particles, whereas 0.02 M gives no product. At the highest molar ratio (30 : 1), no precipitate is formed, as it is decreased to 15 : 1 star-like particles form and a further decrease to 7.5 : 1 results in the star-like particles becoming filled to form almost spherical particles.

If the concentration of zinc nitrate is kept constant and the hydroxide concentration is altered, both the pH and molar ratios change. A 2 M NaOH solution gives a pH of 13.87, a 30 OH^- : 1 Zn^{2+} ratio and no precipitate. A 0.5 M NaOH solution gives a final pH of 13.27, a ratio of 7.5 OH^- : 1 Zn^{2+} and aggregated platelet type particles. Therefore rather than a certain pH resulting in no precipitate, it appears that it is a 30 : 1 molar ratio of hydroxide to zinc cation leads to no precipitate forming. Similarly, the cases which result in the lower ratio of 7.5 : 1 give the large spherical type products.

The decrease in OH^- concentration to 0.5 M gives large spherical type particles. In this case however, the particles do not show the expected spines forming the star-like particles. Rather, aggregated platelet type particles result. This morphology is formed because the initial precipitate of ZnO, which forms when a small amount of NaOH is added to the zinc solution, never re-dissolves. The final concentration of OH^- never reaches a high enough level to cause the first ZnO precipitate to dissolve and so precipitation of ZnO star-like particles does not take place at around 55 – 60 °C as it does for the other samples. The final particles are a result of continued growth of these initial particles. By comparing Figures 2.4 and 2.9 C, it is evident that the original morphology is largely retained.

A high concentration of zinc nitrate results also results in spherical type particles, this time caused by filling in of the star-like particles, Figure 2.9 (A) & (B). This is a dendritic[20] growth process. The twinned particles form re-entrant corners that are favourable to further nucleation and growth. Between the spines of the star-like particles new growth sites are encouraged, which causes this filling in, resulting in the formation of the almost spherical particles. Although the molar ratio is the same as the case above, the pH means the initial ZnO phase dissolves and the second precipitate of star-like ZnO takes place.

In an attempt to completely fill these particles, a solution of 0.1 M zinc nitrate was used. This however resulted in similar particles forming. The high concentrations of zinc cation present at precipitation simply results in the formation of more nuclei, which grow into filled stars, rather than there being enough Zn^{2+} present to completely fill the stars. In an attempt to overcome this, a sample of filled stars was grown from a 0.08 M solution of $Zn(NO_3)_2.6H_2O$. After two hours ageing, when all nucleation should have been completed, the concentration of Zn^{2+} was increased by addition of zinc nitrate. This however resulted in aggregation of the filled star-like particles already formed (Figure 2.10). In the experiments where the OH^- concentration was doubled or the Zn^{2+} concentration was halved, the high relative concentration of hydroxide ion in solution appears to inhibit the precipitation of ZnO.

2.4.4 Effect of zinc salt counter-ion on star-like ZnO particles.

A change in zinc salt counter-ion is seen to have a noticeable effect on the morphology of the ZnO. Figure 2.11 shows that although the needle-like particles, which make up the spines of the stars, are present when zinc sulphate or chloride are used in place of zinc nitrate, they form non-uniform aggregates. Also, the crystallinity of the samples formed from zinc sulphate and chloride are not as good as that of the zinc nitrate product. It can be assumed therefore that nitrate ion plays a role in the formation of the star-like particles. In previous studies, the counter-ion effect is explained by the adsorption of the anions onto the surface of the growing particles.[21] By preventing growth at some surfaces, the particles grow only in certain directions and hence the final morphology is determined.

In this ZnO system studied, the nitrate anion appears to have an effect on the twinning of ZnO hexagonal lattice. Adsorption of the nitrate ion onto a surface of the growing ZnO nuclei would prevent growth in the direction of that surface, causing strain on the growing crystal and hence encouraging twinning to take place. If this is the case, the sulphate and chloride ions must not adsorb onto the crystal in this preferential manner.

PART 2 – GROWTH OF NEEDLE-LIKE ZnO – (PATH B)

2.5 RESULTS

The second pathway the reaction can follow (Figure 2.1) is that which results in the formation of needle-like ZnO. $Zn(NO_3)_2.6H_2O$ (0.04 M) and NaOH (1 M) are added together and stirred at room temperature prior to ageing. Consequently, the precipitate forming after 10 to 15 minutes is rhombic $Zn(OH)_2$. The suspension of these $Zn(OH)_2$ particles are then subjected to ageing (heating to reflux temperature and holding the solution at that temperature). After ageing the particles are found to be ZnO with a needle-like morphology.

2.5.1 Growth of rhombic $Zn(OH)_2$ particles.

If the NaOH / $Zn(NO_3)_2.6H_2O$ reaction mixture is stirred at room temperature, after approximately 10 to 15 minutes a precipitate forms. This precipitate has been identified as $Zn(OH)_2$, with a rhombic morphology. The growth of these particles was studied by sampling the reaction mixture over 2 hours stirring at room temperature. Figure 2.14 shows the XRD patterns obtained for the samples withdrawn at regular intervals throughout the reaction. All patterns are consistent with $Zn(OH)_2$ (wulfingite, Appendix II). Between 15 and 30 minutes the crystallinity of the particles is seen to improve, with no significant change occurring after that time.

After the particles were removed, the filtrate was retained and titrated against EDTA to determine the concentration of Zn^{2+} remaining in solution. Figure 2.15 shows the concentration profile obtained for the 2-hour stirring reaction.

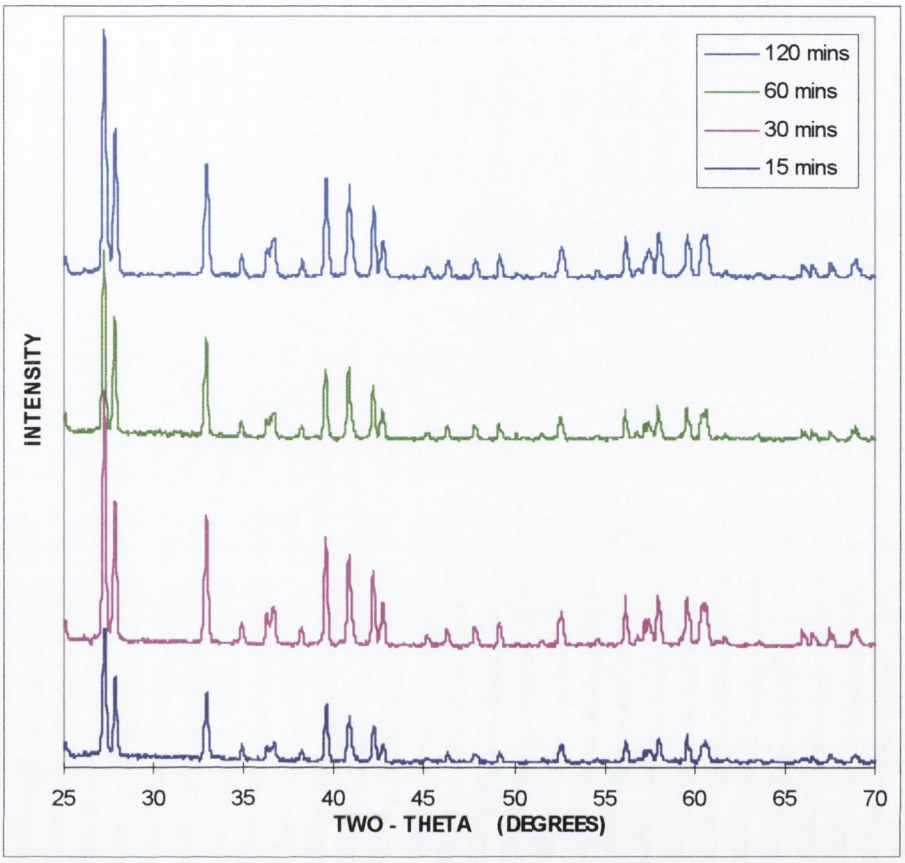

Figure 2.14 XRD patterns for $Zn(OH)_2$ particles prepared by stirring NaOH (1 M) with $Zn(NO_3)_2.6H_2O$ (0.04 M) at room temperature for 15, 30, 60 and 120 minutes.

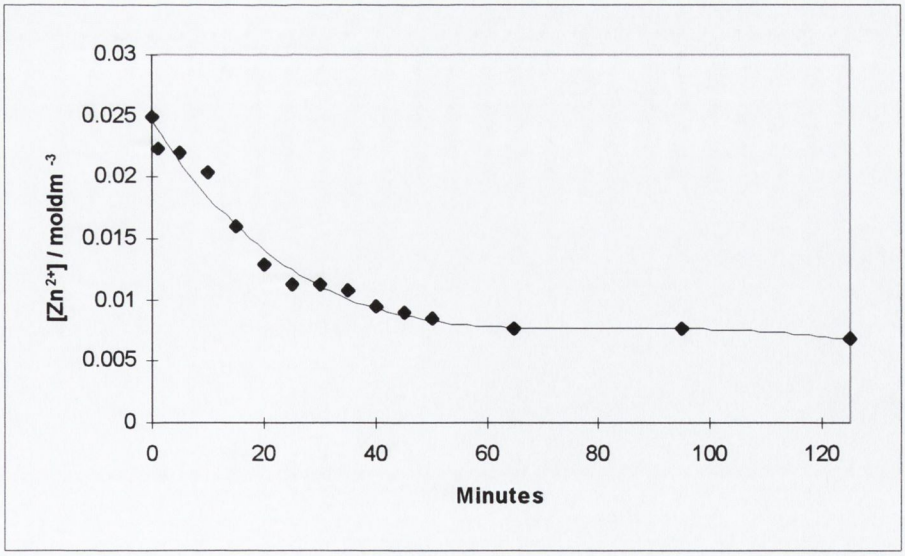

Figure 2.15 $[Zn^{2+}]$ profile for NaOH (1 M) and $Zn(NO_3)_2.6H_2O$ (0.04 M), stirred at room temperature for 125 minutes.

The growth of the $Zn(OH)_2$ was also followed by SEM. Figure 2.16 shows particles withdrawn from the dispersion at various intervals. The particles are seen to precipitate with a rhombic morphology, gradually getting larger and more uniform with time; increasing from around 5 μm at precipitation to approximately 10 μm in size after 2 hours.

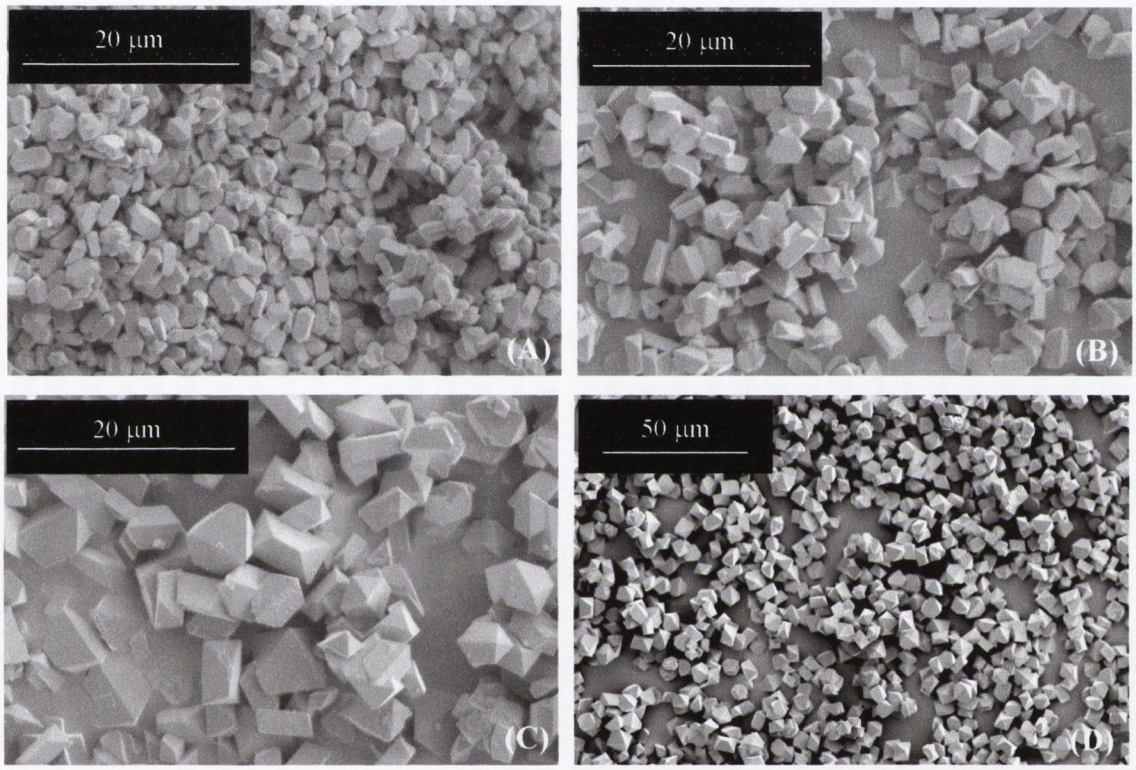

Figure 2.16 Growth of $Zn(OH)_2$ particles prepared by stirring NaOH (1 M) and $Zn(NO_3)_2.6H_2O$ (0.04 M) together at room temperature (A) at precipitation and for (B) 30 minutes, (C) 45 minutes and (D) 120 minutes after precipitation.

In order to further characterise the rhombic $Zn(OH)_2$ particles, differential scanning calorimetry (DSC) was carried out on a sample prepared by stirring $Zn(NO_3)_2.6H_2O$ (0.04 M) with NaOH (1 M) for two hours. The temperature was ramped at 10 °C / min. from -50°C to 300°C. After the scan was completed, the sample was quench cooled in the chamber and a second scan was carried out. Figure 2.17 shows the two DSC scans. The two peaks that are visible in the first scan at 136 and 256 °C, do not appear in the

second scan. These peaks are thought to be related to H_2O loss from the $Zn(OH)_2$ lattice. As no peak is visible at 0 °C, neither peak is not attributed to the loss of bulk water.

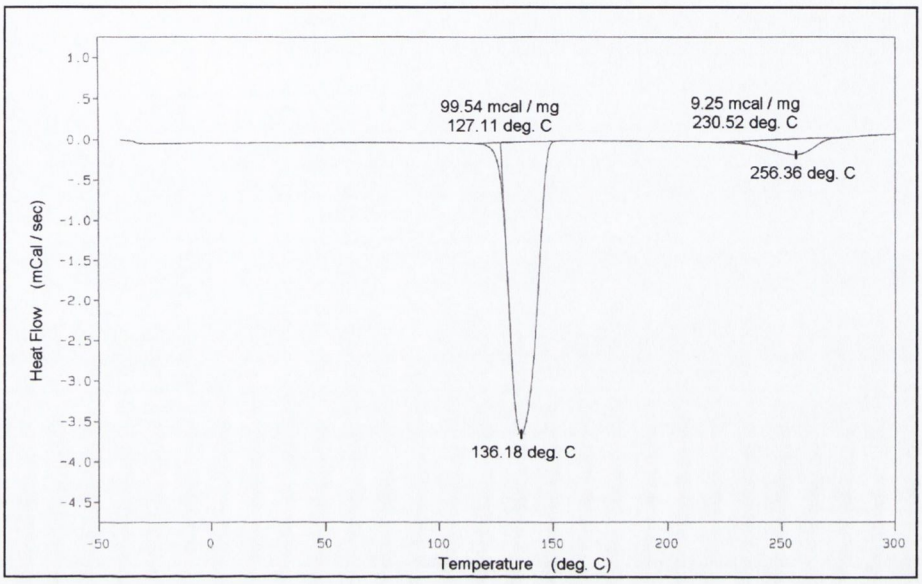

Figure 2.17 DSC of $Zn(OH)_2$ sample, first and second scan.

2.5.2 Effect of pre-stirring time.

As was seen above, stirring the sodium hydroxide and zinc salt solutions together, results in the formation of $Zn(OH)_2$ particles. When heating is then carried out on these particles suspended in the mother liquor, ZnO needle-like particles are formed. The effect of the pre-stirring was examined not only with respect to the morphology of the final particles but also their dimensions. Size distributions were determined using light microscopy. Table 2.6 outlines the effect of pre-stirring on the resultant particles.

Table 2.6 Effect of pre-stirring on particle size, morphology and crystalline phase when $Zn(NO_3)_2.7H_2O$ (0.04 M) is treated with NaOH (1 M) and aged for two hours.

Pre-stirring time (hours)	Precipitation temperature (°C)	Precipitated crystalline phase and morphology	Final crystalline phase and morphology	Final particle length distribution (μm)	Final particle width distribution (μm)
0	55 – 60	Star-like ZnO	Star-like ZnO	4.5 – 8.5	-----
1	20 – 25	Rhombic $Zn(OH)_2$	Needle ZnO	2.5 – 8.3	0.7 – 1.5
2	20 – 25	Rhombic $Zn(OH)_2$	Needle ZnO	2.5 – 7.0	0.6 – 1.3
5	20 – 25	Rhombic $Zn(OH)_2$	Needle ZnO	2.5 – 8.0	0.6 – 1.2
24	20 – 25	Rhombic $Zn(OH)_2$	Needle ZnO	3.0 – 9.5	0.7 – 1.4

It can be seen that no pre-stirring results in the precipitation of star-like ZnO, as was discussed in section 2.3. Pre-stirring always results in the formation of $Zn(OH)_2$ rhombic particles and their subsequent decomposition to form ZnO on heating. However, the length of time for which pre-stirring is carried out appears to have a slight effect on the dimensions of the needle-like ZnO formed. As the most uniform sample of needle-like particles was formed from 2 hours pre-stirring, these were the conditions employed for all of the needle-like particle formation studies.

2.5.3 Growth of needle-like ZnO from rhombic $Zn(OH)_2$.

In this study it can be shown that needle-like ZnO can be produced by the thermal decomposition of the $Zn(OH)_2$ rhombic particles in an alkaline suspension. $Zn(NO_3)_2.6H_2O$ (0.04 M) and NaOH (1 M) were stirred together for two hours and then aged for given times. Reflux temperature is reached after 30 – 35 minutes.

Samples were withdrawn at various times through the reaction to study the growth of the particles. Figure 2.18 shows the XRD patterns of samples withdrawn for up to 60 minutes ageing and Figure 2.19 shows the SEM images of the same samples.

XRD clearly shows the transformation from $Zn(OH)_2$ to ZnO taking place between 30 and 60 minutes. The pattern for $Zn(OH)_2$ decreases in intensity, simultaneously with the appearance of ZnO peaks, which gradually become dominant until $Zn(OH)_2$ is no longer evident.

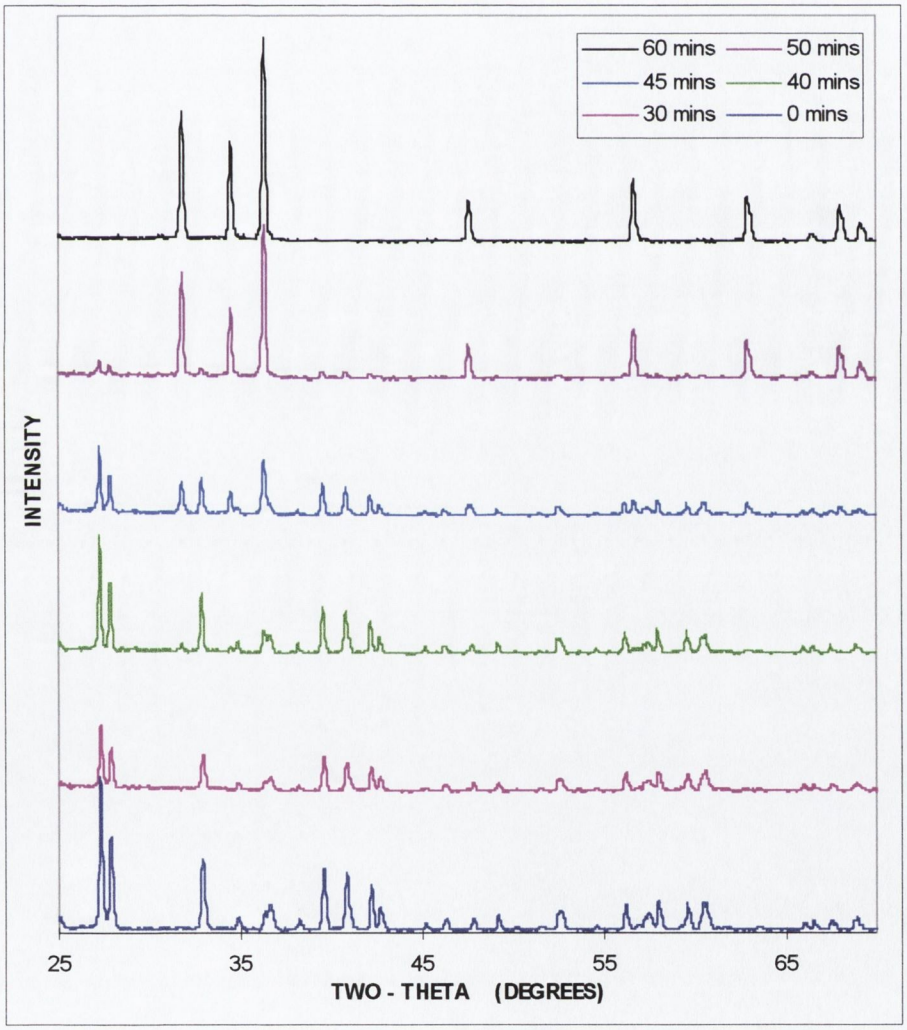

Figure 2.18 XRD patterns for growth of ZnO needle-like particles by thermal decomposition of $Zn(OH)_2$ rhombic particles.

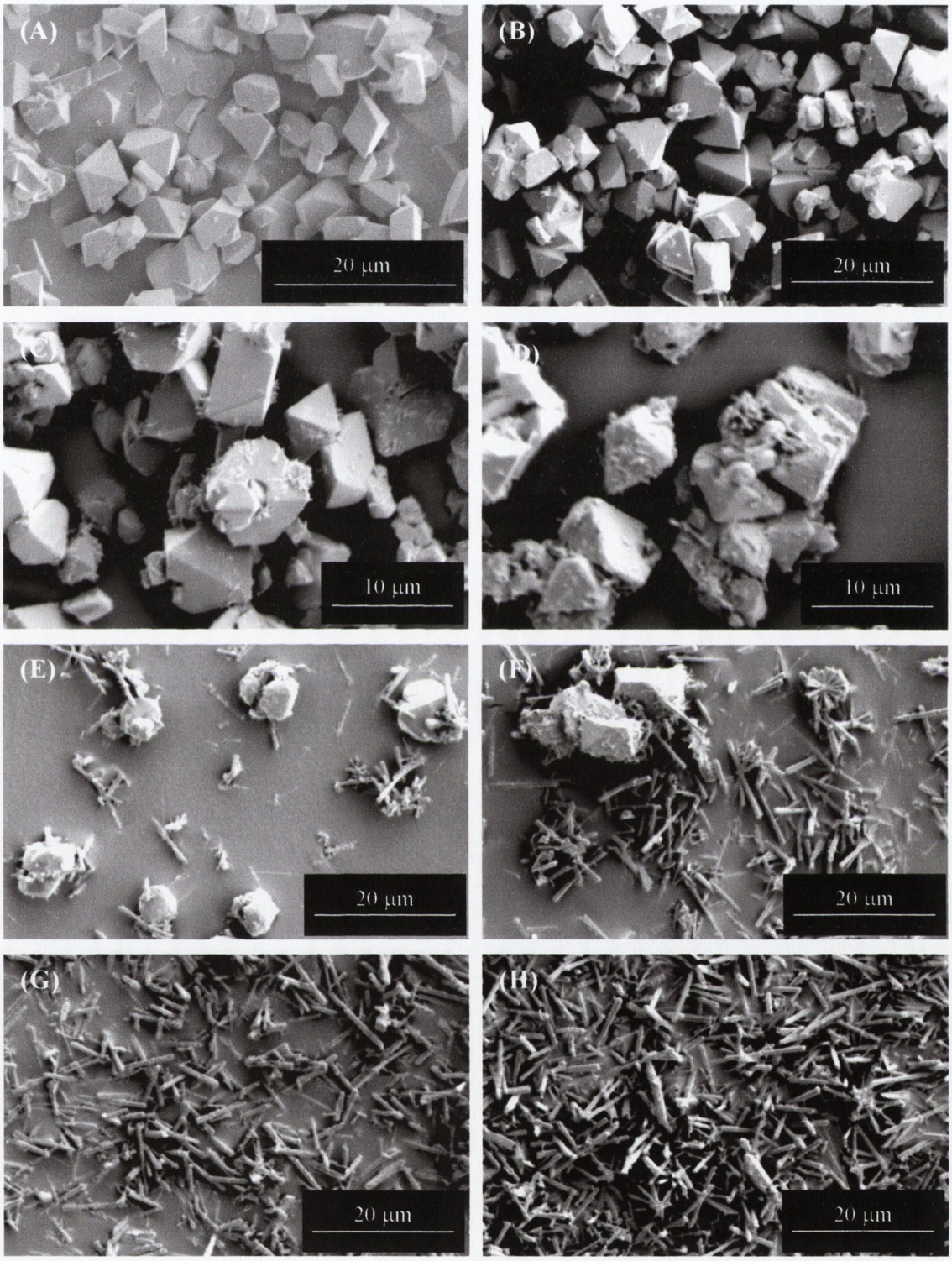

Figure 2.19 Growth of needle-like ZnO by thermal decomposition of $Zn(OH)_2$. $Zn(NO_3)_2.6H_2O$ (0.04 M) and NaOH (1 M) stirred for two hours followed by (A) 0 minutes, (B) 30 minutes, (C) 35 minutes, (D) 40 minutes, (E) 45 minutes, (F) 50 minutes, (G) 55 minutes and (H) 60 minutes ageing.

Raman spectroscopy was used to distinguish between ZnO and $Zn(OH)_2$ in the mixed samples. Figure 2.20 shows spectra for a sample of pure rhombic $Zn(OH)_2$ (Figure 2.19A above) and of only needle-like ZnO (Figure 2.19H above). These spectra were then used as standards.

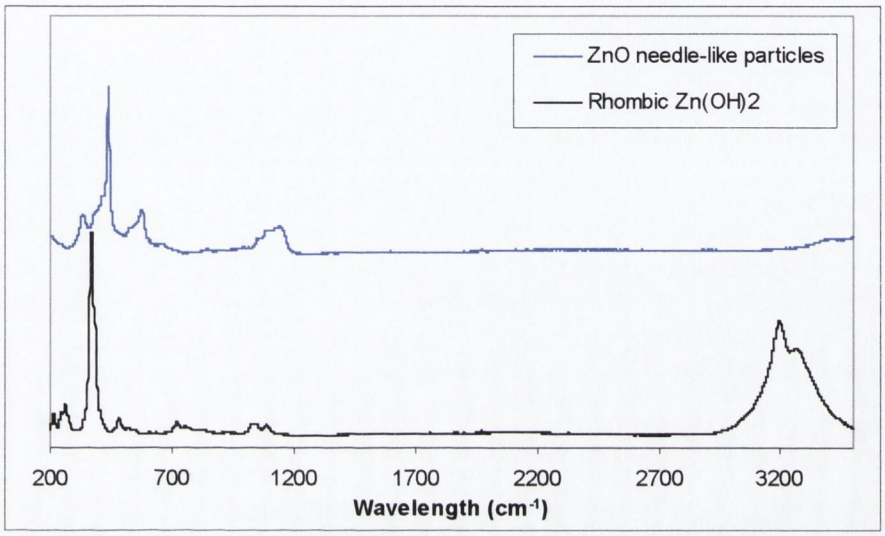

Figure 2.20 Raman spectra of ZnO needle-like particles and $Zn(OH)_2$ rhombic particles.

Using light microscopy, an individual particle can be pinpointed, the spectrum for which can then be acquired. Using a mixed sample (Figure 2.19 D above), a rhombic particle was isolated (Figure 2.21 A), followed by a needle-like particle (Figure 2.21 B) and both spectra were recorded. The spectra (seen in Figure 2.22) can be compared to the standard spectra above and be used confirm the particle composition for each morphology.

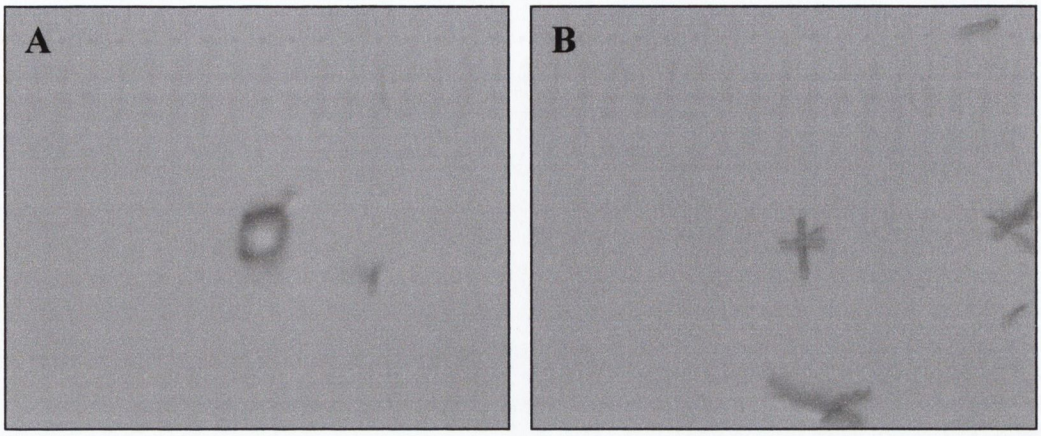

Figure 2.21 (A) Rhombic particle and (B) needle-like particle isolated under a light microscope, from a mixed sample of ZnO and $Zn(OH)_2$ represented in Figure 2.19A above; particles prepared from $Zn(NO_3)_2.6H_2O$ (0.04 M, 250 ml) and NaOH (1 M, 150 ml), stirred at room temperature for two hours followed by 40 minutes ageing.

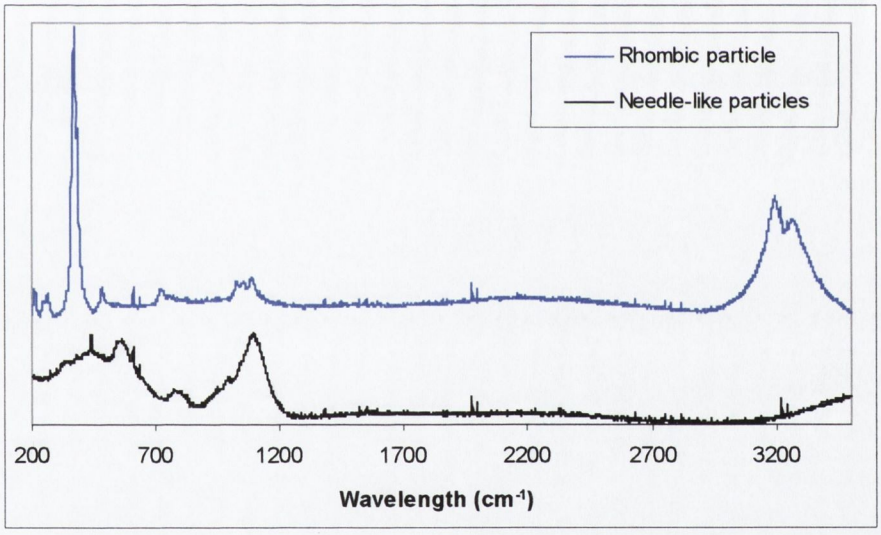

Figure 2.22 Raman spectra of samples represented in Figure 2.21 above, mixed ZnO and $Zn(OH)_2$ particles prepared from $Zn(NO_3)_2.6H_2O$ (0.04 M, 250 ml) and NaOH (1 M, 150 ml), stirred at room temperature for two hours followed by 40 minutes ageing.

After the samples were withdrawn from the reaction, the filtrate was retained and titrated against EDTA, to determine the concentration of Zn^{2+} remaining in solution. Figure 2.23 shows the concentration profile obtained.

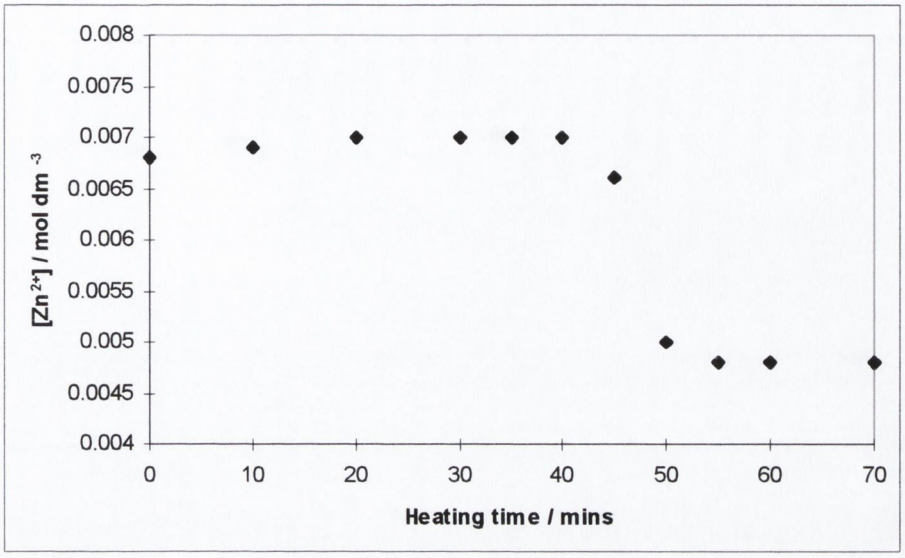

Figure 2.23 $[Zn^{2+}]$ profile for NaOH (1 M) and $Zn(NO_3)_2.6H_2O$ (0.04 M), aged for 70 minutes after 2 hours pre-stirring at room temperature.

2.5.4 Effect of ageing times on needle-like ZnO particle formation.

The length of time for which the solution is aged was varied in order to determine the effect of ageing time on the resultant needle-like particles. Table 2.7 outlines the yield and dimensional changes of the particles with increased ageing time. Yields are calculated based on a 100% ZnO composition.

Table 2.7 Effect of ageing time on needle-like ZnO production.

Heating time (hours)	Mean width	Width distribution	Mean length	Length distribution	Yield (± 5 %)
5	1.0 μm	0.6 – 1.3 μm	4.5 μm	2.5 – 7.5 μm	0.73 g / 89 %
8	0.9 μm	0.6 – 1.2 μm	5.0 μm	3.0 – 8.0 μm	0.62 g / 76 %
15	1.1 μm	0.6 – 1.5 μm	5.1 μm	3.0 – 8.5 μm	0.72 g / 89 %
24	1.0 μm	0.6 – 1.4 μm	6.4 μm	3.0 – 9.5 μm	0.71 g / 87 %

Figure 2.24 shows the particle length distributions for the needle-like particles reported in Table 2.7. The distribution is seen to increase slightly with time and the average particle length also increases gradually. The width distribution does not appear to be affected by ageing time.

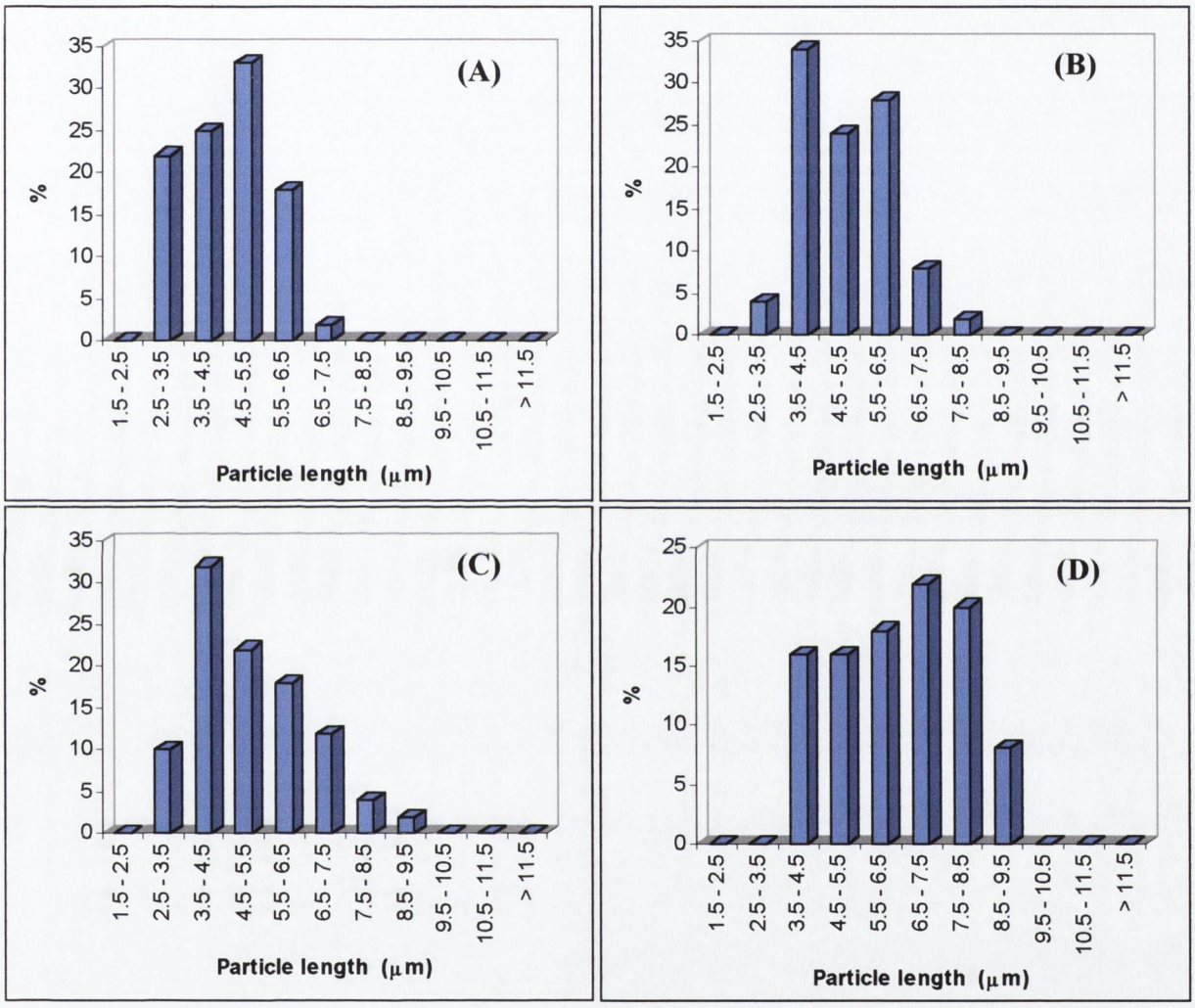

Figure 2.24 Needle-like particle length distribution after (A) 5, (B) 8, (C) 15 and (D) 24 hours ageing.

2.5.5 Effect of reactant concentrations on needle-like ZnO particles.

The concentration of both the zinc nitrate and the sodium hydroxide were altered to examine their effect on the particles formed. Table 2.8 outlines the effect of

concentration on the morphology of the particles and Figure 2.25 shows two of the morphologies produced.

Table 2.8 Effect of reactant concentrations on ZnO particles produced by stirring $Zn(NO_3)_2.6H_2O$ and NaOH for two hours followed by five hours ageing.

$[Zn(NO_3)_2.6H_2O]$ mol dm^{-3}	[NaOH] mol dm^{-3}	Morphology	Yield (± 5 %)
0.04	0.5	Spherical platelet aggregates	0.79 g / 97 %
0.04	2	Needle-like	0.01 g / 7 %
0.04	1	Needle-like	0.73 g / 90 %
0.02	1	Needle-like	0.24 g / 58 %
0.08	1	Needle-like	1.41 g / 87 %

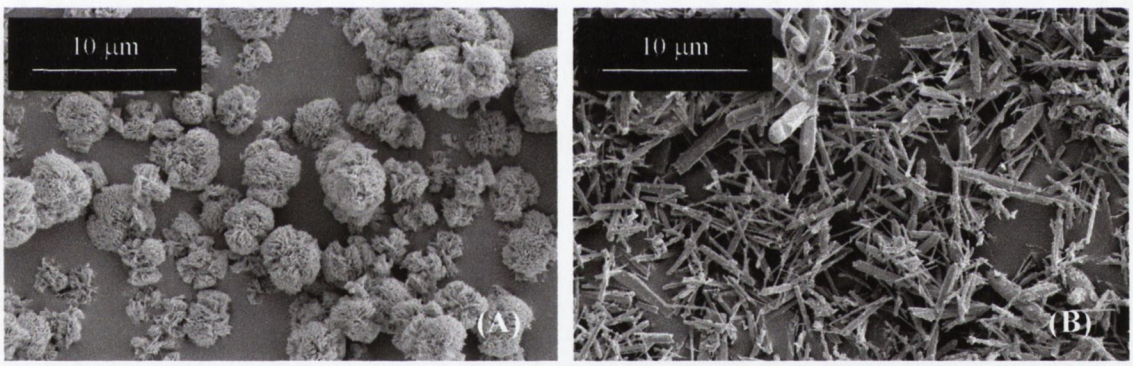

Figure 2.25 ZnO particles produced when (A) $Zn(NO_3)_2.6H_2O$ (0.04 M) and NaOH (0.5 M) and (B) $Zn(NO_3)_2.6H_2O$ (0.08 M) and NaOH (1 M), are stirred for 2 hours then aged for 5 hours.

2.5.6 Effect of zinc salt counter-ion on needle-like ZnO particles.

In order to determine the effect of zinc counter-ion on the morphology of the ZnO particles, identical reactions were carried out, varying only the zinc salt used. The morphology and composition of the particles produced when zinc sulphate or zinc chloride is substituted for zinc nitrate is shown in Table 2.9. Zinc chloride results in a sample similar to that produced from zinc nitrate. However, zinc sulphate gives a highly disperse sample.

Table 2.9 Morphology and composition of samples obtained when different zinc salt solutions (0.04 M) and NaOH (1 M) are stirred for two hours then aged for five hours.

Zinc salt	Morphology	Particle sizes	Composition
Nitrate	Needle-like	2.5 – 7.5 μm	ZnO, zincite
Sulphate	Needle-like	Highly disperse	ZnO, zincite
Chloride	Needle-like	2.0 – 8.5 μm	ZnO, zincite

Figure 2.26 shows the particles produced when (A) zinc sulphate and (B) zinc chloride is stirred with NaOH for 2 hours at room temperature then aged for 5 hours.

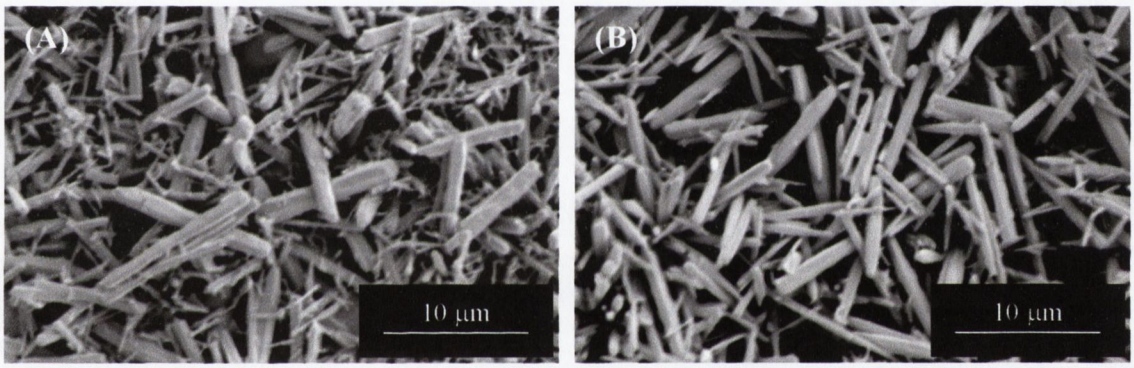

Figure 2.26 ZnO particles prepared from (A) $ZnSO_4.7H_2O$ and (B) $ZnCl_2$ (0.04 M) and NaOH (1 M) stirred for 2 hours and aged for 5 hours.

2.5.7 Band gap determination.

In order to further characterise the ZnO samples prepared and to compare their properties to those achieved by industrial preparations (e.g. burning zinc vapour), band gap measurements were carried out. Using UV/vis. reflectance spectroscopy with a $BaSO_4$ reference, the band gaps were determined. The spectra obtained and their estimated band edges are seen in Figure 2.27. The band edge for needle-like ZnO was found to be approximately 3.4 eV and star-like ZnO gave a similar spectrum, also with a

band gap of 3.4 eV. This is in agreement with literature, which quotes a value of 3.4 eV for bulk ZnO.[22]

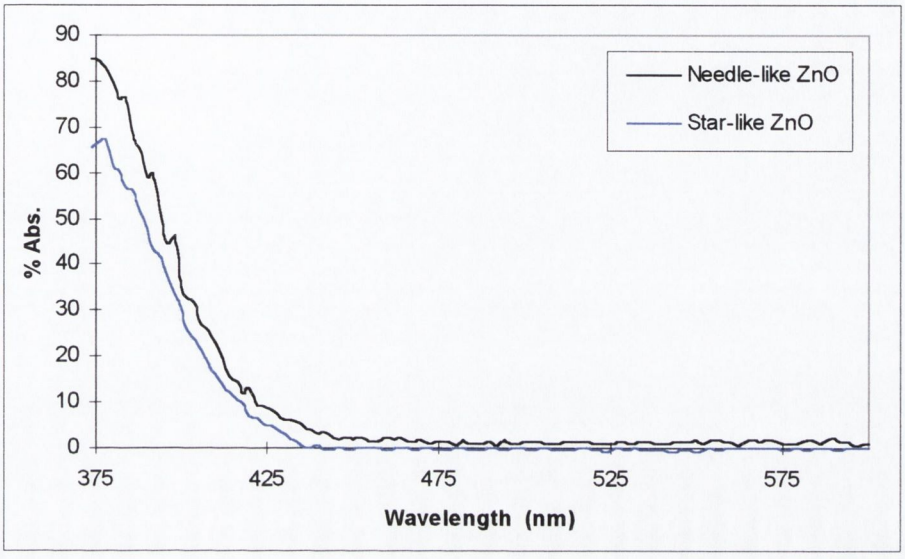

Figure 2.27 UV/vis. reflectance spectra of $Zn(OH)_2$ and needle-like ZnO.

2.6 DISCUSSION

In the second of the two methods studied, a room temperature stirring step is carried out prior to heating. The $Zn(NO_3)_2.6H_2O$ (0.04 M, 250 ml) and NaOH (1 M, 150 ml) are added together and after approximately 10 minutes at room temperature, a white precipitate of $Zn(OH)_2$ forms. This $Zn(OH)_2$ then undergoes a transformation to needle-like ZnO during the heating stage of the procedure. The growth of both the $Zn(OH)_2$ particles and of the needle-like ZnO is examined.

2.6.1 Growth of $Zn(OH)_2$ rhombic particles.

After the initial precipitate of ZnO dissolves (section 2.2.2), a second precipitate forms within approximately 10 minutes. At room temperature, this second phase precipitated from the zinc nitrate / NaOH solution was characterised as $Zn(OH)_2$

(wulfingite). This is in agreement with the results found for the precipitation studies, (section 2.2.1). Over the course of two hours stirring at room temperature, the crystalline structure of the particles remains unchanged but becomes more crystalline up to 30 minutes. Neither Chittofrati and Matijevic[2] nor O'Brien and co-workers,[4] both of whom studied zinc nitrate / sodium hydroxide systems, stirred their solutions prior to the formation of ZnO particles and hence did not report the formation of $Zn(OH)_2$ particles. In many of the cases where inorganic base hydrolysis is carried out on metal ions, organic bases are added as complexing agents to prevent the formation of the $Zn(OH)_2$ phase.[3]

The $Zn(OH)_2$ particles precipitate after around 10 minutes stirring at room temperature with a rhombic morphology (Figure 2.16). This morphology reflects the orthorhombic lattice structure of the $Zn(OH)_2$ crystal.[14] The particle sizes range from approximately 1 μm to 5 μm in size. After 30 minutes, the particles have increased in size, with the largest now around 7 μm. They reach a maximum size of around 8 to 9 μm after 45 minutes and 10 μm by 60 minutes stirring. Over the next 75 minutes no further increase in size is observed and from Figure 2.16(D) it can be seen that they have become substantially monodisperse, approximately 6 – 10 μm. Prolonged stirring, up to 24 hours, showed no change in the particle crystalline structure or morphology, with the size distribution also remaining apparently unchanged.

In the first 30 minutes of the reaction, the concentration of Zn^{2+} in solution drops from 0.025 M to 0.01 M (Figure 2.15). The drop in concentration then slows considerably and from 30 to 45 minutes the concentration falls to 0.008 M. The Zn^{2+} concentration then begins to level off and stops decreasing after around 60 minutes, remaining almost constant at approximately 0.0076 M. From the solubility studies carried out by Moir,[23] it would appear that the solubility of $Zn(OH)_2$ in the reaction mixture is approximately 0.015 M. On the other hand, Wood[24] found that in a 0.3871 M solution of NaOH, $Zn(OH)_2$ solubility was 0.0057 M. According to IUPAC solubility

data for $Zn(OH)_2$,[7] the numerous reports on $Zn(OH)_2$ solubility in NaOH solutions are inconsistent and therefore unreliable. Hence, it is fair to assume that the value at which the concentration of Zn^{2+} in solution is levelling off (0.0076 M), is most likely related to the solubility of $Zn(OH)_2$ in the reaction mixture.

The growth of these rhombic $Zn(OH)_2$ particles does not fit the LaMer[10] or aggregation[11] growth mechanisms exclusively. However, by combining the two, the growth can be explained. As with the LaMer theory, the particles precipitate and grow discreetly without aggregation. Nevertheless, nucleation does not only occur once, instead a number of nucleation events take place. This is evident by the broad size distribution and precipitation sized particles (< 5 μm) present in the sample up to around 45 minutes stirring. This is also reflected in the titration data, which indicates precipitation and diffusional growth up to 60 minutes, seen by the steady drop in $[Zn^{2+}]$. After this point a self-sharpening procedure most likely occurs, as the $Zn(OH)_2$ particles have a broad size distribution at 45 minutes and the final particles, after 120 minutes, are seen to be quite monodisperse. This is similar to what occurs in Den Ouden and Thompson's model of growth by diffusion.[13]

According to general inorganic textbooks,[14] $Zn(OH)_2$ loses water at an appreciable rate at temperatures of approximately 120 °C. In order to convert $Zn(OH)_2$ entirely to ZnO, temperatures of around 900 °C are required because migration of water through the lattice is difficult. A more recent report[25] however, suggests that conversion of $Zn(OH)_2$ to ZnO is complete at 300 °C. DSC on the solid (Figure 2.17) showed a large peak for water at 136 °C and a smaller one at 256 °C. As no peak was seen around 0 °C, it is assumed that the water is not simply surface water. Instead, the peaks are related to H_2O loss from the lattice and hence, the conversion of $Zn(OH)_2$ to ZnO. The existence of two distinct peaks suggests that there is more than one site in the lattice from which water is lost. A third scan carried out on the sample, after one weeks exposure to the air, was analogous to the second scan, i.e. no rehydration had taken place.

2.6.2 Growth of needle-like ZnO particles.

As was discussed in the previous section, when the zinc nitrate and sodium hydroxide are stirred together at room temperature, $Zn(OH)_2$ rhombic particles are precipitated and grow to a uniform size. If these particles are then aged in the mother liquor at reflux temperature (101°C), a thermal decomposition reaction takes place, forming ZnO. The growth of needle-like ZnO was studied by XRD and SEM.

Previous studies on thermal decomposition show that the decomposition can take place by dissolution-reprecipitation[26] or by a crystallization-recrystallization[27] phase transformation. Dissolution-reprecipitation involves complete dissolution of the first phase and the subsequent precipitation of the second and final phase. Crystallisation-recrystallization on the other hand, involves formation of the second phase by a lattice rearrangement solid phase transformation of the first, without dissolving. That is, something is lost from the lattice e.g. H_2O or CO_2, while the lattice rearranges to form the new phase. Matijevic and co-workers showed that $Fe(OH)_2$ decomposed to form Fe_3O_4 by recrystallization,[27] whereas, to produce hematite, Fe_2O_3, the ferric hydroxide was dissolved and reprecipitated.[26] Louër and co-workers,[28, 29] have studied decomposition of zinc hydroxide carbonate, zinc hydroxide nitrate, zinc oxalate and zinc acetate, all resulting in a ZnO product. Unlike this study however, these decomposition reactions were all solid state and not dispersion reactions and also concentrated on XRD studies rather than analysis of the morphology of the decomposition product.

X-ray diffraction (Figure 2.18) shows that the particles have a $Zn(OH)_2$ (wulfingite) composition after the two hour stirring step. When they are subjected to heating, they slowly begin to transform into ZnO (zincite). After 30 minutes heating the particles appear unchanged in morphology and size and the XRD is still showing a pattern for $Zn(OH)_2$ only. From 35 to 40 minutes, small particles are beginning to appear on the

surface of the rhombic hydroxide (Figure 2.19 C). After 45 minutes, it is evident that these particles have a needle-like morphology. The XRD shows the pattern for $Zn(OH)_2$ but also, from 40 minutes, the pattern for ZnO is beginning to appear. By 50 minutes, the ZnO pattern is predominant, with the $Zn(OH)_2$ pattern intensity reduced considerably. This is reflected by SEM, where the needle-like particles are more dominant and have increased in size after 50 minutes heating. By 55 minutes, the SEM shows only needle-like particles and the XRD shows the pattern for ZnO alone. This evidence on its own however, does not indicate whether the mechanism of transformation is by dissolution or by a lattice rearrangement. For that, the concentration of Zn^{2+} in the solution must be examined.

The concentration of Zn^{2+} would be expected to increase slightly and then fall gradually if the $Zn(OH)_2$ was dissolving prior to the formation of the ZnO. This however is not the case. The concentration of the zinc cation (Figure 2.23) remains at approximately 0.0076 M for the first 40 minutes, the same level at which it was at the beginning of the reflux reaction. The apparent increase seen in the Zn^{2+} concentration over this time is related to the increase in solution temperature, as the reaction is quenched at the temperature in question, (101 °C reached after ~ 35 minutes). The zinc ion concentration then drops over the next ten minutes (40 to 50 minutes) to around 0.0046 M and again levels off. The initial concentration is equivalent to the solubility of $Zn(OH)_2$ in the solution,[7] as discussed in section 2.6.1. After 40 minutes, the SEM shows the appearance of the ZnO needle-like particles and the concentration of the Zn^{2+} in the solution begins to drop. This is due to the fact that the ZnO is less soluble than the $Zn(OH)_2$ in the solution. After 55 minutes, only ZnO particles are seen in the sample and the concentration has levelled off at approximately 0.0047 M, a value assumed to be related to the solubility of ZnO in the solution at around 70 to 80 °C ($\approx$ 0.004 M at 25 °C).[9]

It can therefore be assumed that the growth of ZnO needle-like particles from rhombic $Zn(OH)_2$, is a decomposition reaction with particles forming as a result of a recrystallization and without dissolution of the $Zn(OH)_2$. The needle-like morphology reflects the structure of the ZnO lattice. The hexagonal structure can be seen by the prismatic shape of the needles and the *a:c* axial ratio of 1:1.6 is expressed by the elongation in the c-axis direction. As the aspect ratio of the particles is far greater than 1.6, the growth is obviously exaggerated in that direction. The net polarization of the ZnO c-axis has been previously put forward as an explanation for the directional aggregation in ZnO growth from zinc nitrate-HMT solutions[6] and is discussed in detail in Chapter 4 (section 4.3.1.2). This net polarization may also be the reason why ZnO particles grown by a phase transformation of $Zn(OH)_2$ have extended growth along the c-axis.

As the hydroxide is a layered lattice (see Figure 1.4, Chapter 1), loss of H_2O would cause fragmentation, resulting in the ZnO particles produced having smaller dimensions than the parent zinc hydroxide. The uniformity of the ZnO particles produced would therefore be related to the uniformity of the $Zn(OH)_2$ precursor.

2.6.3 Effect of pre-stirring time.

The pre-stirring times do not seem to have an appreciable effect on the dimensions of the needle-like particles which formed from the decomposition of the $Zn(OH)_2$. The width of the particles seemed to be relatively unaffected, as was the length distribution of the particles, which appeared to broaden very slightly with increased stirring times. The largest particles increase in size by only 1 μm from 2 to 24 hours ageing. As no palpable effect is observed with longer stirring times, two hours pre-stirring was chosen for all decomposition reactions.

2.6.4 Effect of ageing times on ZnO needle-like particle formation.

By varying the amount of time for which the ageing step is carried out, the dimensions of the needle-like particles formed can be altered. The ageing time was varied between 5 and 24 hours and is reported in section 2.5.4. The width of the needle-like particles does not change significantly with time and the average width of the particles also remains comparatively unchanged. In contrast, the length of the needle-like particles is seen to be affected by ageing time. The smallest particle length stays at approximately 2.5 – 3.0 μm, however, the largest of the particles gradually increases from 7.5 μm after 5 hours to 9.5 μm after 24 hours. The mean particle length also increases with time. After 5 hours, the particles have an average particle length of 4.5 μm and this increases slowly to 5.1 μm only after another 10 hours (15 hours in total). However, with prolonged ageing, after 24 hours, the mean particle length has increased to 6.4 μm. As the ZnO needle-like particles are formed from the decomposition of $Zn(OH)_2$, which is completed after 55 to 60 minutes heating, any subsequent growth of the particles must result from a dissolution and reprecipitation of the existing ZnO particles. The results suggest that this is a slow process, as significant changes in the particle dimensions are only seen after 24 hours ageing. The yield obtained appears unaffected by the ageing time, giving a yield of 85 ± 5 % in all cases.

2.6.5 Effect of reactant concentrations on ZnO needle-like particles.

The concentrations of both the zinc nitrate and the NaOH solutions were altered. The standard concentrations used were $Zn(NO_3)_2.6H_2O$ (0.04 M) and NaOH (1 M), resulting in a uniform sample of needle-like ZnO. By doubling the zinc nitrate concentration, no effect on the particles is observed and although halving the zinc nitrate concentration still resulted in needle-like particles, the size distribution was seen to broaden greatly. The samples are no longer uniform. The cause of this is most likely the size of the $Zn(OH)_2$ particles from which the ZnO forms. With only half the amount

of Zn^{2+} cations available for growth, a uniform sample of $Zn(OH)_2$ particles would not be produced. The particles still grow to approximately 10 μm, however, no excess Zn^{2+} is available for self-sharpening to take place. Therefore, as the $Zn(OH)_2$ sample in not uniform, it does not decompose to form a monodisperse sample of ZnO.

When twice the hydroxide ion concentration is used (2 M), a very low yield (~ 7 %) is obtained and the particles are needle-like in morphology. This is in contrast to that observed for the production of the star-like particles. When NaOH (2 M) is used in the star-like particle preparation, the Zn^{2+}: OH^- molar ratio is sufficiently high to inhibit the precipitation of the ZnO and hence no product forms. However, for production of the needle-like ZnO, precipitation of $Zn(OH)_2$ must take place first and the Zn^{2+}: OH^- molar ratio is not at a level which inhibits the zinc hydroxide precipitation. Nevertheless, the higher pH causes an increase in solubility of the $Zn(OH)_2$, as well as the ZnO, which results in a low yield.

When half OH^- concentration is used (0.5 M NaOH), spherical platelet particles are formed, similar to those obtained in the case of the star-like ZnO preparation procedure (as discussed in section 2.4.3). Again this can be accounted for by the fact that the initial ZnO phase precipitated does not dissolve. The solution pH never reaches a level at which the initial ZnO precipitate becomes fully soluble. Instead, continued growth of these particles takes place, resulting in spherical platelet aggregations.

2.6.6 Effect of the zinc counter-ion on the production of needle-like ZnO.

By altering the zinc salt used, the effect of the counter-ion on the reaction was monitored. It was found that when zinc nitrate, which produces uniform ZnO needle-like particles, is replaced by zinc sulphate or zinc chloride, needle-like ZnO particles are also obtained. In the case of zinc sulphate, the needle-like particles are non-uniform, with a broad distribution of width and length. Zinc chloride, on the other hand, produces

a sample with a distribution similar to that obtained with zinc nitrate. As a complete study of the growth process involved from zinc sulphate solution was not carried out, no obvious reason is evident for this decrease in sample uniformity. It is probable however, that the lack of uniformity of the sample is related to the $Zn(OH)_2$ phase formed prior to the ZnO particles. If this $Zn(OH)_2$ sample is non-uniform, the ZnO sample will reflect that lack of uniformity.

2.7 CONCLUSIONS

- By mixing a zinc nitrate aqueous solution with an NaOH solution, both ZnO and $Zn(OH)_2$ can be produced. Controlling the temperature of precipitation determines the phase that is produced. At room temperature, rhombic $Zn(OH)_2$ is produced whereas, when precipitation temperatures greater than 55°C are employed, ZnO is formed.

- When ZnO is precipitated directly, usually at 55 – 60 °C, particles with a star-like morphology are produced. This star-like morphology is a result of complex crystal twinning of the hexagonal ZnO lattice at $(11\bar{2}2)$ planes. By ageing the reaction solution at reflux temperatures, the size and uniformity of the star-like particles increases. The particles grow by a diffusional mechanism, increasing in size until the solubility of ZnO in the solution is reached. Increases in the initial concentration of zinc nitrate results in the star-like particles forming approximately spherical particles. These particles are a result of dendritic growth of the star-like particles.

- Rhombic $Zn(OH)_2$ particles are formed when precipitation is allowed to take place at room temperature. Again the particles grow by a diffusion mechanism but in this case a self-sharpening step also takes place. When the solution is stirred at room temperature, the particles increase in size and in uniformity until the $Zn(OH)_2$

solubility is reached. A monodisperse sample of $Zn(OH)_2$ results after two hours stirring.

- By thermally decomposing the $Zn(OH)_2$ particles in suspension, needle-like ZnO can be produced. These particles form by a recrystallization mechanism. Loss of H_2O from the lattice causes decomposition of the layered $Zn(OH)_2$ structure to give hexagonal ZnO. The uniformity of the ZnO needle-like particles reflects the uniform nature of the $Zn(OH)_2$ pre-cursor.

2.8 REFERENCES

1. E. Matijevic, *Pure & Appl. Chem.*, 1978, **50**, 1193-1210
2. Chittofrati, E. Matijevic, *Colloids and Surfaces*, 1990, **48**, 65-78
3. E. Matijevic, *Chem. Mater.*, 1993, **5**, 412-426
4. T. Trindade, J.D. Pedrosa de Jesus, P.O'Brien, *J. Mater. Chem.*, 1994, **4**, 1611-1617
5. Matijevic, *Acc. Chem. Res.*, 1981, **14**, 22-29
6. M. Andres-Verges, A. Mifsud, C.J. Serna, *J. Chem. Soc. Faraday Trans.*, 1990, **86**, 959-963
7. *IUPAC Solubility Data Series Vol. 23*, Pergamon Press, Oxford, 1986, 156-269
8. *Powder Diffraction File: Inorganic Phases*, JCPDS, International Centre for Diffraction Data, USA
9. T.P. Dirske, C. Postmus, R. Vandenbosch, *J.Am.Chem. Soc.*, 1954, **76**, 6022-6024
10. V. LaMer, R.H. Dinegar, *J. Am. Chem. Soc.*, 1950, **72**, 4847-4854
11. P.J. Murphy, A.M. Posner, J.P.Quirk, *J. Colloid Interface Sci.*, 1976, **56**, 284
12. M. Ocaña, R. Rodriguez-Clemente, C.J. Serna, *Adv. Mater.*, 1995, **7**, 212-216
13. C.J.J. Den Ouden, R.W. Thompson, *J. Colloid Interface Sci.*, 1991, **143**, 77
14. *Comprehensive Inorganic Chemistry Vol. 3*, Ed. J.C. Bailar, H.J. Emeléus, R. Nyholm, A.F. Trotman-Dickenson, Pergamon Press, 1975

15. S.W.K. Morgan, *ZINC and its alloys and compounds*, Ellis Horwood Ltd., England, 1985
16. E. Matijevic, *Faraday Discuss.*, 1991, **92**, 229-239
17. F.A. Sigoli, M.R. Davolos, M. Jafelicci Jr., *J. Alloys and Compounds*, 1997, **262-263**, 292-295
18. J.M. Cowley, A.L.G. Rees, J.A. Spink, *Proc. Phys. Soc.*, 1951, **64B**, 638-644
19. M.N. Fuller, *J. Appl. Phys.*, 1944, **15**, 164
20. J.C. Brice, *Crystal Growth Processes*, John Wiley & Sons, Blackie & Son, Glasgow, 1986
21. M.P. Morales, T. González-Carreño, C.J. Serna, *J. Mater. Res.*, 1992, **7**, 2538
22. J.D. Lee, *Concise Inorganic Chemistry 4th Ed.*, Chapman & Hall, London, 1992
23. J. Moir, *Proc. Chem. Soc.*, 1905, **21**, 301-311
24. J.K. Wood, *J. Chem. Soc.*, 1910, **97**, 878
25. C-H. Lu, C-H. Yeh, *Ceramics International*, 2000, **26**, 351-357
26. M. Ozaki, S. Katohvil, E. Matijevic, *J. Colloid Interface Sci.*, 1984, **102**, 146
27. T. Sugimoto, E. Matijevic, *J. Colloid Interface Sci.*, 1980, **74**, 227
28. N. Audebrand, J.P. Auffrédic, D. Louër, *Chem. Mater.*, 1998, **10**, 2450-2461
29. Benabad, M.T. Mesnier, J.C. Niepce, D. Louër, *Mat. Sci. Monograph*, 1985, **28B**, 895

Chapter 3

Growth of ZnO and $Zn(OH)_2$ microparticles by forced hydrolysis; microwave oven heating.

3.1 INTRODUCTION

In recent years, the use of microwave ovens in the laboratory has been widely investigated. It has been found that reaction times can be greatly reduced for some organic reactions,[1] for sample preparations, such as acid digestion pre-treatment for analytical methods[2] and for materials processing, e.g. sintering of ceramics.[3]

It has also been reported that domestic microwave ovens (DMO's) can be modified to better facilitate reaction apparatus, for instance by installing a reflux condenser.[4] Alterations can also be made to exercise control over the temperature and pressure of reactions in a microwave oven. A number of publications outline simple modifications that can be carried out to any DMO.[e.g. 5]

3.1.1 Inorganic synthesis using microwave ovens.

The use of microwave heating has also been applied to inorganic synthesis. In 1999, Rao *et al*[6] published a comprehensive review of the synthesis of inorganic solids using microwaves by both solid state and solution reactions. Solid state reactions were found to be greatly enhanced, taking place at temperatures much lower than those required under conventional heating, e.g. SiC production occurred at 1250 K rather than 1673 K.[7] Reaction times were also reduced for the production of many materials such as niobates and titanates. An example of this is the production of $KNbO_3$, prepared in 12 minutes using a DMO,[6] in contrast to 30 hours at 1273 K by conventional heating methods.

For solution inorganic synthesis, the majority of work carried out has been in the production of hydroxyapatite (HAp). This material is used extensively in the manufacturing of prosthetics. The hydrothermal process for HAp synthesis is very slow and eloborate, requiring a critical pH, high temperatures and long ageing times.[8] When prepared using microwave heating methods however, HAp forms within 25 minutes.[9]

Other reactions in aqueous media include the production of zeolites and aluminium phosphates,[10] for which the reaction times have been reduced from 1 - 2 days to 20 minutes in a microwave oven.

3.1.2 Microwave heating of inorganic oxides.

Until 1988,[11] it was generally assumed that inorganic oxides did not strongly absorb microwaves. For this reason many of the containers produced for microwave ovens are made from ceramic materials. Baghurst and Mingos[11] showed that although many inorganic oxides such as SnO, CaO and Fe_2O_3 do not absorb strongly at the operating frequency of a domestic microwave oven (2.45 GHz), there are a substantial number that do. These include ZnO, V_2O_5, CuO, MnO_2, PbO_2 and WO_3. The rapid heating of these compounds, when exposed to microwaves, reflects their strong absorption; for example, a sample of V_2O_5 can reach temperatures of over 700 °C and melt within one minute at 500 W in a microwave oven.

Coupling of some inorganic oxides with microwave energy has been explained by their conductivity. Semiconductors and ion conductors conduct by the movement of electrons or ions through their lattice. This movement of ions or electrons within the solid results in high loss tangents, that is, an efficient conversion of microwave to kinetic energy.[12] As the temperature of a semiconductor body increases, so too does its conductivity and thus coupling with microwaves becomes more efficient. This can result in thermal runaway.

The interaction of inorganic oxides with microwaves can be exploited in the production of ceramics and mixed oxides. Baghurst and Mingos[11] showed that heating CuO and Fe_2O_3 together in a DMO at 500 W gave $CuFe_2O_4$ within 30 minutes, whereas the conventional preparation takes approximately 23 hours.

In the thermal decomposition of PbO_2 to Pb_3O_4,[11] the temperature reached approximately 200 °C after 7 minutes and decomposition took place. Even though microwave irradiation continued, the temperature of the sample began to fall after this time. This drop in temperature was attributed to the poor microwave absorption of the product.

3.1.3 Microwave heating of ZnO.

Baghurst and Mingos[11] also showed strong microwave coupling in ZnO. A sample of 5 to 10 g was exposed for 1 minute at 500 W and was found to reach temperatures in excess of 800 °C. This strong coupling can be attributed to the fact that ZnO is a semiconductor.

Microwave heating of ZnO has mostly been applied to the varistor industry. High temperature sintering is an important step in processing varistors and ZnO is a chief component of these materials. Among others, Levinson *et al*[13] studied sintering of ZnO based varistor ceramics and found no significant performance differences between those processed by conventional heating and by microwave heating. Varistor production also requires the preparation of ZnO doped precursors. Varma *et al*[14] were first to apply a novel microwave decomposition method to varistor fabrication. This rapid method (approximately 8 minutes at 600 W) was found to yield high density materials, which when sintered at high temperatures have desirable properties for use as varistors.

3.1.4 Microwave deshielding.

As was mentioned in section 3.1.1, Rao and co-workers[6, 9] found that when they prepared hydroxyapatite (HAp) using a microwave oven procedure, the reaction took place in a substantially shorter time than when HAp was prepared by conventional hydrothermal methods.[8] They attribute this faster reaction to microwave coupling of

water bound to the Ca^{2+} ions in the aquation sheath. The rotational excitation of the water molecules by microwaves disengages them from the Ca^{2+} ions. This has the effect of deshielding / denuding the Ca^{2+} ions and enabling them to interact directly with the phosphate and hydroxyl ions more readily than when they have to get out of the aquation sheaths by themselves.

3.1.5 Microwave oven power levels.[15]

The power settings of a domestic microwave oven are assigned values in watts. These levels however are not strictly correct. Each power level is merely a fraction of the overall operating power of the oven. By cutting the magnetron in and out at regular intervals throughout the heating time, lower average power levels are obtained. Therefore, when using a 750 W microwave oven, 150 W is achieved by operating the magnetron for only $1/5^{th}$ of the time set. In other words, if a microwave is set to operate at 150 W for ten minutes, the magnetron will only be in operation at regular intervals for a total of two of the ten minutes.

3.1.6 Aims.

Although microwave heating has been applied to a large number of reactions, controlled particle growth has yet to be investigated. In this study, the reactions used in Chapter 2 to produce ZnO star-like and needle-like particles have been carried out in a domestic microwave oven. The effect of microwave heating and conventional heating on the morphology and size of the particles is compared. Heating times and power settings were varied to investigate the effect each has on the resulting particles. The particle growth at each power setting was investigated.

3.2 RESULTS

As was discussed in Chapter 2, the addition of NaOH to $Zn(NO_3)_2.6H_2O$ results in the formation of ZnO and $Zn(OH)_2$. At room temperature, $Zn(OH)_2$ is the most stable phase in contact with the reaction mixture. Therefore, stirring the reaction mixture prior to heating yielded rhombic crystals of $Zn(OH)_2$, which were subsequently thermally decomposed to form needle-like ZnO. Alternatively, star-like ZnO was prepared when precipitation took place above 55 °C. This was achieved by heating the reaction mixture directly, i.e. no pre-stirring step. Precipitation took place at approximately 60 °C and the stable precipitate in that case was ZnO. Similar experiments to those of Chapter 2 are carried out in this study, however, a microwave heat source is used as an alternative to conventional heating methods.

$Zn(NO_3)_2.6H_2O$ (0.04 M, 50 ml) and NaOH (1 M, 30 ml) were added together and heated in sealed Teflon® vessels (acid digestion bombs), at three different power settings, (150, 300 and 450 W), for times ranging between one and fifteen minutes. Due to constraints of the apparatus longer times and higher power settings were not studied (see Chapter 6, section 6.2.3.1). Experiments were carried out both with and without pre-stirring and in the cases of stirred reactions, two hours pre-stirring at room temperature was employed. No stirring was carried out during the heating step in either case. As aliquots could not be removed during heating, study of particle growth during a single experiment was not possible. For this reason, growth of the particles was investigated using a number of discrete experiments.

3.2.1 Microwave oven temperatures.

Temperatures in the microwave oven were measured using Fisherbrand irreversible 8-level temperature strips. Strips were attached to the outside of the Teflon® heating vessels. Using the reaction mixture, calibration of the strips was carried out for

temperatures below 100 °C and is shown in Figure 3.1. As the recorded temperature is less than the actual solution temperature, all temperatures quoted in this report are the minimum temperature achieved in the reaction bomb. The temperature range of the strips lies between 40 °C and 260 °C.

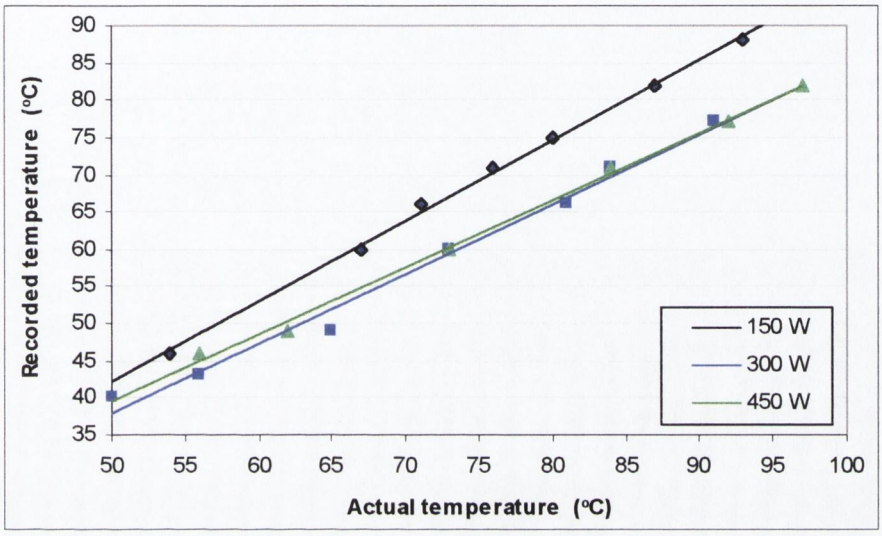

Figure 3.1 Calibration of temperature strips used in microwave studies, (actual temperature determined by mercury thermometer after heating had ceased).

The recorded temperatures when heating the reaction mixture for various times and at different power settings are shown in Table 3.1. The temperature of the solution decreases rapidly after irradiation has ceased and the bomb pressure is released.

Table 3.1 Minimum temperatures obtained when $Zn(NO_3)_2.6H_2O$ (0.04 M, 50 ml) and NaOH (1 M, 30 ml) is heated in a sealed Teflon® bomb in a microwave oven.

Power (W)	Heating time (minutes)	Recorded temperature (° C)
150	5	54
	10	77
	15	93
300	5	104
	10	154
	15	210
450	5	148
	10	210
	15	> 260

Throughout this report, the temperatures quoted will be those recorded using the temperature strips, with no adjustment according to calibration data.

3.2.2 Particle growth without prestirring – Direct precipitation of ZnO.

Growth of ZnO particles was examined by heating the reaction mixture at three power settings in a domestic microwave oven. Growth up to fifteen minutes at each power setting was monitored.

The XRD of particles grown at 150 W with no pre-stirring are shown in Figure 3.2, with each sample from a separate experiment. Prior to six minutes heating, no precipitate is isolated from the solution and therefore, the six-minute sample represents the initial particles formed. After heating at 150 W for six minutes a temperature of approximately 60 °C is recorded. Fifteen minutes represents the last sample acquired. Both patterns are consistent with ZnO (zincite, see Appendix I) and no apparent change

in crystallinity can be seen. All samples taken between six and fifteen minutes also show patterns consistent with zincite.

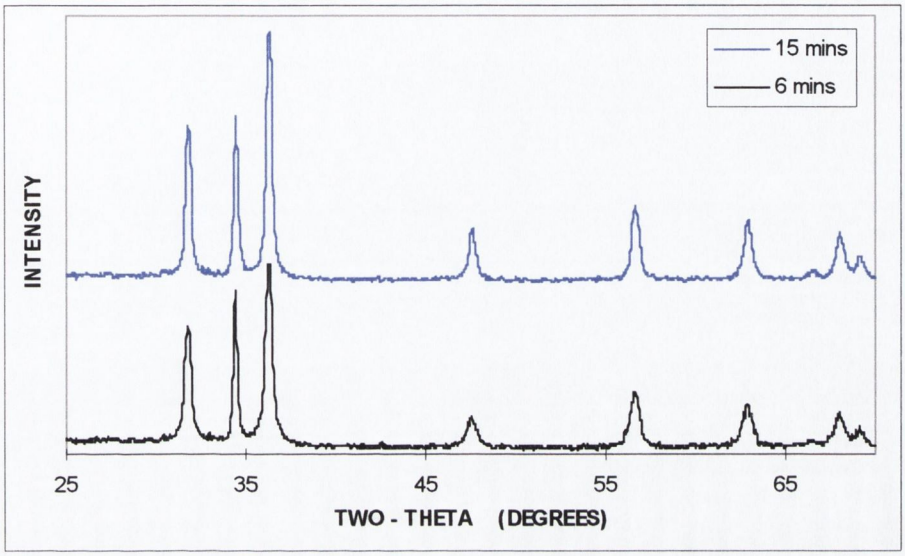

Figure 3.2 XRD patterns of particles formed when $Zn(NO_3)_2.6H_2O$ (0.04 M) and NaOH (1 M) are heated together at 150 W in a DMO for 6 and 15 minutes.

The SEMs of the ZnO particles formed after six and fifteen minutes at 150 W can be seen in Figure 3.3. Both samples show a star-like morphology, with the spines becoming more defined with time.

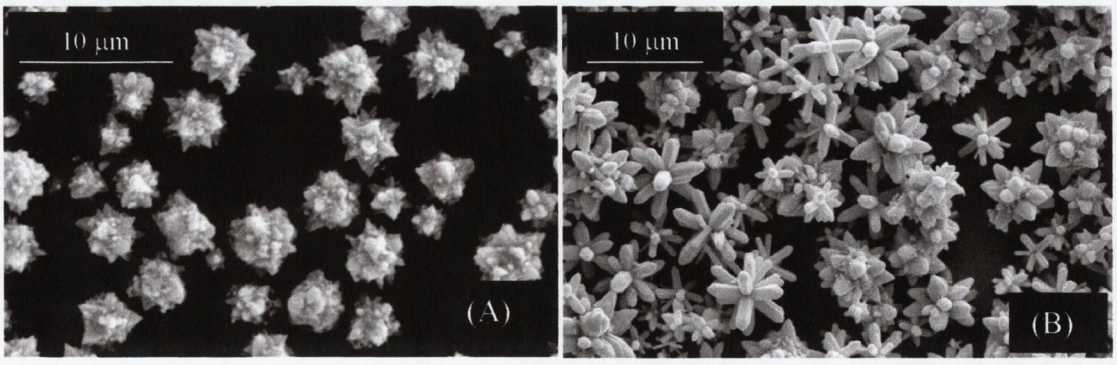

Figure 3.3 SEM of particles formed when $Zn(NO_3)_2.6H_2O$ (0.04 M) and NaOH (1 M) are heated together at 150 W in a DMO for (A) 6 and (B) 15 minutes.

Although the $Zn(OH)_2$ pattern is not seen in the XRD, SEM shows the presence of a small number of rhombic particles in the sample, confirmed to be zinc hydroxide by Raman spectroscopy (see Chapter 2, section 2.5.3). These particles are no longer evident after approximately ten to twelve minutes heating (recorded temperatures of around 75 to 80 °C). An example of this can be seen in Figure 3.4, which shows a sample heated for 8 minutes at 150 W.

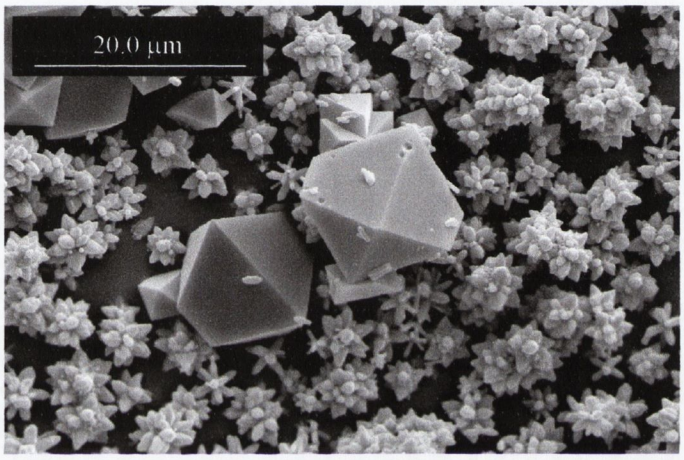

Figure 3.4 ZnO star-like particles and $Zn(OH)_2$ rhombic particles formed when $Zn(NO_3)_2.6H_2O$ (0.04 M, 50 ml) and NaOH (1 M, 30 ml) were heated for 8 minutes at 150 W in a DMO.

Similar results were observed when the reaction was heated at 300 W. When the reaction solution was heated directly after mixing (i.e. no pre-stirring step), the first particles were observed after 2 minutes heating and the solution temperature was recorded (~ 60 °C). The particles formed between two and fifteen minutes were analysed using SEM and XRD. All samples demonstrated diffraction patterns consistent with ZnO, zincite. In Figure 3.5, the XRD patterns of samples heated for two and fifteen minutes are shown, with no obvious change in crystallinity over the reaction time.

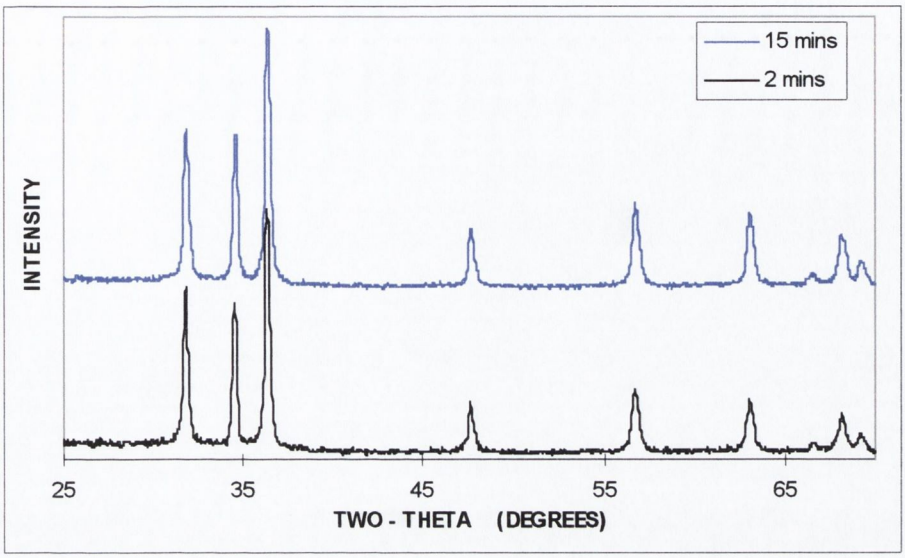

Figure 3.5 XRD patterns of particles formed when $Zn(NO_3)_2.6H_2O$ (0.04 M) and NaOH (1 M) are heated at 300 W in a DMO for 2 and 15 minutes.

The SEM images of the two samples whose XRD patterns are represented above can be seen in Figure 3.6. Both samples have a star-like morphology, with the shape becoming more defined with time. Unlike when heating was carried out at 150 W, no $Zn(OH)_2$ particles were present in the samples grown at 300 W.

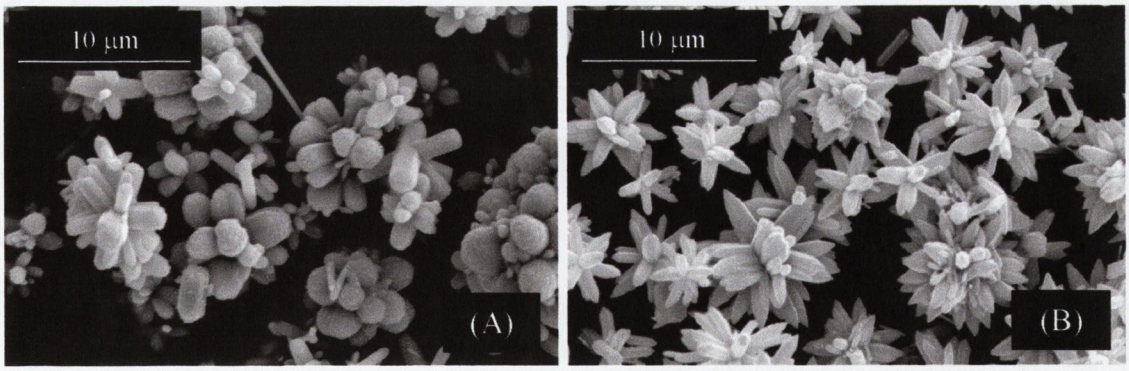

Figure 3.6 SEM of particles formed when $Zn(NO_3)_2.6H_2O$ (0.04 M) and NaOH (1 M) are heated at 300 W in a DMO for (A) 2 and (B) 15 minutes.

Again with heating at 450 W, particles formed after each minute were analysed by XRD and SEM. In this case, the first sample was isolated after one minute heating. Diffraction patterns for all samples are consistent with ZnO (zincite), with no apparent change in crystallinity. Diffraction patterns for samples heated for one and fifteen minutes are shown in Figure 3.7. After one minute, a temperature of at least 55 °C has been reached.

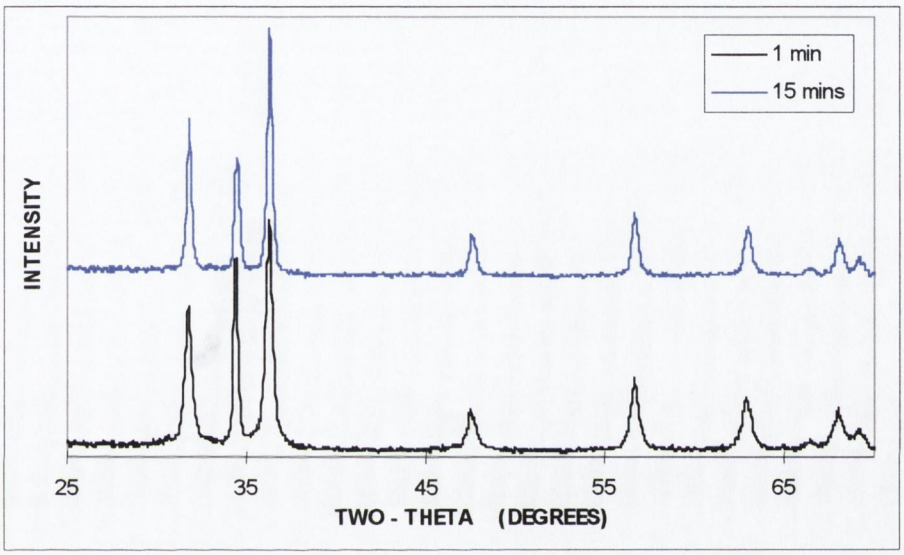

Figure 3.7 XRD patterns of particles formed when $Zn(NO_3)_2.6H_2O$ (0.04 M) and NaOH (1 M) are heated at 450 W in a DMO for 1 and 15 minutes.

The SEM images of particles formed after one and fifteen minutes heating at 450 W are represented in Figure 3.8. Particles form with a star-like morphology, increasing in size with time. No $Zn(OH)_2$ particles are present in any of the samples.

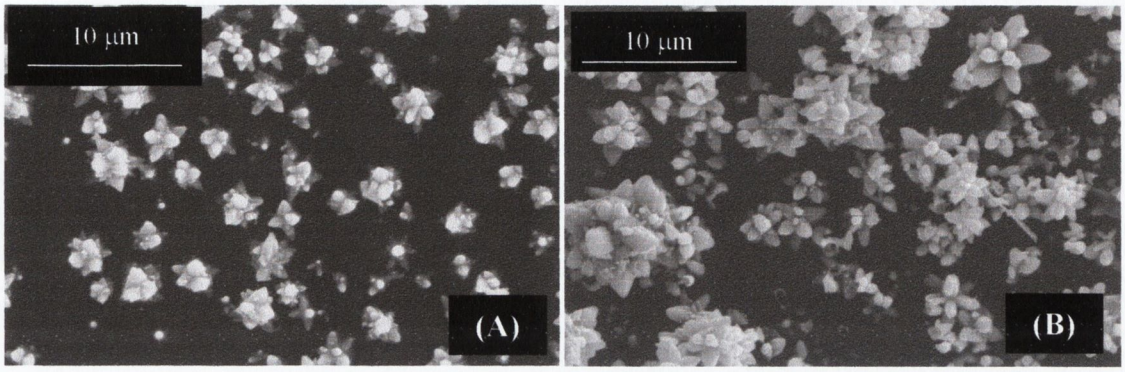

Figure 3.8 SEM of particles formed when $Zn(NO_3)_2.6H_2O$ (0.04 M) and NaOH (1 M) are heated in a DMO for (A) 1 and (B) 15 minutes at 450 W.

3.2.2.1 $[Zn^{2+}]$ analysis. When each sample was prepared and the particles removed from the hot suspension, the filtrate was retained to analyse the concentration of Zn^{2+} remaining in solution. The concentration in the hot solution was determined by EDTA titration using solochrome black indicator at pH 10. After heating is complete, pressure is released from the bomb, causing a volume loss. This volume loss was taken into account when calculating the final concentration of Zn^{2+} in solution. The concentration profiles obtained for the solutions heated at 150, 300 and 450 W can be seen below in Figure 3.9.

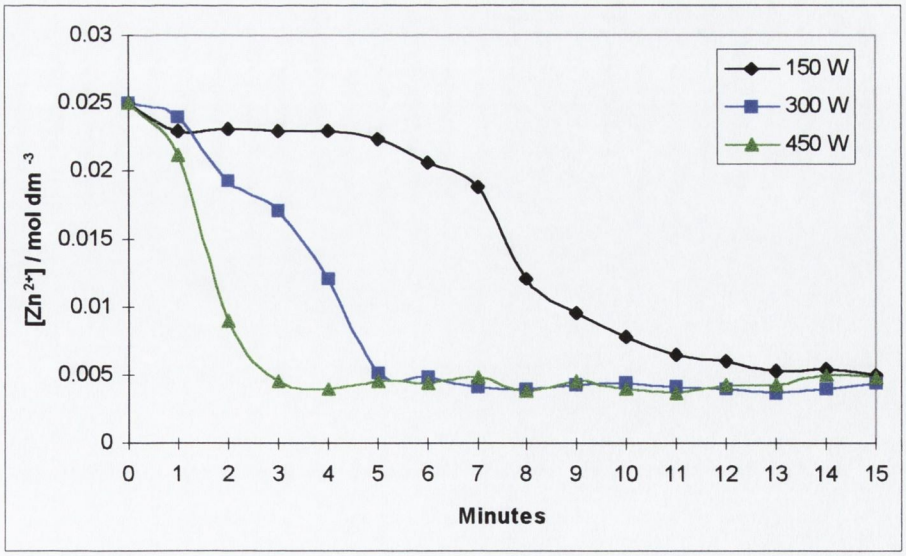

Figure 3.9 $[Zn^{2+}]$ profile obtained when $Zn(NO_3)_2.6H_2O$ (0.04 M) and NaOH (1 M) are heated in a DMO over 15 minutes at 150, 300 and 450 W.

3.2.2.2 Yields. The yields of ZnO obtained when $Zn(NO_3)_2.6H_2O$ (0.04 M) and NaOH (1 M) are heated in a microwave oven, with no pre-stirring step, at 150, 300 and 450 W are reported in Table 3.2.

Table 3.2 Typical yields of ZnO obtained when $Zn(NO_3)_2.6H_2O$ (0.04 M) and NaOH (1 M) are heated in a DMO at 150, 300 and 450 W.

Power (W)	Heating time (mins)	Typical yield* (± 5 %)
150	6	1 mg / 6 %
	10	70 mg / 43 %
	15	130 mg / 80 %
300	2	28 mg / 17 %
	6	120 mg / 74 %
	15	130 mg / 80 %
450	1	15 mg / 9 %
	3	132 mg / 81 %
	15	130 mg / 80 %

* All yields are calculate on the basis of a 100 % ZnO sample composition

The times chosen above (Table 3.2) correspond to initial particle formation (6, 2 and 1 minutes), the time at which $[Zn^{2+}]$ begins to level off (10, 6 and 3 minutes) and the final sample withdrawn (15 minutes), for each power setting respectively.

3.2.2.3 Star-like ZnO morphology. In Chapter 2 (section 2.4.1) the formation of star-like ZnO particles was discussed. It is proposed that these particles form by twinning of the hexagonal lattice along the $(11\bar{2}2)$ plane.[16] A split particle can be seen in Figure 3.10, which shows the core of the star-like particle. A direct comparison between this particle and the diagram of a twinned ZnO lattice (Figure 2.12) can be made.

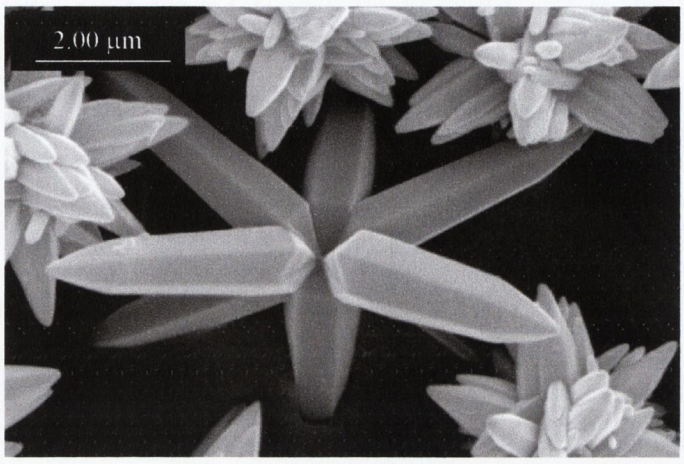

Figure 3.10 Star-like particle growth; $Zn(NO_3)_2.6H_2O$ (0.04 M) and NaOH (1 M) heated for 15 minutes at 150 W in a DMO.

3.2.2.4 Band gap determination. In order to establish if the microwave synthesized ZnO band gap differed from that produced by conventional heating processes, ZnO band gaps were determined using UV/vis. reflectance spectroscopy and a $BaSO_4$ reference. ZnO was produced from $Zn(NO_3)_2.6H_2O$ (0.04 M, 50 ml) and NaOH (1 M, 30 ml) heated for fifteen minutes at either 150, 300 or 450 W.

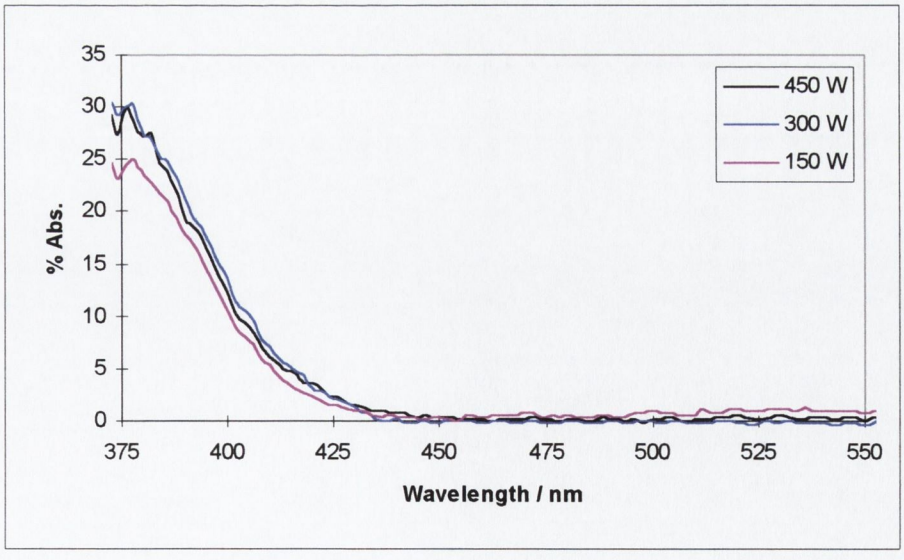

Figure 3.11 UV/vis. reflectance spectra for ZnO produced from $Zn(NO_3)_2.6H_2O$ (0.04 M, 50 ml) and NaOH (1 M, 30 ml) heated for fifteen minutes at 150, 300 and 450 W.

No significant variation in the spectra is observed between the three different power settings. The band edges are all approximately 420 ± 2 nm, corresponding to a band gap of approximately 3.4 eV, equivalent to that of ZnO produced by conventional methods (section 2.5.7).

3.2.3 Particle growth with pre-stirring.

As described in Chapter 2, when a two hour pre-stirring step is carried out at room temperature, $Zn(OH)_2$ with a rhombic morphology forms, the growth of which was studied (see section 2.5.1).

The $Zn(OH)_2$ suspension was heated at the three power settings, 150, 300 and 450 W. Individual experiments for heating from one to fifteen minutes were carried out and the resulting particles analysed by SEM and XRD. After heating at 150 W, the diffraction patterns for all samples were consistent with $Zn(OH)_2$ (wulfingite, see Appendix II) and those recorded for samples heated for one and fifteen minutes can be seen in Figure 3.12.

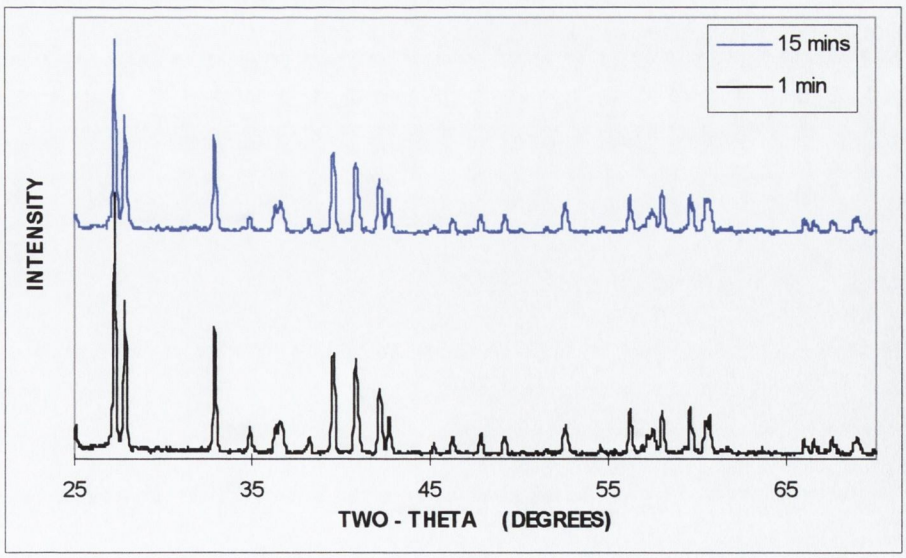

Figure 3.12 XRD patterns of particles formed when $Zn(NO_3)_2.6H_2O$ (0.04 M) and NaOH (1 M) are stirred together for two hours at room temperature, then heated at 150 W in a DMO for 1 and 15 minutes.

Figure 3.13 shows the morphology of the same particles whose XRD patterns are shown above. The rhombic morphology of the $Zn(OH)_2$ is unchanged after fifteen minutes heating at 150 W.

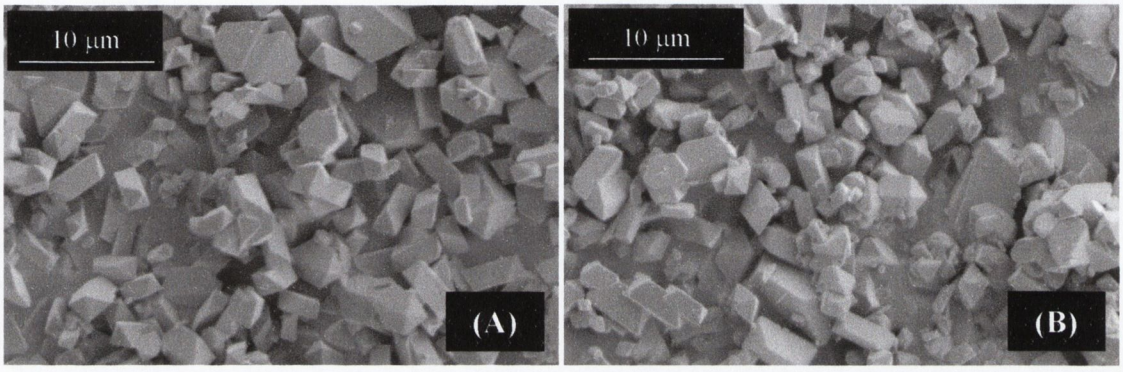

Figure 3.13 SEM of particles formed when $Zn(NO_3)_2.6H_2O$ (0.04 M) and NaOH (1 M) are stirred together for two hours, followed by heating at 150 W in a DMO for (A) 1 and (B) 15 minutes.

In contrast, heating at 300 W had the result that $Zn(OH)_2$ rhombic particles decomposed to form ZnO. Experiments were carried out heating for one to fifteen minutes and samples obtained corresponding to each minute. Figure 3.14 shows the XRD patterns obtained for a selection of the samples. The transition from $Zn(OH)_2$ to ZnO can be clearly seen to take place between three and six minutes. Three minutes heating at 300 W corresponds to a temperature of approximately 71 °C.

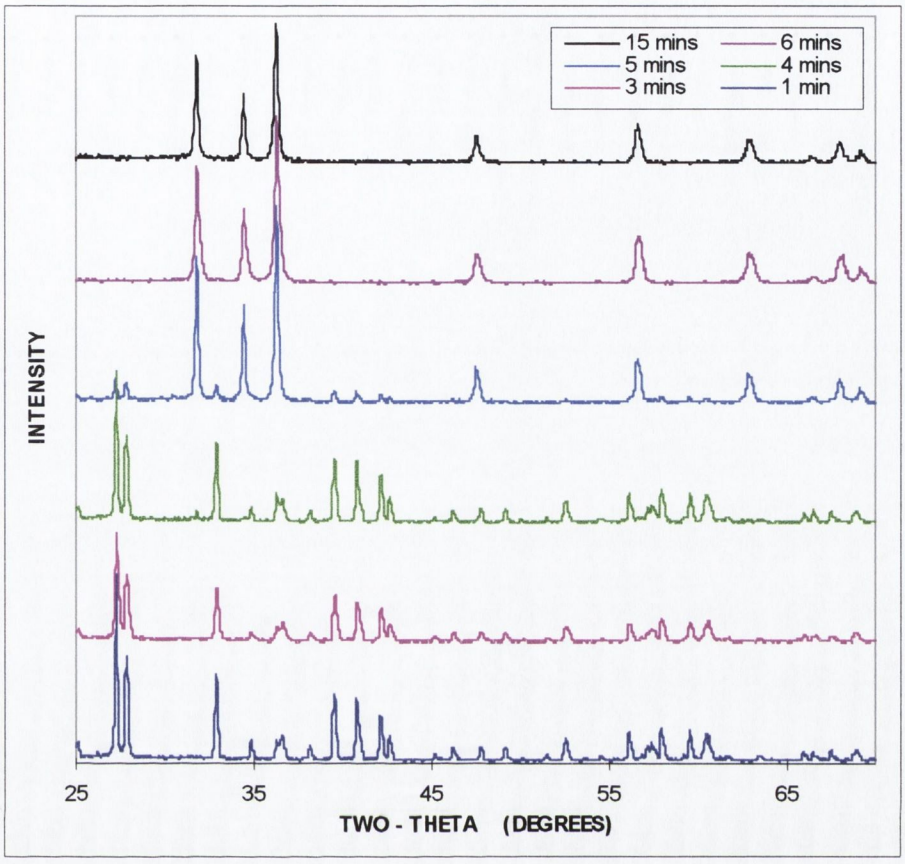

Figure 3.14 XRD patterns for samples formed when $Zn(NO_3)_2.6H_2O$ (0.04 M, 50 ml) and NaOH (1 M, 30 ml) are stirred for two hours at room temperature, followed by heating at 300 W in a DMO for 1, 3, 4, 5, 6 and 15 minutes.

The samples were also analysed by SEM. Figure 3.15 shows the morphology of the samples whose diffraction patterns are represented above. The morphology of the $Zn(OH)_2$ particles is rhombic. Up to four minutes, no discernible difference is seen in the particles. After five minutes, rod-like and twinned rod-like particles can be seen as well as large spheroid particles and after six minutes only the rod-like morphology is visible. The spheroid particles have been identified by Raman spectroscopy as $Zn(OH)_2$, having lost some of their definition.

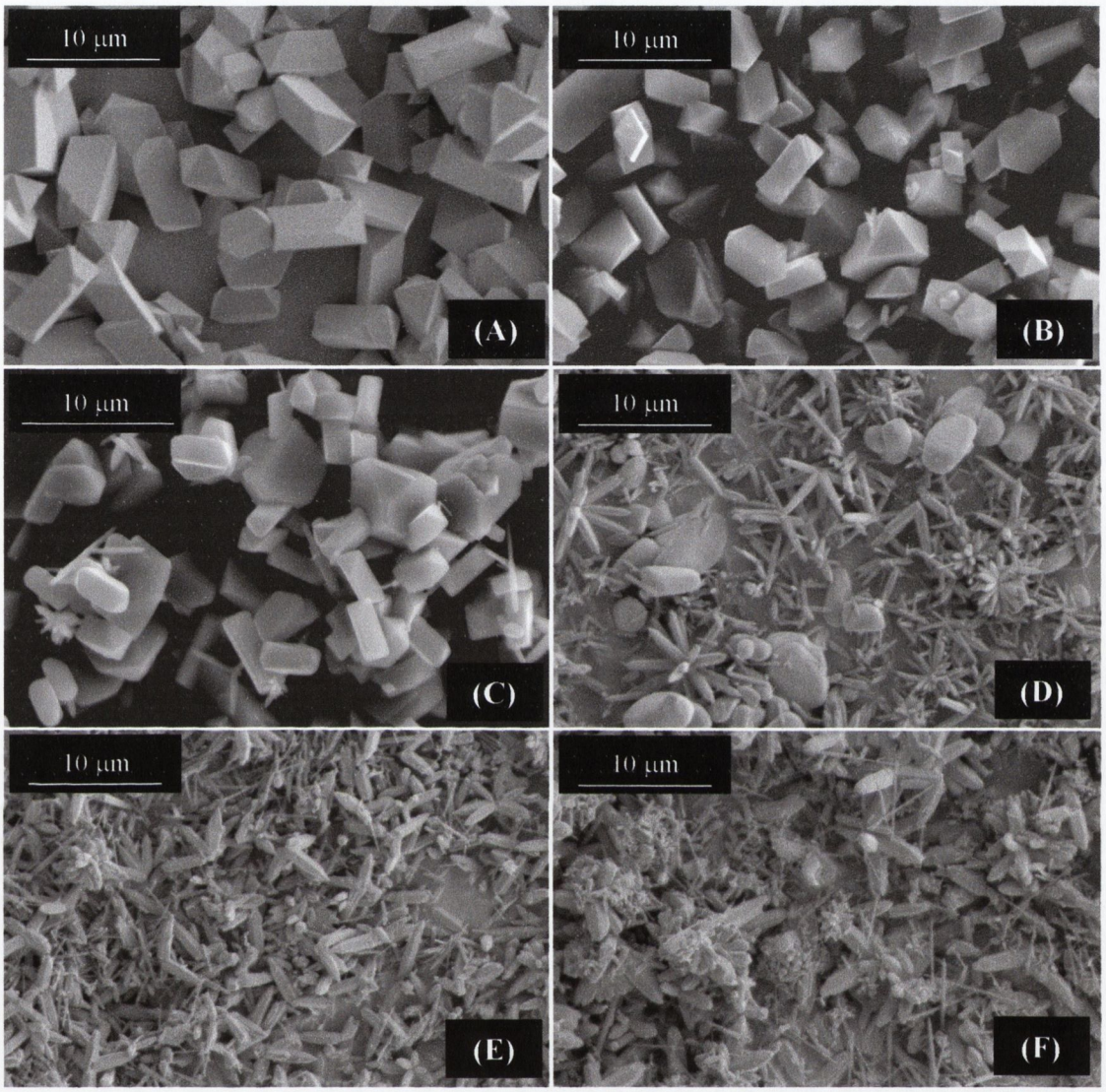

Figure 3.15 SEM of particles formed when $Zn(NO_3)_2.6H_2O$ (0.04 M) and NaOH (1 M) are stirred for two hours at room temperature, followed by heating at 300 W in a DMO for (A) 1, (B) 3, (C) 4, (D) 5, (E) 6 and (F) 15 minutes.

Likewise, heating at 450 W also results in the decomposition of $Zn(OH)_2$ to give ZnO. The XRD patterns for a selection of the samples obtained between one and fifteen minutes heating can be seen in Figure 3.16. The transition from $Zn(OH)_2$ to ZnO takes place between three and five minutes. Three minutes heating at 450 W corresponds to a temperature of approximately 104 °C.

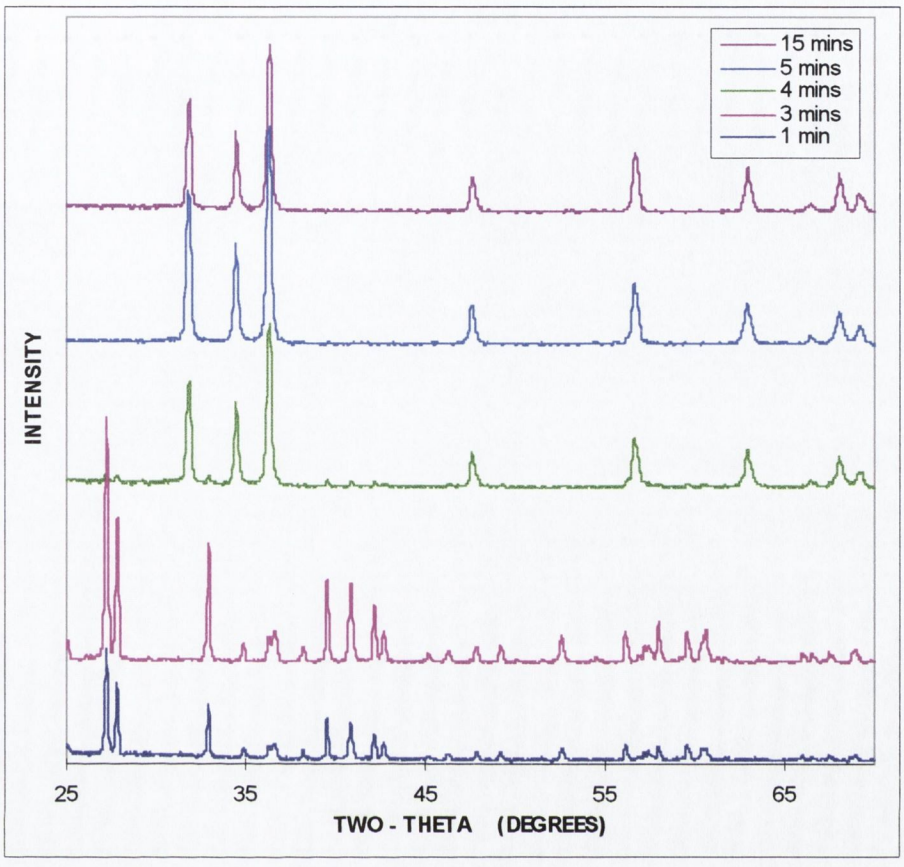

Figure 3.16 XRD patterns of samples formed when $Zn(NO_3)_2.6H_2O$ (0.04 M) and NaOH (1 M) are stirred at room temperature for two hours then heated in a DMO for 1, 3, 4, 5 and 15 minutes at 450 W.

This phase transformation, from $Zn(OH)_2$ to ZnO, was also followed by SEM (Figure 3.17). The morphology of the particles changes as the conversion from $Zn(OH)_2$ to ZnO takes place. After three minutes, no morphology changes can be seen and the rhombic $Zn(OH)_2$ is still evident. However, after four minutes the rod-like morphology of ZnO is dominant, with only a small amount of $Zn(OH)_2$ seen as spheroid type particles. No $Zn(OH)_2$ remains after five minutes heating has elapsed.

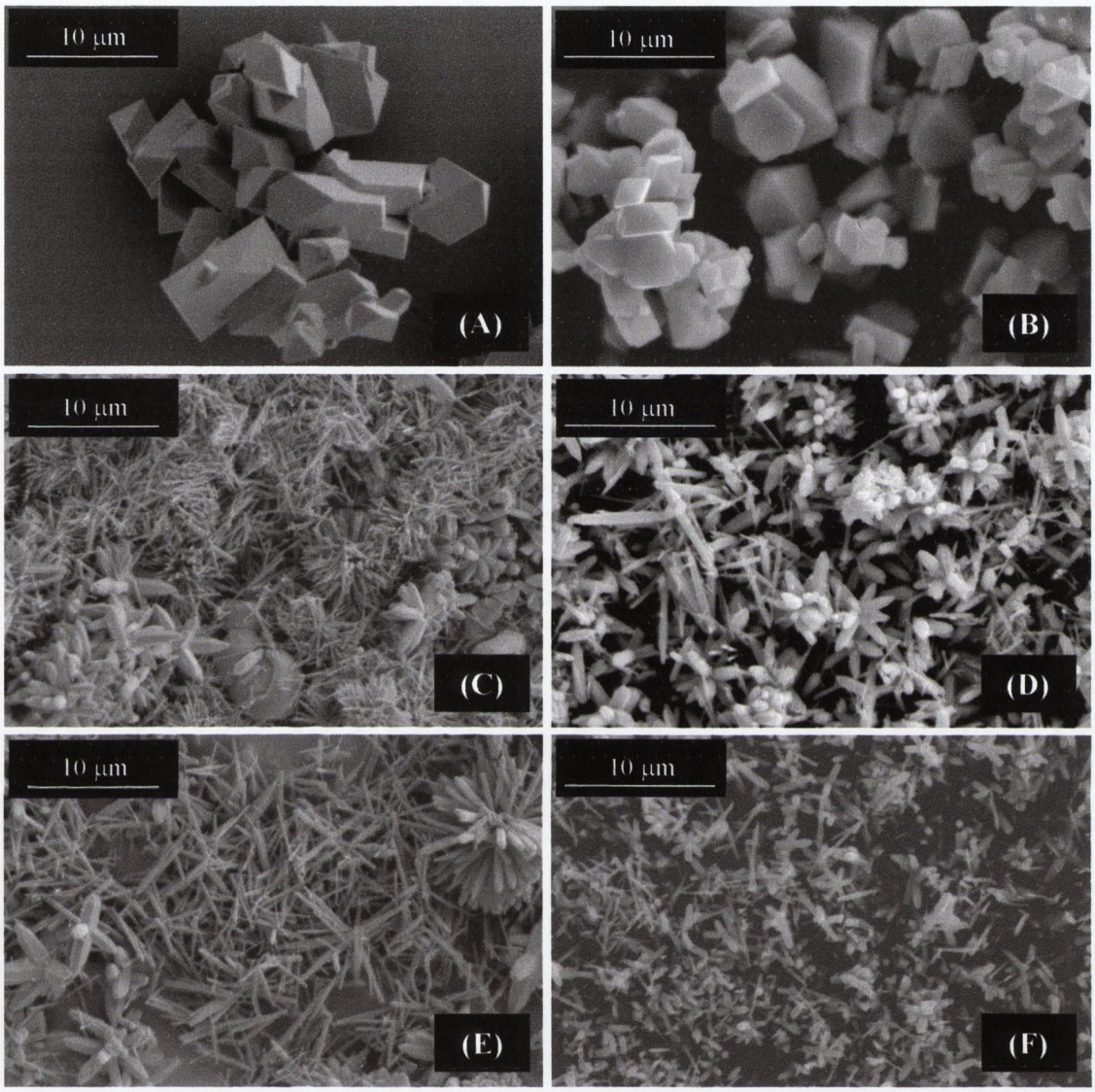

Figure 3.17 SEM of particles formed when $Zn(NO_3)_2.6H_2O$ (0.04 M) and NaOH (1 M) are stirred for two hours at room temperature then heated in a DMO at 450 W for (A) 1 (B) 3, (C) 4, (D) 5, (E) 6 and (F) 15 minutes.

3.2.3.1 $[Zn^{2+}]$ analysis. As with the case of no pre-stirring, the filtrate from the growth experiments was retained and analysed for $[Zn^{2+}]$. Figure 3.18 shows the concentration profiles at each of the three power settings. Due to the two hour pre-stirring step, the initial concentration is lower (approximately 0.0076 M) than when no

pre-stirring has been carried out (0.025 M, Figure 3.9), as $Zn(OH)_2$ has already precipitated from the solution.

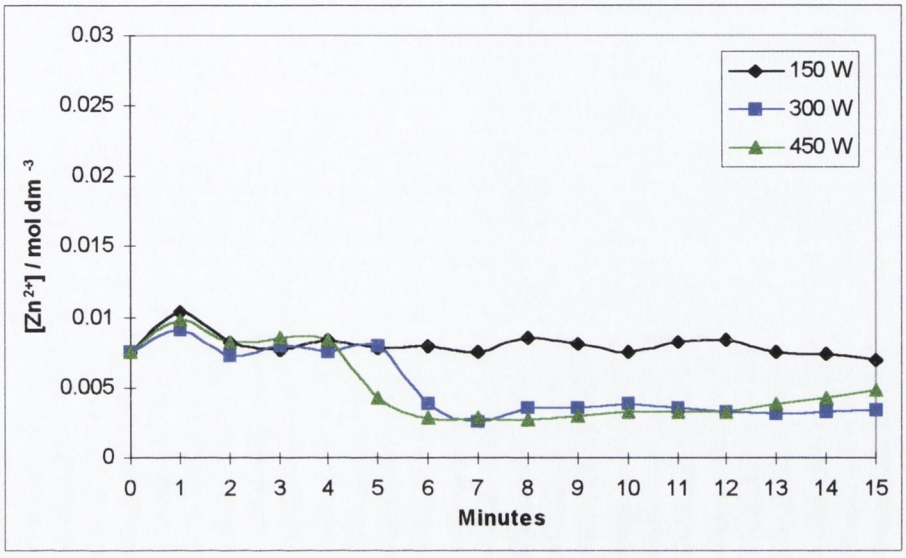

Figure 3.18 $[Zn^{2+}]$ profile obtained when $Zn(NO_3)_2.6H_2O$ (0.04 M) and NaOH (1 M) are stirred for two hours at room temperature then heated in a DMO over 15 minutes at 150, 300 and 450 W.

3.3 DISCUSSION

ZnO was prepared by two different methods. In both procedures, the reaction mixture consisted of $Zn(NO_3)_2.6H_2O$ (0.04 M, 50 ml) and NaOH (1 M, 30 ml). The first technique involves directly heating the reaction solution after mixing and hence, forming a ZnO precipitate. The second procedure involved a two hour pre-stirring step at room temperature, resulting in the formation of $Zn(OH)_2$ rhombic crystals, which then decomposed on heating to form ZnO.

Growth of ZnO particles by both methods was studied at three different microwave oven power settings. Power levels of 150, 300 and 450 W were used and by carrying out similar experiments, varying only the power setting, the effect of microwave operating power on the particles produced can be determined.

Section 3.3.1 will deal with the growth of ZnO particles when no pre-stirring step is employed and section 3.3.2 will cover growth of ZnO by thermal decomposition of $Zn(OH)_2$ produced by a two hour pre-stirring step.

3.3.1 Growth of ZnO particles – No pre-stirring step.

Table 3.3 outlines the main results obtained when no pre-stirring step took place, i.e. after mixing, the solution was heated immediately.

Table 3.3 Growth of ZnO particles from $Zn(NO_3)_2.6H_2O$ (0.04 M) and NaOH (1 M), heated directly after mixing in a DMO.

Power (W)	Precipitated particles	Precipitation time (mins)	Precipitation temperature* (°C)	Final particles
150	Star-like ZnO	6	60	Star-like ZnO
300	Star-like ZnO	2	60	Star-like ZnO
450	Star-like ZnO	1	55	Star-like ZnO

* Minimum temperature as recorded using Fisherbrand temperature strips

At 150 W, a precipitate formed in solution after approximately five to six minutes heating. At this time, a temperature in the region of 60 °C is recorded. The particles formed after six minutes at 150 W were identified by XRD as ZnO (zincite). This is expected, as studies carried out in the reaction solution (Chapter 2, Table 2.1) show that precipitation above 50 °C will yield ZnO. When the heating time is increased, XRD indicates that the composition of the sample remains unchanged and the diffraction patterns obtained do not suggest any increase in crystallinity with time.

The morphology of the particles isolated after six minutes are spherical-type with small spines protruding from the surface and are an average of 4 μm in diameter. As the heating time increases the spines are seen to increase in length, until star-like particles

with an average diameter of around 7.5 μm are achieved at fifteen minutes heating (Figure 3.3). A particle size distribution in the range 3 to 10 μm results.

The concentration of Zn^{2+} ions in solution was monitored over fifteen minutes (Figure 3.9). The concentration remains at approximately that of the initial solution (0.025 M) until heating for five minutes is carried out. Between five and six minutes the concentration begins to decrease. This coincides with the time at which turbidity and hence precipitation is first observed. The concentration of Zn^{2+} in solution continues to decrease until around thirteen minutes heating, at which point it begins to level off in the region of 0.005 M. This concentration is slightly higher than that of the solubility of ZnO in the reaction solution at room temperature (0.004 M).[17] As filtration takes place while the solution is still hot, almost boiling, it is expected that the ZnO solubility will be higher than 0.004 M. An examination of the yield obtained shows that the ZnO yield continually increases from six to fifteen minutes by 6 to 83 ± 5 %. This yield increase is in agreement with the steady drop in Zn^{2+} concentration in solution and also with the increase in particle sizes. Taking into account the solubility of ZnO in the solution, a maximum yield of 82 ± 2 % is predicted.

These star-like particles can therefore be seen to grow by the same mechanism as that observed under conventional heating methods (see section 2.4). Precipitation takes place around 60 °C and as the heating time is increased, the particle sizes increase due to growth by diffusion. However, up to thirteen minutes, the smallest particles are equivalent size to those seen at nucleation. This implies that a number of nucleation events are taking place. The steady drop in zinc cation concentration in solution also indicates a number of nucleations. As no narrowing of the particle size distribution is observed, it can be concluded that self-sharpening is not occurring.

When growth of ZnO is studied at 300 and 450 W, similar results are obtained. At higher power settings however, the temperature increases at a faster rate and so precipitation takes place after a shorter time.

For 300 W heating, again precipitation occurred at approximately 60 °C. In this case however, 60 °C was reached after only two minutes. The particles formed after each minute show an XRD pattern consistent with ZnO, with no indication of any increase in crystallinity with time. The initial particles formed have a star-like morphology with an average particle diameter of 5 μm. After approximately six minutes the spines of the star-like particles have increased in length to give an average particle diameter of 7 μm (Figure 3.6). After this time, no increase in average particle size is observed. Also, the size distribution (3 – 10.5 μm after fifteen minutes) is not seen to narrow, implying that self-sharpening is not occurring.

The concentration of Zn^{2+} in solution, when heated at 300 W (Figure 3.9), begins to decrease almost immediately until approximately five to six minutes heating has elapsed. After this time the concentration levels off at around 0.0045 M, again slightly higher than the solubility of ZnO in the solution (0.004 M at 25 °C),[17] due to the higher temperature. The yield of ZnO obtained is also seen to increase until after six minutes heating, at which point it also levels off at 77 ± 5 %. This is in agreement with the trend seen for the drop in Zn^{2+} concentration and also with the change in particle size.

Again particles grown at 450 W in the microwave oven, follow a similar process to those grown at 150 and 300 W. At all stages of the reaction, the isolated particles exhibit XRD patterns consistent with ZnO (zincite), the degree of crystallinity appearing unchanged with increasing heating times. A precipitate is observed after one minute of heating, when a temperature of the order of 55 °C is attained. This is consistent with the precipitation studies from Chapter 2 (section 2.2.1), that ZnO is expected to precipitate from the reaction solution at this temperature.

The first sample, obtained after one minute heating, has a star-like morphology with particles approximately 4 μm to 5 μm in diameter (Figure 3.8). As was observed at the other power settings, the particles increase in size with time. After approximately three to four minutes heating, a particle size of around 7 μm is achieved. This average size does not change considerably with prolonged heating, with size distribution remaining in the range 2.5 – 10.0 μm. The Zn^{2+} concentration in solution decreases rapidly for the first three minutes of the reaction, at which time the ZnO solubility is reached and the concentration becomes constant at around 0.0045 M. The yield also increases up to three minutes and then remains approximately constant at 80 ± 5 %.

3.3.1.1 Effect of power setting. From the results presented above, it can be concluded that the power level at which the reaction is carried out, affects only the rate at which the particles are formed. In all cases, the first precipitate forms between 55 and 60 °C and has a star-like morphology. The particles have an average size of 4 μm to 5 μm when first isolated and increase in size to around 7 μm and a size distribution between 2.5 and 10.5 μm, at which point the solubility of ZnO in the solution is reached and the particles stop growing. The yield reaches a maximum of 78 ± 5 %.

Table 3.4 summarizes the differences observed when the particles are grown at three different power settings and with no pre-stirring step. The time and temperature at which precipitation takes place and at which the particles are seen to have terminated growth are compared. Also included is the yield that is obtained when the growth is completed.

Table 3.4 ZnO star-like particle growth from $Zn(NO_3)_2.6H_2O$ (0.04 M) and NaOH (1 M) heated in a DMO.

Power (W)	Precipitation time (mins)	Precipitation temperature* (°C)	Growth completion time (mins)	Growth completion temperature* (°C)	Final yield (± 5 %)
150	6	60	13	82	80
300	2	60	5	104	74
450	1	55	3	104	81

* Temperature recorded using Fisherbrand strips

These results show that when the heating rate is increased, so too is the rate at which the particles form. From precipitation until the final particles are obtained, takes seven, three and two minutes, at 150, 300 and 450 W respectively. The rate of ZnO particle growth is therefore, related to the rate of heating.

It is interesting to note that at the higher two power settings (300 and 450 W), growth is concluded at approximately the same temperature. This is also indicative of the faster growth kinetics at higher powers, as at 300 W, 104 °C is reached after 5 minutes but at 450 W, it is reached within 3 minutes. At 150 W however, growth is completed at a lower temperature. This is because of the slower heating rate, 104 °C is not reached within the reaction time, that is, the length of time taken to reach the ZnO solubility level in solution. Particles are growing at lower temperatures and hence take more than twice the length of time to form than those prepared at higher power settings.

3.3.1.2 Microwave *vs.* conventional heating. In Chapter 2, similar experiments were carried out on a larger scale and heated using conventional means (round bottom flask in an oil bath). The maximum temperature achieved in that case was 101 °C. The solution was heated until reflux was attained and then was held at this temperature for at least two hours. When no pre-stirring step was used, the star-like particles formed and

grew by a diffusional growth mechanism;[18] that is, during heating, many nucleation events took place after which the particles continued to grow until the Zn^{2+} supply was exhausted (ZnO solubility was reached). No self-sharpening step was observed. As was discussed above, this growth pattern was also observed in the microwave heating method.

The obvious advantage that microwave heating has over conventional heating methods however, is the speed at which the reaction takes place. The fastest growth was observed for 450 W heating. Table 3.5 compares conventional growth to 450 W microwave growth.

Table 3.5 Comparison of conventional and microwave heating methods for ZnO star-like particle preparation, from $Zn(NO_3)_2.6H_2O$ (0.04 M) and NaOH (1 M).

Heating method	Precipitation time (mins)	Precipitation temperature (°C)	Total heating time (mins)	Average particle size (μm)	Size distribution (μm)	Typical yield (± 5%)
Oil bath	10 -15	55 - 60	120	6.3	4.5 – 8.5	60
DMO at 450 W	< 1	55 - 60	3	7.0	2.5 – 10	80

The microwave method is much faster than conventional heating and a higher yield is obtained. Using a microwave oven, ZnO star-like particles can be produced within three minutes. When compared to conventional methods, at least two hours heating is required to obtain particles of a similar size. However, using conventional heating, the size distribution of the particles is narrower. Band gap and XRD analysis indicate that the two ZnO samples are comparable and SEM shows that the morphology is similar in both cases (Figures 2.6 F and 3.10). It is therefore concluded, that the use of microwave for controlled synthesis of ZnO star-like particles is extremely useful. Similar particles

can be produced in times over 80 times faster than those necessary by conventional heating processes.

3.3.1.3 Why faster reactions? It is evident from this study, that the kinetics of ZnO formation are greatly increased when microwave heating methods are employed. The reaction mimics that which occurs under conventional heating, with the exception of the reaction rate. The most apparent reason for these reduced reaction times is the enhanced rate of heating which occurs with microwaves. By conventional heating, the reaction mixture reaches 101 °C after approximately 35 minutes heating. In the microwave however, this temperature is attained after only 5 minutes at 300 W. Therefore, faster particle growth is to be expected.

Fast synthesis of inorganic solids from aqueous solutions using microwave oven heating, has previously been attributed to the absence of an aquation sheath surrounding the cations in solution. As was discussed in section 3.1.4 of this chapter, Rao and co-workers[6, 9] found that the production of hydroxyapatite (HAp) was greatly enhanced by microwave heating. They proposed that the rotational excitation of the water molecules effectively deshields the hydrated cation, making it react much quicker than if it had to escape the aquation sheath unaided.

It is proposed that the same mechanism is taking place in the synthesis of ZnO star-like particles. The microwave rotational energy causes a disruption in aquation sheath of the hydrated Zn^{2+} cations in solution. In this 'deshielded' form, the cations are more open to attack from the hydroxide ion and hence react more quickly. When the microwave operating power is increased, the rate at which the aquation sheath is disrupted increases. This is because at lower power levels the magnetron cuts in and out to allow a lower average operating wattage.[15] This cutting in and out of power effectively interrupts the rotational excitation of the water molecules, eliminating the deshielding effect during stoppage in exposure. Hence, at lower operating powers the

deshielding effect will be less pronounced. At higher operating powers, when the magnetron is in operation for longer times, the formation of the ZnO particles proceeds more rapidly.

Baghurst and Mingos[11] showed that ZnO was an efficient absorber of microwaves, evidenced by rapid heating rates of the solid. It is therefore fair to assume that as the ZnO particles form, they are heated to a much higher temperature than that recorded for the solution. This could result in superheated pockets within the reaction, surrounding the growing particles. These areas of high temperature would hence contribute to the enhanced rate of growth observed and explain the difference in time scales between the conventionally heated reaction and that heated by microwave energy. When the microwave source is switched out, rapid cooling of the solid occurs and therefore the solution itself is not seen to reach these high temperatures. However, at 450 W, when the magnetron is in operation for more than half of the reaction time, the solution temperature exceeds that which can be recorded using the temperature strips (260 °C).

3.3.1.4 Star-like morphology. In Chapter 2 (section 2.4.1) the formation of the star-like morphology was discussed in detail. Fuller[16] attributed the star-like structure to twinning along the $(11\bar{2}2)$ planes. This results in the formation of spines, each of which is a ZnO crystal, approximately tetrahedral to one another joined at a common base.

Figure 3.10 shows a split particle, broken either during growth or during sample preparation for SEM. This image clearly shows the core of a star-like particle. Comparing Figure 2.12 (Chapter 2), showing two hexagonal lattices twinned along their $(11\bar{2}2)$ planes, to Figure 3.10, suggests that this type of twinning is taking place, as proposed by Fuller.[16]

3.3.1.5 $Zn(OH)_2$. When heating is carried out at 150 W, a small amount of $Zn(OH)_2$ is observed alongside star-like ZnO for the first three to four minutes after precipitation

(Figure 3.3). As the $Zn(OH)_2$ pattern is not observed with XRD and only a small number of particles are observed under SEM, it is assumed that the percentage composition is extremely low. After ten minutes, when a temperature of 75 °C is reached, the $Zn(OH)_2$ particles are no longer present, neither are they observed in samples prepared at 300 or 450 W. This is because the heating rates in these cases are considerably faster and 75 °C is reached before three and two minutes heating for 300 and 450 W respectively. Consequently, the $Zn(OH)_2$ would form and re-dissolve within the first minute of particle formation and hence, the particles are not observed at higher power levels.

The presence of $Zn(OH)_2$ for short times after precipitation is also seen in the case of conventional heating preparation of ZnO star-like particles. For the first ten minutes after precipitation, a small number of $Zn(OH)_2$ rhombic particles can be observed. Again, their presence is not indicated by XRD, only by SEM and Raman spectroscopy. When a temperature of approximately 65 – 70 °C is reached the zinc hydroxide particles are no longer observed in the sample.

3.3.2 Growth of ZnO particles – two hour pre-stirring.

In the second method investigated for ZnO formation, after the $Zn(NO_3)_2.6H_2O$ (0.04 M, 50 ml) and NaOH (1 M, 30 ml) are mixed, stirring at room temperature for two hours is carried out. In Chapter 2 (section 2.6.1), the white precipitate, which formed after approximately fifteen minutes room temperature stirring, was identified as $Zn(OH)_2$ rhombic particles. After two hours stirring, the particles had grown to a size of approximately 10 μm and the sample was quite monodisperse. The concentration of Zn^{2+} remaining in solution was approximately 0.0076 M. When conventional heating and ageing of the suspension at reflux temperature (101 °C) was then carried out, the $Zn(OH)_2$ particles underwent a thermal decomposition to form ZnO needle-like particles.

As with conventional heating, microwave oven heating resulted in the decomposition of $Zn(OH)_2$ to form ZnO. The main observations made when the $Zn(OH)_2$ suspension was heated in a DMO are outlined in Table 3.6.

Table 3.6 Growth of ZnO particles from $Zn(NO_3)_2.6H_2O$ (0.04 M) and NaOH (1 M), stirred at room temperature for two hours, followed by heating in a DMO.

Power (W)	Initial particles (ppt after ~ 10 mins stirring)	Time range for decomposition (mins heating)	Decomposition temperature range (°C)	Final particles
150	Rhombic $Zn(OH)_2$	---	---	Rhombic $Zn(OH)_2$
300	Rhombic $Zn(OH)_2$	3 – 6	71 – 116	Needle-like ZnO
450	Rhombic $Zn(OH)_2$	3 – 5	104 – 148	Needle-like ZnO

The $Zn(OH)_2$ suspension solution was heated in a DMO for one to fifteen minutes. When the 150 W power setting was used, no change in the particle morphology was observed over the course of fifteen minutes heating (Figure 3.13). This was confirmed by XRD, which continued to consist of the $Zn(OH)_2$ (wulfingite) pattern only. A temperature of 93 °C was recorded for the solution after fifteen minutes. Titration analysis of the reaction solution after heating also showed no significant change in concentration of Zn^{2+} during the heating step of the reaction (Figure 3.18).

In Chapter 2 (section 2.6.2), it was determined that, after heating at 101 °C for thirty five to forty minutes, the $Zn(OH)_2$ particles suspended in solution began to decompose to form ZnO needle-like particles. Although a temperature of approximately 93 °C is achieved when the same solution is heated at 150 W in a microwave oven, ageing at this temperature does not take place. When the maximum temperature is reached, the microwave irradiation is ceased and the sample begins to cool rapidly. It is therefore evident that this heating is not sufficient to cause a phase transformation of the $Zn(OH)_2$ particles to take place.

In contrast to 150 W, when the suspension is heated at 300 W, needle-like particles are formed after 6 minutes heating. A sample produced after each minute (one to fifteen) was analysed by SEM and XRD (Figures 3.15 and 3.14 respectively). For heating times up to three minutes, the particles remain unchanged in morphology and the XRD consists only of $Zn(OH)_2$. However, the sample removed after four minutes heating begins to show changes. A close examination of the XRD data shows the formation of ZnO peaks at very low intensities. A small number of needle-like ZnO particles can also be observed in the SEM, however, the most abundant particles are still rhombic $Zn(OH)_2$.

After five minutes, ZnO is the dominant pattern in the XRD, with $Zn(OH)_2$ having a very weak signal. The SEM reflects the same; needle-like and twinned needles of ZnO are profuse, with a small quantity of poorly defined $Zn(OH)_2$ particles evident. After a total of six minutes heating, the XRD shows only the pattern for ZnO and no $Zn(OH)_2$ particles can be seen in the SEM. Instead needle-like and complex twinned needles of ZnO are observed, (Figure 3.15). The sample is highly dispersed in both the length and the width of the particles. The decomposition of $Zn(OH)_2$ to ZnO took place over 3 minutes, between approximately 71 and 116 °C and within a total of six minutes of heating at 300 W. Heating was continued until fifteen minutes had elapsed. From six to fifteen minutes, no significant changes occurred in the particles. The sample produced after fifteen minutes consists of highly disperse needle-like and twinned needle-like ZnO.

The concentration of Zn^{2+} in solution was monitored using EDTA titration (Figure 3.18). The concentration remains reasonably unchanged from the start of heating until five minutes have elapsed. Between five and six minutes, the zinc cation concentration drops to approximately 0.004 M and remains steady at that value for the remainder of the reaction. This coincides with the transformation of $Zn(OH)_2$ to ZnO observed by

XRD and SEM. The concentration is seen to drop from the approximate solubility concentration of the hydroxide to that of the oxide in the reaction solution.[17, 19]

The results obtained when the suspension is heated at 450 W are very similar to those for 300 W heating. Up to three minutes heating, no changes in composition or morphology are observed in the sample and the sample consists only of rhombic $Zn(OH)_2$. After four minutes heating, the XRD (Figure 3.16) indicates that the composition of the sample is now predominantly ZnO, with only small traces of $Zn(OH)_2$ remaining. SEM (Figure 3.17) shows a profusion of highly disperse ZnO needles and twinned needle-like particles along side a small amount of poorly defined $Zn(OH)_2$. When five minutes heating has elapsed, only ZnO particles can be seen under SEM and the XRD pattern now only consists of ZnO. Prolonged heating, up to fifteen minutes, shows no change in the particle composition or morphology. The concentration of Zn^{2+} in solution was monitored by EDTA titration (Figure 3.18) and is observed to drop between three and six minutes, to a value consistent with the solubility of ZnO in the reaction solution (0.004 M at 25°C).[17] This drop coincides with the appearance of ZnO in the sample and the loss of $Zn(OH)_2$.

Although decomposition does not occur at 150 W, at 300 and 450 W the ZnO particles appear to form by the same mechanism as that observed by conventional heating methods (Chapter 2, section 2.6.2). Under conventional heating techniques, the thermal decomposition of $Zn(OH)_2$ to produced ZnO needle-like particles, takes place by a solid phase transformation. The hydroxide lattice loses water and undergoes a rearrangement to form ZnO, without a dissolving – re-precipitation step taking place. When ZnO is produced using the same experimental procedure, only heating using a microwave oven, the same mechanism for ZnO formation takes place. Titration of the reaction solution before, during and after the decomposition reaction shows that no increase in Zn^{2+} ions in solution occurs. If the $Zn(OH)_2$ particles dissolved, an increase in concentration would be recorded, followed by a steady decrease as ZnO began to

form would be expected and XRD would not show the co-existence of both ZnO and $Zn(OH)_2$. As this is not observed, the evidence strongly suggests solid-state transformation.

3.3.2.1 Effect of power setting. Table 3.7 outlines the effect of power setting on decomposition times and temperatures.

Table 3.7 Effect of DMO power setting on decomposition of $Zn(OH)_2$ to ZnO suspended in reaction solution.

Power (W)	Decomposition start temperature (°C)	Decomposition start time (mins)	Decomposition end temperature (°C)	Decomposition end time (mins)
150*	---	---	---	---
300	71	3	116	6
450	104	3	148	5

* No decomposition of $Zn(OH)_2$ observed for 150 W, max. temperature reached ≈ 93 °C after 15 minutes.

At 150 W no decomposition of the $Zn(OH)_2$ particles takes place during the fifteen minutes heating. No change in the particle morphology or composition is seen. In contrast, at 300 and 450 W the rhombic $Zn(OH)_2$ decomposes to form needles of ZnO. The sample size in both cases is highly disperse, with a large amount of twinning occurring.

The only difference been the 300 and 450 W power setting appears to be the rate at which the decomposition reaction takes place. At 300 W, decomposition takes place over 3 minutes, whereas at 450 W formation of ZnO takes only two minutes from start to finish. In both cases, the first ZnO particles are detected by three minutes after heating began.

Unlike with the formation of star-like ZnO (no pre-stirring), the rate of heating for the solution does not appear to be the determining factor for ZnO production. Decomposition of the $Zn(OH)_2$ does not begin to take place at the same solution temperature at each power level. At 300 W, decomposition begins at 71 °C and at 450 W the temperature has reached 104 °C before decomposition commences. In contrast, at 150 W, even though the temperature exceeds 93 °C decomposition does not transpire at all. It is proposed therefore, that the increased rate of decomposition with power is related to heating rates of solids, rather than or in conjunction with that of the solution. This will be discussed in detail in section 3.3.2.3 below.

3.3.2.2 Microwave *vs.* conventional heating processes. In Chapter 2 (section 2.5.3), ZnO needle-like particles were prepared by thermal decomposition of $Zn(OH)_2$. The $Zn(OH)_2$ particles were found to undergo a phase transformation by lattice rearrangement, to produce ZnO particles. As was mentioned above, this growth pattern was also observed when suspensions were heated by microwave irradiation. The fastest decomposition under microwave heating was observed at 450 W. These results are compared to those obtained for conventional heating. Table 3.8 outlines the differences between the particles produced by microwave and conventional heating.

Table 3.8 Comparison of conventional and microwave heating methods for ZnO needle-like particle preparation, from $Zn(OH)_2$ decomposition : $Zn(NO_3)_2.6H_2O$ (0.04 M) and NaOH (1 M) stirred for two hours, followed by heating.

Heating method	Start of decomposition		End of decomposition		ZnO produced	
	(mins)	(°C)	(mins)	(°C)	Morphology	Size (μm)
Oil bath	35	101	55 - 60	101	Needle-like	(5 ± 2.5) x (1 ± 0.3)
DMO at 450 W	3	104	5	148	Needle-like and twinned	Highly disperse

For complete conversion of $Zn(OH)_2$ to ZnO, microwave heating reduces decomposition times 20 fold. However, at these decomposition rates, control over the growth of ZnO is lost and the particles are produced with an extremely broad size distribution. This broad size distribution may be explained by the rate at which water is lost from the $Zn(OH)_2$ lattice. Uniformity of ZnO needle-like particles is dependent on the uniform decomposition of $Zn(OH)_2$. At the high temperature reached by microwave heating, the loss of lattice water and the re-crystallization process takes place over a very short time and therefore, formation of the particles is not controlled. Under conventional heating however, $Zn(OH)_2$ decomposition takes place at a much slower rate and hence the re-crystallization process can take place uniformly.

Particle twinning is also dramatically increased in the case of microwave heating. When particles are formed under strained conditions, it is sometimes energetically favourable for atoms or ions in the lattice to adopt an alternative position.[20] When this occurs, the external shape of the crystal is altered and this is referred to as twinning. The high temperatures and pressures reached within the reaction bomb, when microwave heating is employed, causes extra strain on the growing ZnO crystals and hence a substantial amount of twinning takes place.

3.3.2.3 Why faster decomposition? As mentioned in section 3.3.2.1 above, the enhanced rate of decomposition of $Zn(OH)_2$ may not be a result of solution temperature. Solid materials can also absorb microwave energy. The means by which solids are heated using microwave energy, is related to the movement of electrons or ions through the lattice.[12] Baghurst and Mingos[11] have investigated the rate of heating of a number of inorganic oxides, including ZnO.

In section 3.3.1.3, the heating of ZnO particles as they form, is proposed as one of the reasons that the rate of growth of star-like ZnO is greatly enhanced by microwave heating. In the same way, heating of needle-like ZnO particles as they form may also contribute to the increase in the rate of decomposition of $Zn(OH)_2$. By SEM it can be

seen that the new ZnO particles begin to form on the surface of the hydroxide. If these growing ZnO particles increase in temperature due to microwave energy, they can in turn cause heating of the hydroxide particles, resulting in their decomposition.

Alternatively or complementary to that process, the $Zn(OH)_2$ particles may be susceptible to microwave energy. To our knowledge, there have been no reports to date, examining the ability of inorganic hydroxides to absorb microwaves. Zinc hydroxide particles (dry) are known to completely decompose to form ZnO at temperatures of approximately 900 °C.[21] If the $Zn(OH)_2$ rhombic particles were heated independently by the microwave energy, the high temperatures attained would cause an increase in their decomposition rate (in suspension) when compared to conventional heating processes. Some preliminary studies suggest that irradiation of dry $Zn(OH)_2$ in the microwave oven does result in absorption of microwaves and a subsequent increase in temperature. However, the temperature rise is thought to be less significant than that observed for ZnO.

3.4 CONCLUSIONS

- Using microwave energy, the heating processes are much more complex than conventional heating. Conduction, convection and radiation all contribute to increases in temperature throughout the suspension; most constituents of the mixture are being heating not only by their surroundings but also independently, by interaction with microwave energy. The interaction of growing particles, decomposing particles and the reaction solution, with the microwave radiation can result in changes in growth rates.

- **ZnO star-like particles** form when microwave heating of zinc nitrate solutions, in the presence of hydroxide ions is carried out. The particles are comparable to those

prepared when the solution is heated by conventional means, with size distributions of 4.5 to 8 μm for conventional heating and 2.5 to 10 μm by microwave heating.

- The rate of growth of ZnO particles is greatly enhanced by microwave heating, with reactions taking place over 80 times faster that those heated over an oil bath. The increased reaction rate is thought to be via two mechanisms. Firstly, microwave rotational excitation of the water molecules causes Zn^{2+} cations to become dehydrated and hence more open to attack from the other reactants (hydroxide) in solution. Secondly, the rapid heating rate of the growing ZnO particles causes pockets of high temperature in solution and hence faster growth at their surface.

- Microwave heating favourably enhances the growth of ZnO star-like particles. With no loss of control to the particle growth, ZnO stars can be produced in much shorter times.

- **ZnO needle-like particles** are the result when the reaction solution is pre-stirred at room temperature. During stirring $Zn(OH)_2$ rhombic particles precipitate and heating this suspension then results in the thermal decomposition of $Zn(OH)_2$ to form needle-like ZnO.

- The rate of decomposition of $Zn(OH)_2$ in the suspension is greatly enhanced by microwave heating; a 20 fold increase is observed. As with the formation of star-like ZnO, the enhanced rate can be attributed to the rapid heating of the growing particles. ZnO needle-like particles absorb microwave energy, increase in temperature and hence surface growth is promoted. It is suggested, that the $Zn(OH)_2$ particles may also absorb a small amount of microwave energy and thus be heated somewhat independently from their surroundings, increasing the rate at which water is lost from the lattice.

- Microwave heating, although enhancing the growth rate of needle-like ZnO growth, results in a loss of control over the reaction. The sample uniformity, which is obtained when conventional heating is used, has not been reproduced using microwave heating. The increased rate of growth using microwave heating, does not allow recrystallization in a controlled manner.

3.5 REFERENCES

1. R. A. Abramovich, D.A. Abramovich, K. Iyanar, K. Tamareselvy, *Tet. Lett.*, 1991, **32**, 5251-5254
2. F.E. Smith, E.A. Arsenault, *Talanta*, 1996, **43**, 1207-1268
3. W.H. Sutton, *Mat. Res. Soc. Symp. Proc.*, 1992, **269**, 3-20
4. D.R. Badhurst, D.M.P. Mingos, *J. Organometallic Chem.*, 1990, **384**, C57-C60
5. M.Pagnotta, A. Nolan, L. Kim, *J. Chem. Ed.*, 1992, **69**, 599-600
6. K. J. Rao, B. Vaidhyanathan, M. Ganguli, P. A. Ramakrishnan, *Chem. Mater.* 1999, **11**, 882 – 895
7. P.D. Ramesh, B. Vaidhyanathan, M. Ganguli, K.J. Rao, *J. Mater. Res.*, 1994, **2**, 3025
8. A. Puloff, A. Posner, *Science*, 1956, **124**, 583
9. B. Vaidhyanathan, K. J. Rao, *J. Bull. Mater. Sci.* 1996, **19**, 1163
10. H. Kosslich, H.L. Zutowa, U. Lohse, H. Landmesser, R. Fricke, J. Caro, *J. Ceram. Trans.*, 1997, **80**, 523
11. D.R. Baghurst, D.M.P. Mingos, *J. Chem. Soc. Chem. Comm.*, 1988, 829-830
12. D.M.P. Mingos, *Adv. Mater.*, 1993, **5**, 857-859
13. L.M. Levinson, H.A. Comanzo, W.N. Schultz, *Mat. Res. Soc. Symp. Proc.*, 1992, **269**, 311-321
14. H.K. Varma, S. Ananthakumar, K.G.K. Warrier, A.D. Damodaran, *Ceramics International*, 1996, **22**, 53-56
15. Information obtained from Sanyo Ireland Ltd.
16. M.N. Fuller, *J. Appl. Phys.*, 1944, **15**, 164

17. T.P. Dirske, C. Postmus, R. Vandenbosch, *J. Am. Chem. Soc.*, 1954, **76**, 6022-6024
18. C.J.J. Den Ouden, R.W. Thompson, *J. Colloid Interface Sci.*, 1991, **143**, 77
19. J.K. Wood, *J. Chem. Soc.*, 1910, **97**, 878
20. J.C. Brice, *Crystal Growth Processes*, John Wiley & Son, Blackie & Son, Glasgow, 1986
21. *Comprehensive Inorganic Chemistry Vol. 3,* Ed J.C. Bailar, H.J. Emeléus, R. Nyholm, A.F. Trotman-Dickenson, Pergamon Press, Oxford, 1975

Chapter 4

Alternative hydrothermal preparation methods for ZnO microparticles.

4.1 INTRODUCTION

The preparation of uniform metal oxide particles by a number of different methods has been described in literature. In this chapter, the urea hydrolysis method and forced hydrolysis by hexamethylenetetraamine (HMT) will be discussed.

4.1.1 Urea hydrolysis.

By taking advantage of the thermal decomposition of urea at elevated temperatures, metal oxide particles can be produced with a relatively narrow size distribution. In a neutral solution, the urea decomposition reaction takes places as follows:

$$CO(NH_2)_2 + 3\ H_2O \rightarrow 2\ NH_4^+ + 2\ OH^- + CO_2 \qquad \text{equation 4.1}$$

The urea acts as a reservoir for hydroxyl ions, which are slowly released into the reaction mixture and react with metal ions to give a metal hydroxide / oxide. This urea hydrolysis method has been used to produce a number of different metal oxides and hydroxides, such as zinc oxide,[1] nickel hydroxide,[2] iron oxyhydroxide,[3] zirconia[4] and mixed oxides systems.[5, 6] Soler-Illia *et al*[7] have published a review of the method.

Tsuchida and Kitajima[1, 8] used the urea hydrolysis method to prepare ZnO. By ageing a zinc salt in the presence of urea at 95°C, they showed that using zinc sulphate resulted in rod-like ZnO and zinc nitrate gave rise to needle-like ZnO. Variations of this method can also be found in literature,[9, 10] whereby a basic zinc carbonate is formed by urea hydrolysis at lower temperatures (usually 90°C) and then thermally decomposed to form zinc oxide. The basic carbonate forms as follows:

$$CO(NH_2)_2 + OH^- + H_2O \rightarrow CO_3^{2-} + NH_3 + NH_4^+ \qquad \text{equation 4.2}$$

$$5\,Zn^{2+} + 2\,CO_3^{2-} + 6\,OH^- \rightarrow 2ZnCO_3.3Zn(OH)_2 \qquad \text{equation 4.3}$$

The urea in solution reacts with some of the hydroxide that is released during the urea decomposition reaction, to produce a carbonate ion and so competes with the ZnO formation reaction. These carbonate ions go on to react with more hydroxyl ions and zinc cations to form a basic zinc carbonate.

When the basic carbonate, of general formula $Zn_5C_2O_{12}H_6$, is formed from zinc sulphate heptahydrate, rod-like crystals result. On heating, the basic carbonate decomposes to ZnO and if the decomposition is carried out at a slow rate, the particles can retain their morphology, hence producing rod-like ZnO.[9] Therefore, this method is also regarded as a good route to uniform particle formation. In this chapter, however, only the direct formation of ZnO will be studied. The method employed by Tsuchida and Kitajima[1] will be followed using zinc sulphate solutions and the effect of ageing time on the particle size distribution will be reported.

4.1.2 Forced hydrolysis - complex formation with HMT.

In the forced hydrolysis procedure, an aqueous metal salt solution is aged at elevated temperatures and the hydrated metal ion slowly deprotonates to form a metal hydrous oxide. However, in the case of some metal ions, which are not easily hydrolysed, a small amount of base is added to increase the pH and hence encourage deprotonation. It has been shown that the base employed can have a marked effect on the morphology of the precipitated oxide and hydrous oxide particles and there have been a number of studies carried out examining the effects of the base on various metal systems. Matijevic and co-workers have published numerous papers on this subject,[11, 12] one particularly dealing with the effects of bases on ZnO formation.[13]

The organic base can also play a second role in the system. When a metal salt solution is mixed with an organic base, (usually an amine), a metal-base complex is formed. Thermal decomposition of this complex results in the slow release of metal ions into solution, thus allowing a slow and controlled growth of metal oxide particles. This method has been extensively studied for zinc oxide formation, using a number of different organic bases. Nishizawa *et al*[14] showed how the thermal decomposition of a Zn-EDTA complex resulted in needle-like crystals and O'Brien and co-workers[15] investigated the role of EDTA, TEA and various other organic bases in ZnO and ZnS systems. For the purposes of this study the use of HMT for ZnO production will be examined. The structure of HMT is as follows:

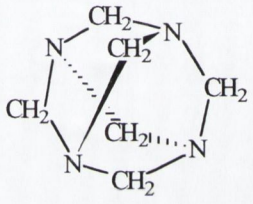

Figure 4.1 Structure of hexamethylenetetraamine (HMT).

Andres-Verges *et al*[16] and Fujita *et al*[17] reported rod-like and needle-like ZnO respectively by ageing zinc salts in the presence of HMT.

The only report to date of the growth stages of uniform ZnO crystals from salt solutions is from the ZnO-HMT system. Andres-Verges *et al*[16] have shown that ZnO rods grow from an addition of smaller particles to each other, aggregating along the c-axis. These reactions were carried out using HMT and zinc nitrate, heated in sealed tubes. In this chapter, the HMT particle growth study will be repeated and the effects of heating in an unsealed vessel and of microwave treatment will be studied.

4.1.3 Aims.

ZnO rod-like particles will be produced by two methods, previously reported in the literature. Firstly, urea hydrolysis will be carried out on zinc sulphate solutions, yielding uniform ZnO particles and the effect of ageing times will be determined. Secondly, the growth of ZnO particles will be followed using HMT forced hydrolysis of zinc nitrate solutions. Also, for the first time, microwave heating will be applied to this method. A comparison will be drawn between particles formed by conventional heating and those produced using microwave heating techniques.

4.2 RESULTS

4.2.1 Urea hydrolysis.

To a dilute aqueous zinc sulphate heptahydrate solution (1×10^{-3} M), a urea solution (0.03 M) was added. The mixture was then heated with a ramp of approximately 0.5 °C / min until a temperature of 95 °C was reached. The method is similar to that outlined by Tsuchida and Kitajima.[1, 8] The white precipitate (which forms at approximately 90 °C) was aged (held) at 95 ± 2 °C in the solution for given times. After filtration, the white solid was studied by SEM, XRD and light microscopy. The effect of ageing time on the size, morphology and composition of the samples was studied.

4.2.1.1 Particle morphology and composition. XRD data for particles produced when the zinc sulphate solution was aged for three hours in the presence of urea can be seen in Figure 4.2. The diffraction data was matched to library data and is found to be consistent with that of ZnO, zincite (Appendix I). Figure 4.3 shows the SEM of the same particles. The hexagonal prismatic nature of the ZnO particles is clearly evident in the rod-like morphology. The morphology and composition of the particles produced is seen to be independent of length of time for which the sample is aged at 95 ± 2 °C.

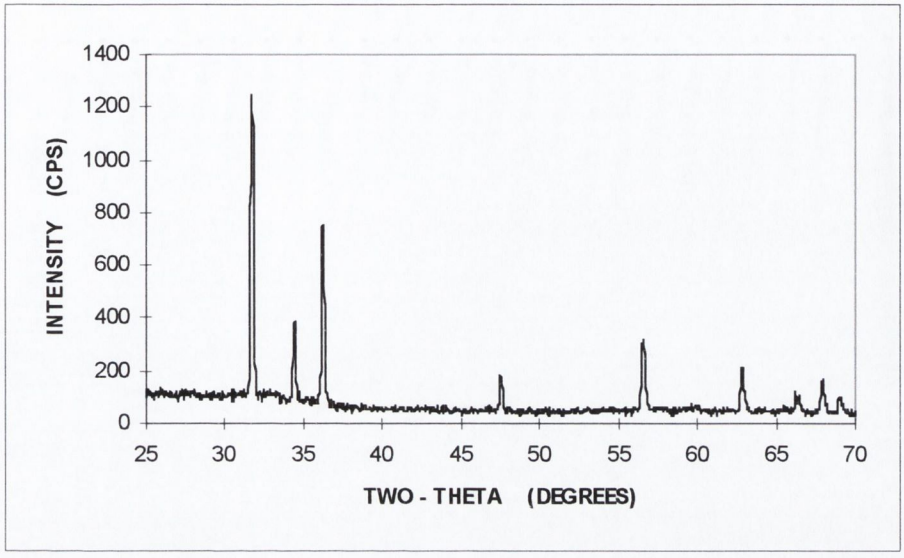

Figure 4.2 XRD pattern of precipitate formed from zinc sulphate heptahydrate (1×10^{-3} M) and urea (0.03 M) heated at 0.5 °C / min. then aged for 3 hours at 95 ± 2 °C.

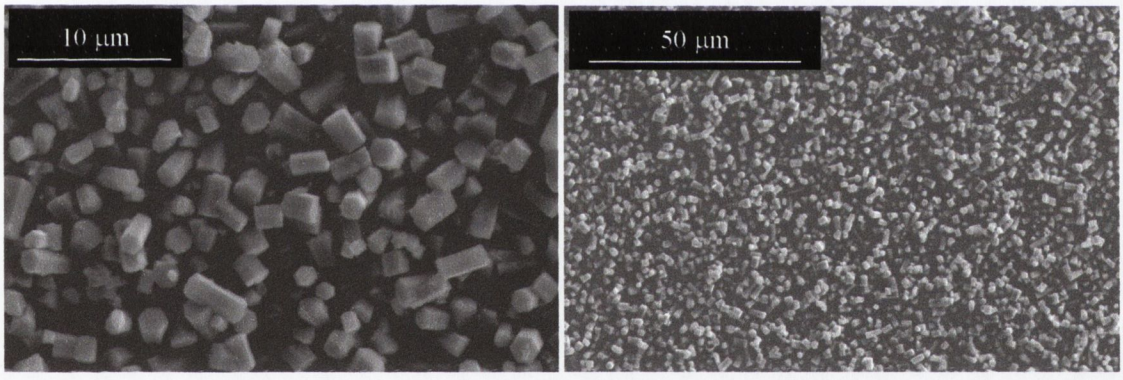

Figure 4.3 SEM of precipitate formed from zinc sulphate heptahydrate (1×10^{-3} M) and urea (0.03 M) heated at 0.5 °C / min. then aged for 3 hours at 95 ± 2 °C.

4.2.1.2 Effect of ageing time. By altering the ageing time at 95 ± 2 °C, the particle size distributions and yield can be altered. Table 4.1 outlines the effect of increasing ageing time.

Table 4.1 Effect of ageing time on particles produced by the urea hydrolysis method.

Ageing time (hours)	Composition and morphology	Mean particle length (μm)	Length distribution (μm)	Mean particle width (μm)	Width distribution (μm)	Average yield
1	Rod-like ZnO	3.0	2.3 - 3.9	1.4	0.9 – 1.9	4 mg, 20 %
3	Rod-like ZnO	5.0	2.5 – 6.5	1.3	0.9 – 1.7	13 mg, 65 %
5	Rod-like ZnO	5.0	3.0 – 6.0	1.3	0.9 – 1.8	16 mg, 80 %

The size distribution of samples was estimated by measuring approximately 150 particles, using light microscopy. Figure 4.4 shows the image of particles, which were aged for three hours, under the light microscope. The particle size distributions reported in Table 4.1 can be seen in Figure 4.5 below. A comparable scale is used in all cases except for the length of particles prepared after 1 hour ageing. This scale is smaller due to the narrow size distribution obtained in that case.

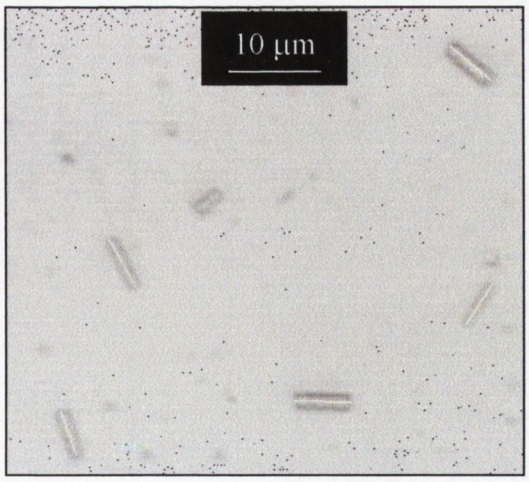

Figure 4.4 Precipitate formed from zinc sulphate heptahydrate (1×10^{-3} M) and urea (0.03 M) heated at 0.5 °C / min. then aged for 3 hours at 95 ± 2 °C, imaged by light microscopy.

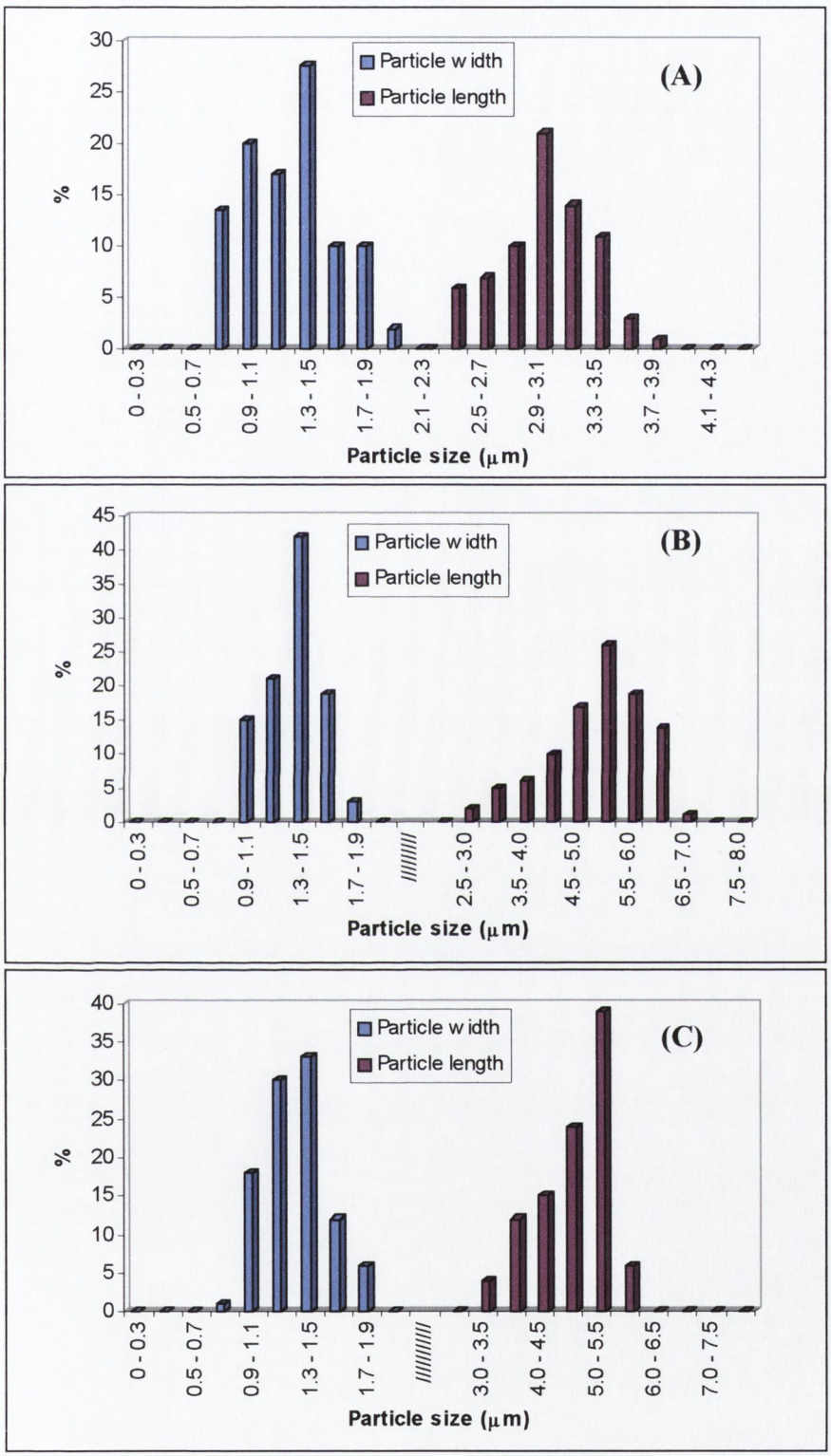

Figure 4.5 Size distributions of precipitate formed from zinc sulphate heptahydrate (1×10^{-3} M) and urea (0.03 M) heated at 0.5 °C / min. then aged for (A) 1 hour, (B) 3 hours and (C) 5 hours, at 95 ± 2 °C.

4.2.1.3 Effect of ageing temperature. If the ageing temperature is not held constant at 95 ± 2 °C and drops to around 90 °C for any length of time, a mixed sample of ZnO and zinc basic carbonate is formed. An example of such a sample can be seen in Figure 4.6. The carbonate formed appears to have no defined morphology.

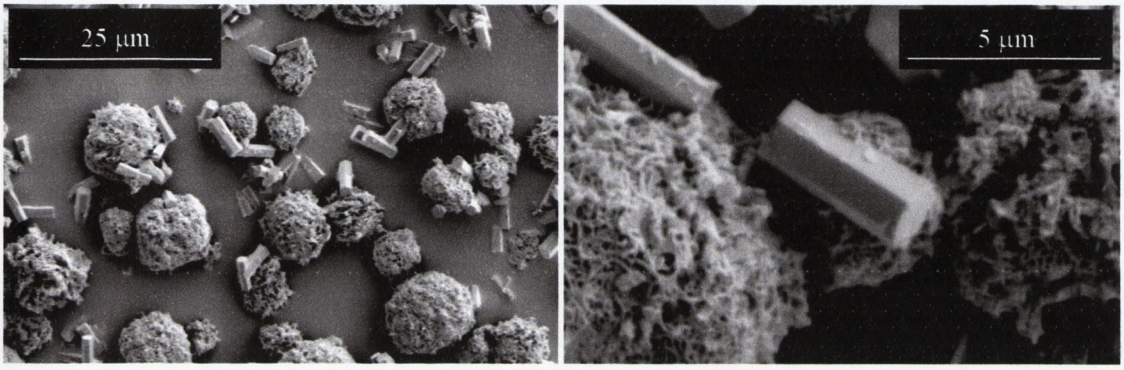

Figure 4.6 SEM of precipitate formed from zinc sulphate heptahydrate (1 x 10^{-3} M) and urea (0.03 M) heated at 0.5 °C / min. then aged for 3 hours at 95 ± 5 °C.

The XRD pattern for this sample is shown in Figure 4.7. This pattern shows both ZnO (zincite), the peaks for which are marked with an asterisk (*) and a basic zinc carbonate (hydrozincite, see Appendix 3), which accounts for the remaining peaks. The zinc basic carbonate however is only partially crystalline.

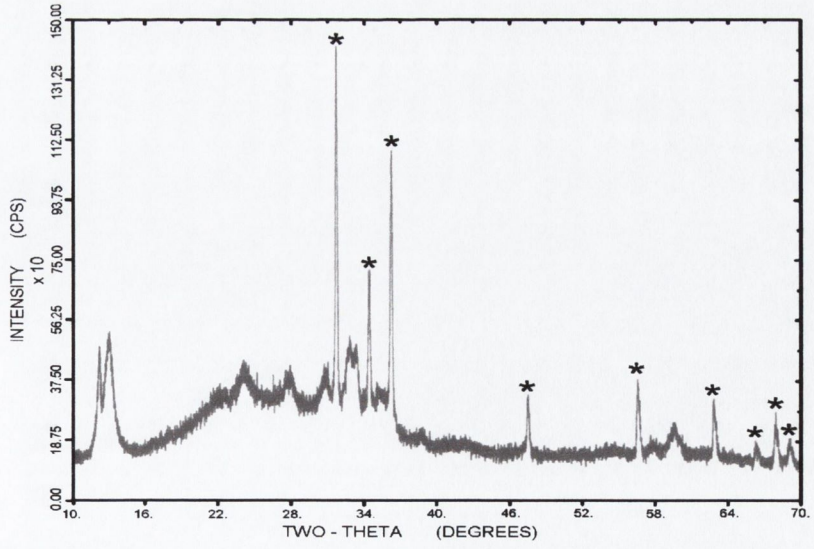

Figure 4.7 XRD pattern of precipitate formed from zinc sulphate heptahydrate (1 x 10^{-3} M) and urea (0.03 M) heated at 0.5 °C / min. then aged for 3 hours at 95 ± 5 °C, (* = peaks due to ZnO).

4.2.2 Forced hydrolysis using HMT.

ZnO particles were prepared from a zinc nitrate solution (0.05 M, 250 ml) and HMT solution (0.05 M, 250 ml) at pH 5. The method is that used by Andres-Verges *et al*[16] with the exception that heating was carried out in open vessels under reflux conditions, as opposed to sealed vessels. However, when microwave heating was used, the reaction was carried out in sealed Teflon® bombs.

4.2.2.1 ZnO formation from HMT – Conventional heating. Zinc nitrate and HMT were heated together in a round-bottomed flask. After turbidity (approximately twenty minutes heating), the samples were aged at 100 °C; ageing times therefore refer to time after turbidity. Figure 4.8 shows the XRD pattern obtained for a sample aged for 30 minutes at 100°C. This sample is seen to be ZnO, consistent with the zincite structure.

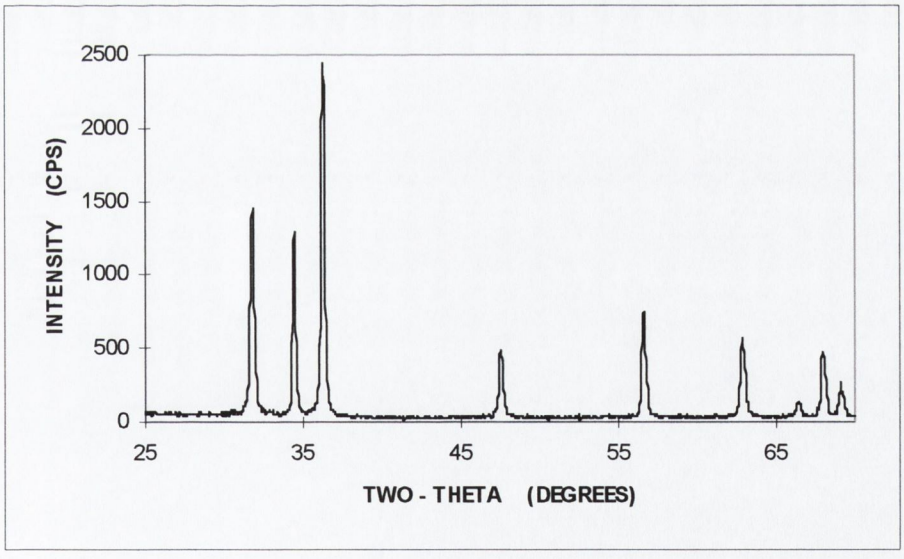

Figure 4.8 XRD pattern obtained for a sample prepared from $Zn(NO_3)_2.6H_20$ (0.05 M) and HMT (0.05 M) aged for 30 minutes at 100°C and pH 5.0.

Figure 4.9 shows these particles, aged for 30 minutes, as observed under SEM. A rod-like morphology is clearly observed, in agreement with that seen by Andres-Verges *et al.*[16] Some twinning of the crystals can also be observed.

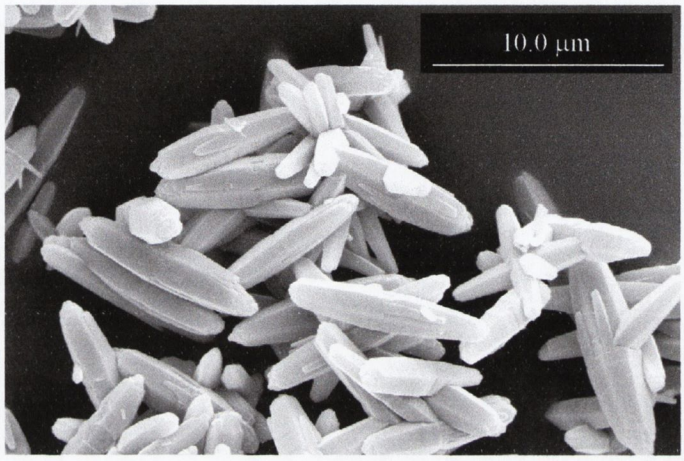

Figure 4.9 SEM of ZnO sample prepared from $Zn(NO_3)_2.6H_20$, (0.05 M) and HMT (0.05 M) aged for 30 minutes at 100 °C and pH 5.0.

In order that the growth of these particles could be monitored, samples were removed from the suspension at given times during the reaction and analysed by XRD and SEM. All samples gave XRD patterns consistent with ZnO (zincite). Figure 4.10 shows the formation of the rod-like particles by SEM, from precipitation (turbidity) to 30 minutes ageing after precipitation.

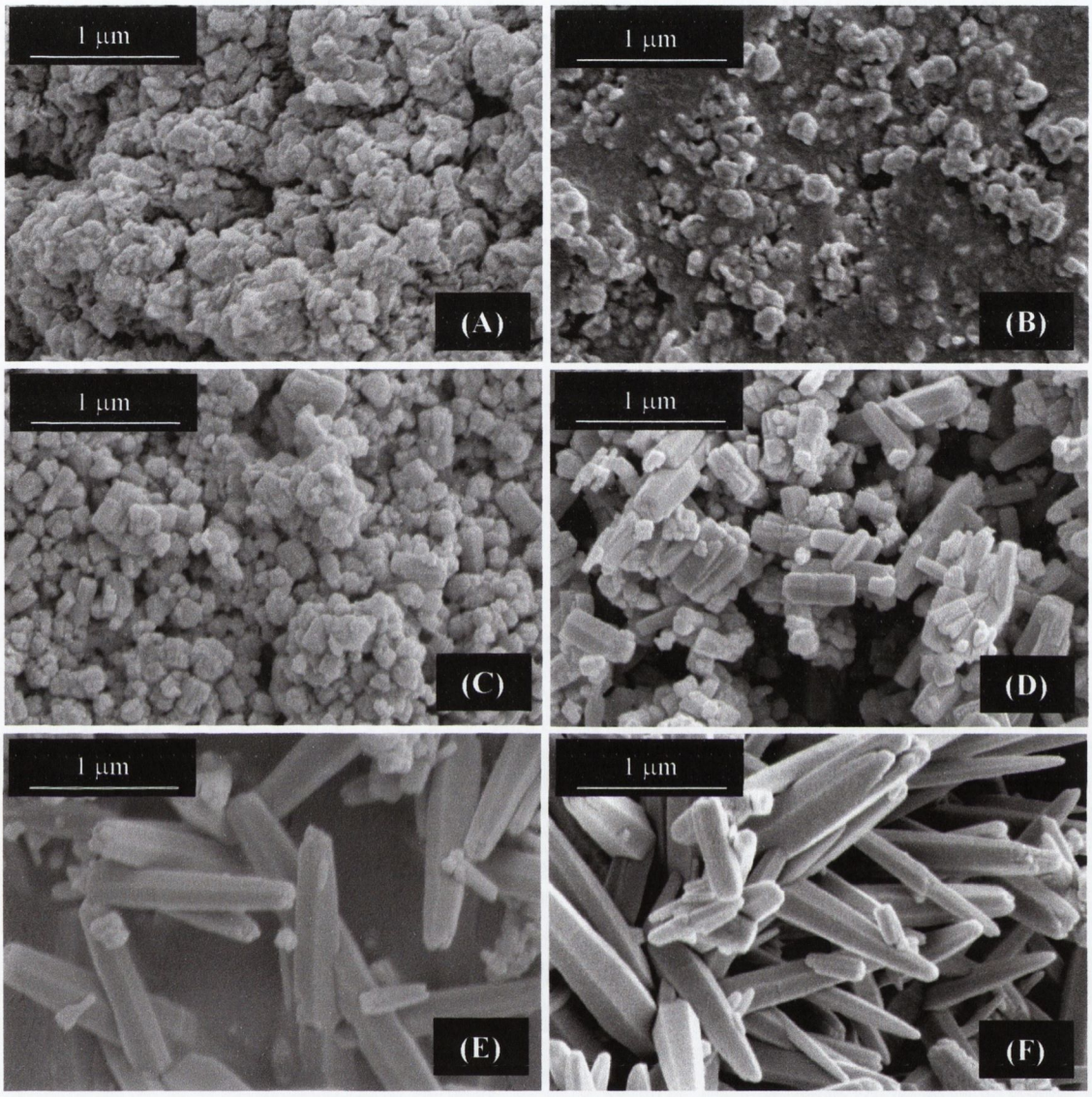

Figure 4.10 Growth of ZnO particles from $Zn(NO_3)_2.6H_20$, (0.05 M, 250 ml) and HMT (0.05 M, 250 ml) at (A) precipitation, (B) after 3 minutes, (C) 6 minutes, (D) 10 minutes, (E) 20 minutes, (F) 30 minutes, ageing at 100 °C and pH 5.0.

The formation of the rod-like particles appears to begin between approximately six and ten minutes ageing. Figure 4.11 shows one of the particles from Figure 4.10(D) at higher magnification. A ridge in the middle of the particle, indicating particle addition, can be seen clearly.

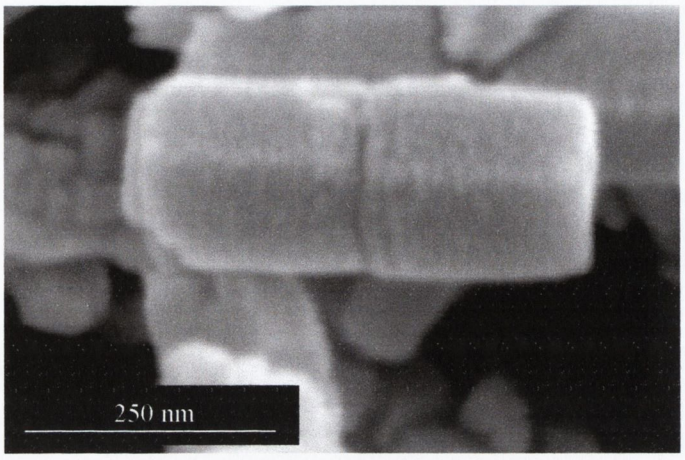

Figure 4.11 ZnO formed from $Zn(NO_3)_2.6H_20$, (0.05 M) and HMT (0.05 M) aged for 10 minutes at 100 °C and pH 5.0.

4.2.2.2 ZnO formation from HMT complex – Microwave heating. A similar experiment was carried out, on a smaller scale, using a microwave heat source. $Zn(NO_3)_2.6H_2O$ (0.05 M, 40 ml) and HMT (0.05 M, 40 ml) were added together in a Teflon® bomb, which was then sealed and heated at different power settings for up to fifteen minutes.

Similar to conventional heating, all particles produced using a microwave heat source also showed a zincite crystal structure by XRD. Table 4.2 below summarises the effect of microwave power settings and heating times on the particles produced. Reactions were also carried out for five minutes; however, no precipitate had formed after that time at any of the power settings.

Table 4.2 Effect of microwave power and heating time on ZnO particles produced from $Zn(NO_3)_2.6H_2O$ (0.05 M, 40 ml) and HMT (0.05 M, 40 ml).

Power (W)	Heating time (mins)	ZnO Morphology	Yield
150	10	Spherical-type aggregates	12 mg / 7 %
	15	Rod-like	63 mg / 39 %
300	10	Rod-like	144 mg / 88 %
	15	Rod-like	130 mg / 80 %
450	10	Rod-like	136 mg / 84 %
	15	Rod-like	120 mg / 74 %

In all the cases reported above, where rod-like ZnO particles were produced, the samples had a broad size distribution. Examples of the rod-like particles can be seen in Figure 4.12. The particles produced when the reaction mixture was heated for fifteen minutes at 300 and 450 W are both seen.

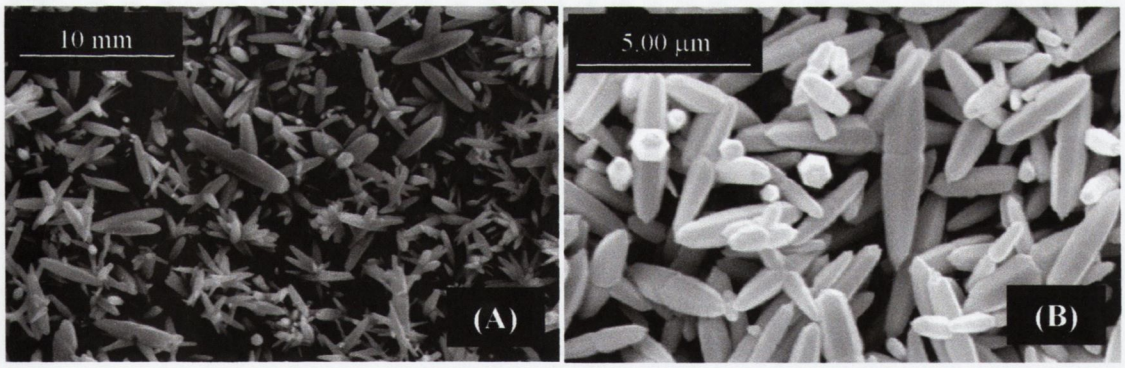

Figure 4.12 ZnO particles produced from $Zn(NO_3)_2.6H_2O$ (0.05 M, 40 ml) and HMT (0.05 M, 40 ml) heated for fifteen minutes at (A) 300 W and (B) 450 W.

Spherical-type aggregate particles were produced following heating at 150 W for ten minutes, with rod-like particles the result after fifteen minutes. Figure 4.13 shows the particles formed at 150 W after ten and fifteen minutes.

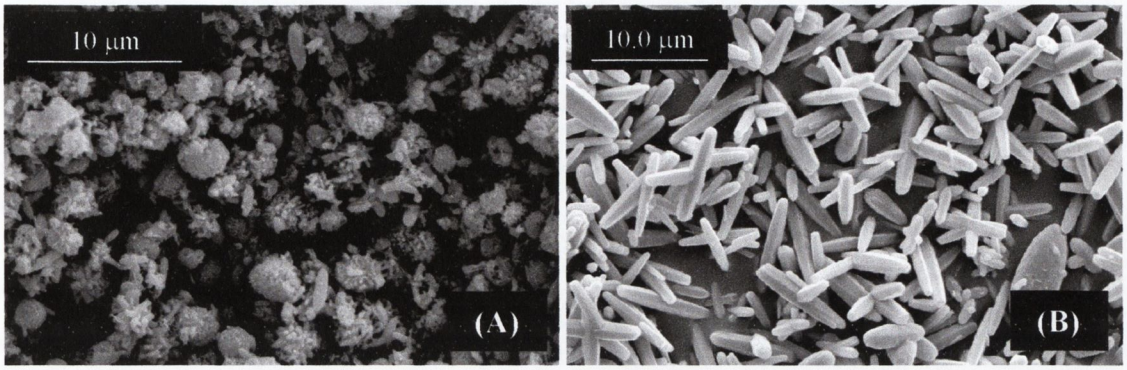

Figure 4.13 Particles produced from $Zn(NO_3)_2.6H_2O$ (0.05 M, 40 ml) and HMT (0.05 M, 40 ml) heated at 150 W for (A) 10 and (B) 15 minutes.

There is evidence to suggest that particles grow by aggregation of smaller sub-units. This can be seen in Figure 4.14 below, where ridges through the centre particles indicate addition of smaller particles to each other. This particle aggregation was seen at all power settings.

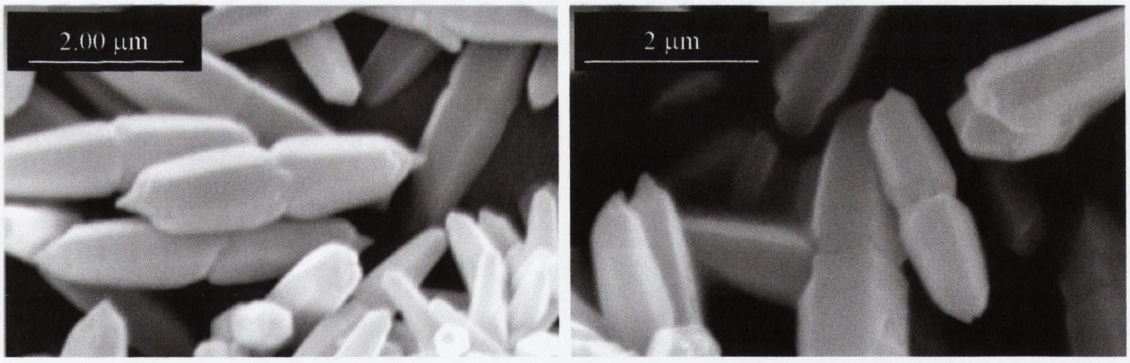

Figure 4.14 Particles produced from $Zn(NO_3)_2.6H_2O$ (0.05 M, 40 ml) and HMT (0.05 M, 40 ml) heated at 450 W for 15 minutes.

4.3 DISCUSSION

The formation of ZnO particles by urea hydrolysis[1, 8, 9] and by HMT forced hydrolysis[16, 17] have both been studied. For urea hydrolysis, reaction conditions used were similar to those reported by Tsuchida and Kitajima,[1] to produce rod-like ZnO particles. Also, the growth study of ZnO rod-like particles by HMT forced hydrolysis, carried out Andres-Verges *et al*[16] was repeated, altering the method by which the reaction was heated.

4.3.1 Urea hydrolysis.

In agreement with literature,[1, 8] the urea hydrolysis method was shown to form uniform particles of ZnO. The urea decomposition reaction acts as a reservoir, slowly releasing hydroxyl ions into the solution. In order that only one burst of nuclei takes place, the initial concentration of the zinc sulphate is kept low (1×10^{-3} M), in accordance with LaMer's theory.[18]

4.3.1.1 Formation of rod-like particles. Direct formation of ZnO took place following the decomposition of urea at elevated temperatures in the presence of zinc sulphate. At approximately 90 °C, the solution became turbid. As the initial concentrations of $ZnSO_4.7H_2O$ in solution are very low, this initial turbidity results from the precipitation of a very small amount of material (< 1 mg). For this reason, no characterisation was carried out on the initial precipitate. After one hour at 95 ± 2 °C however, sufficient precipitate had formed (approximately 4 mg) and was characterised by SEM and XRD. The sample composition was found to be ZnO (zincite) with a rod-like morphology, as is seen in Figure 4.3. In a similar manner to other methods studied (Chapters 2 and 3), this hexagonal prismatic morphology is expected, as the zincite crystal lattice is hexagonal, with an *a:c* ratio of 1:1.6.[19]

4.3.1.2 Effect of ageing times on ZnO particles. Ageing of the urea / zinc sulphate solutions at 95 ± 2 °C was subsequently carried out for times longer than one hour. The SEM and XRD data suggest no change in the particle morphology or crystal structure with longer ageing times, SEM shows rod-like particles and XRD data shows patterns for ZnO. The size of the particles and the yield however, were affected by ageing time. The yield increased from 20% at one hour ageing to 80% after five hours ageing.

The particle size distribution was estimated by measuring particles under a light microscopy (Figure 4.4). Approximately one hundred and fifty particles were measured per sample. With increasing time, the width of particles was seen to remain at an average of 1.3 to 1.4 μm, with a width distribution also remaining relatively unchanged. The average length of the ZnO particles formed increased from 3.0 μm after one hour to 5.0 μm after 3 hours ageing. After one hour ageing, the aspect ratio of the particles is approximately 2.1, slightly more than the axial ratio (1:1.6) and after three hours ageing, the aspect ratio has increased to 3.8, just over twice that of the axial ratio.

It is expected that enhanced growth in the c-axis direction will take place, due to the nature of the ZnO lattice, i.e. polarity along the c-axis. The c-axis layers of a ZnO lattice consist of one type of ion only, Zn^{2+} or O^{2-}, whereas all other axes of the crystal consist of both (see Chapter 1, Figure 1.2). A layer containing only one species will have an effective charge and hence the growing crystal will consist of positively and negatively charged opposite ends of the c-axis, in order that a net neutral charge is maintained. These charged ends of the crystal causes polarity along the c-axis and thus growth is promoted in that direction.

When ageing is increased from three to five hours, the mean length (and hence the aspect ratio) of the particles does not change, however, the length distribution does decrease slightly from 2.5 – 6.5 to 3.0 – 6.0 μm. A self-sharpening process accounts for this narrowing of the size distribution. Self-sharpening[20] occurs because the smaller

particles present in the suspension can grow at a faster rate than the larger ones. In this way, the size distribution of the particles produced narrows. The reduction in size of the largest particles is attributed to dissolution.

4.3.1.3 Effect of ageing temperature – formation of zinc basic carbonate. If the temperature at which the urea / zinc sulphate solution is aged is not controlled accurately, zinc basic carbonate is formed alongside the rod-like ZnO. Carbonate anions are present in solution as a product of urea decomposition. These carbonate ions react with the zinc ions and hydroxide ions to give zinc carbonate species.

It is assumed that the non-uniform particles observed under SEM (Figure 4.6) are those of the carbonate. XRF studies were carried out in an attempted to differentiate between the ZnO and the carbonate but as a graphite coating had to be used on the samples, the % carbon calculated for both were similar and the results were inconclusive.

The basic carbonate has the general formula $Zn_5C_2O_{12}H_6$ but can take on many different forms. In this case, the form observed is thought to be zinc carbonate hydroxide (hydrozincite), $2ZnCO_3.3Zn(OH)_2$. This carbonate type was identified by its XRD pattern. Although the non-uniform particles could always be seen by SEM when the temperature ageing was inadequately controlled, an XRD was only obtained for the carbonate in some cases because the crystallinity of the sample was very poor. When an XRD pattern was obtained, the peaks were broad and ill defined, with some peaks indistinguishable from noise. Appendix III shows the library data for hydrozincite, overlaid on the pattern seen in Figure 4.7.

Castellano and Matijevic[9] observed that by controlling the ageing temperature of the solution at 90 °C instead of 95 °C, the basic carbonate could be formed with a uniform morphology. In this study however, as the carbonate resulted from a lack of control over

the ageing temperature, it appears to have formed with no defined morphology. Thermal decomposition of the zinc basic carbonate to form ZnO in these samples would therefore produce a sample of ZnO with both rod-like particles and non-uniform particles also.

4.3.1.4 Comparison with literature. As Tsuchida and Kitajima[1] did not change urea, zinc salt or ageing times independently of each other, it is difficult to compare results. They did report the rod-like morphology of the ZnO particles and the existence of a zinc carbonate, which they identified as a hydrated zinc carbonate, $4ZnO.CO_2.4H_2O$. The XRD pattern observed in this study however, was a better match with basic zinc carbonate, hydrozincite, $Zn_5(CO_3)_2(OH)_6$. In both this study and that carried out by Tsuchida and Kitajima[A], the zinc carbonate was of low crystallinity. As the XRD patterns for both the hydrated zinc carbonate and of the basic zinc carbonate are very similar, positive identification is difficult.

Tsuchida and Kitajima[1] did not report size distributions for ZnO particles, however, average sizes were given. They reported an average particle size of 1.9 x 4.3 μm for an experiment involving 0.05 M urea and no ageing. In this study, an average size of 1.4 x 3.0 μm was obtained, with a urea concentration of 0.03 M and 1 hour ageing. All other experimental details were the same, (Table 4.1).

4.3.2 HMT forced hydrolysis – Conventional heating.

Using the optimum reaction conditions reported by Andres-Verges *et al*,[16] the growth of ZnO rod-like particles from zinc salt and HMT solutions was followed, heated under reflux conditions.

4.3.2.1 Rod-like particle growth. The growth of ZnO rod-like particles was studied by heating $Zn(NO_3)_2.6H_2O$ (0.05 M, 250 ml) with HMT (0.05 M, 250 ml) to reflux

temperature (~ 100 °C). After approximately twenty minutes heating, the solution became turbid. The turbidity is a result of the precipitation of ZnO. The suspension was then aged for up to thirty minutes after turbidity and particles were removed from the reaction at regular intervals. All samples showed an XRD pattern consistent with zincite.

Figure 4.10 shows the growth of the particles followed by SEM. At precipitation, the sample consists of aggregates of smaller spherical type particles (100 to 200 nm). After three minutes ageing no change is seen in the particles. However, after six and ten minutes, a rod-like morphology is observed along with the spherical type particles. At higher magnification, (Figure 4.11), it can be seen that these rod-like particles are formed by directional aggregation of the spherical type particles. These sub-units appear to aggregate along the c-axis of the ZnO lattice. This c-axis aggregation can be attributed to the net polarity of the lattice in that direction (as discussed above) and is in agreement with what was observed by Andres-Verges *et al.*[16] Over the next twenty minutes the rod-like particles increase in size and by thirty minutes ageing, the particles are up to 10 μm in length. The sample, however, remains with a quite broad size distribution (approximately 2 – 10 μm).

4.3.2.2 Comparison with literature. In this study, growth of ZnO was seen to occur by directional aggregation. This was in agreement with that observed by Andres-Verges *et al.*[16] They found that the spherical ZnO particles began to couple between three and seven minutes and that after thirty minutes, well defined rod-like particles had formed.

The particle growth in this study was also seen to take place by the same method. Precipitation resulted in the formation of spherical particles, which, during three to six minutes ageing at 100 °C, aggregated along the c-axis to form rod-like crystals. The distributions of sample size after 30 minutes ageing appeared to be narrower in the case

of Andres-Verges *et al*[16] but the average particle size was smaller, at only 2 μm. However, as no exact particle dimensions are reported, comparison is difficult. The only differences in experimental procedure between this study and that of Andres-Verges *et al*,[16] is that they heated the solutions in tightly stoppered flasks rather than heating under open reflux conditions. Fujita *et al*[17] also prepared ZnO by HMT forced hydrolysis using acidified zinc chloride solutions and observed needle-like ZnO of 5 μm in size and globular particles 1 μm in size.

4.3.3 HMT forced hydrolysis – microwave heating.

In this method, $Zn(NO_3)_2.6H_2O$ (0.05 M, 40 ml) and HMT (0.05 M, 40 ml) were added together in a Teflon® digestion bomb, sealed and heated at different power settings for up to fifteen minutes. All samples prepared had XRD patterns consistent with ZnO (zincite).

4.3.3.1 Effect of microwave power and ageing times. Solutions were heated for five, ten and fifteen minutes at each power setting (150, 300, 450 W). In all cases, no precipitate had formed after five minutes. After ten minutes at 300 and 450 W, rod-like particles of ZnO had formed; however, at 150 W, spherical particles were present. After fifteen minutes heating at all settings, rod-like ZnO resulted. The size distributions in all cases were quite broad (approximately 1 – 8 μm). It can therefore be concluded that the only difference between the different power settings is the rate at which the particles grow, a product of the increased rate of heating.

The reaction takes place by deprotonation of the hydrated Zn^{2+} cation in solution and also thermally decomposing any HMT-Zn complex that may have formed in the solution, releasing Zn^{2+} into the solution for controlled growth. It is therefore reasonable to assume, that an increased heating rate, caused by an increase in microwave operating power, will result in a decrease in the reaction time.

4.3.3.2. Growth of ZnO particles. In section 4.3.2.1, the growth of ZnO rod-like particles in the presence of HMT was discussed. In agreement with a previous study,[16] it was confirmed that these particles grow by a directional aggregation of spherical sub-units, approximately 100 to 200 nm in size. The directional aggregation takes place along the c-axis and is evident by the ridges seen on the surface of the particles perpendicular to the c-axis of the hexagonal structure.

By microwave heating procedures it can also be shown that the ZnO particles are forming by this mechanism. After ten minutes heating at all power settings, ridged particles are observed (Figure 4.14). For 300 and 450 W, no precipitate is observed after five minutes and rod-like particles are formed after ten minutes. This implies that between five and ten minutes the spherical particles must precipitate and aggregate to form the rod-like particles. This process is slower at 150 W however. Again, no precipitate is observed after five minutes. In contrast to the higher power settings, after ten minutes the spherical particles are observed, with only a small amount of directional aggregation having taken place. This means that precipitation and aggregation takes place at a slower rate at 150 W than at 300 or 450 W. Between ten and fifteen minutes, the spherical particles have fully aggregated to form rod-like ZnO. This slower rate of particle formation can be attributed to the slower rate of heating at lower power settings.

4.3.3.3 Conventional *vs.* microwave. The reactions that are discussed in section 4.3.2 differ from these experiments only in the heating method. Direct comparisons between conventional and microwave heating methods can therefore be drawn. Table 4.3 outlines the differences between the two methods.

Table 4.3 Comparison of conventional and microwave heating for ZnO particle formation from $Zn(NO_3)_2.6H_2O$ (0.05 M) and HMT (0.05 M).

Heating method	Turbidity	Rod-like particle formation	Size distribution
Oil bath (101 °C)	20 mins	40 mins	2 – 10 μm
150 W DMO	5 – 10 mins	15 mins	1 – 8 μm

By conventional heating methods, precipitation takes place after around twenty minutes heating. Six minutes after turbidity, spherical particles are beginning to aggregate to form rod-like ZnO and after ten minutes the rod-like morphology is clearly visible. By twenty minutes ageing the ZnO rods have fully formed, giving a total heating time of around forty minutes. In the microwave experiment, precipitation, aggregation and rod-like particle growth has taken place within fifteen minutes, even at the lowest power setting. Therefore the reaction time is decreased approximately three fold.

In both cases, the reaction mixture consists of hydrated zinc ions which slowly deprotonate to form ZnO. HMT has two roles in the reaction; firstly, it acts as a base to increase the pH of the solution and encourages deprotonation and secondly, it forms a complex with Zn^{2+}. The thermal decomposition of this complex leads to a slow release of Zn^{2+} into solution and hence, controlled particle growth.

Microwave energy may disrupt both of these processes in the reaction. As was discussed in Chapter 3 (section 3.3.1.3), microwave rotational energy can interfere with the aquation sheath surrounding a hydrated ion in solution, resulting in the presence of a partially exposed cation that can react more readily than its fully hydrated equivalent. In the same way, it is possible that microwave energy could cause the Zn-HMT complex to be disturbed. Both of these effects would be expected to enhance the reaction rate when compared to conventional heating. However, the primary influence on this enhanced rate of particle growth is the rapid rate of heating achieved using microwave energy.

Boiling point is reached after around 30 to 35 minutes under conventional heating methods, whereas using microwave power, boiling point and above is reached within 15 minutes, even at the lowest power setting. As the rate of heating is over 2.5 times faster and ZnO particle growth depends on thermal decomposition of the Zn-HMT complex, it would be expected that the growth rate would be enhanced by the same degree.

4.4 CONCLUSIONS

- **Urea hydrolysis** can be used to produce a uniform sample of ZnO rod-like particles with a narrow size distribution. By increasing the ageing time of the reaction, the average particle length can be increased.

- A rigid control must be kept on the ageing temperature, as semi-crystalline zinc basic carbonate can form as a side product if the temperature drops to 90 – 92 °C for any length of time.

- The urea hydrolysis method has the disadvantage that it affords a small amount of product (~ 16 mg), even when almost 80% yield is achieved. This is due to the dilute concentration of the zinc salt and it therefore means that applications of the uniform particles are limited.

- **Forced hydrolysis using HMT** proved also to be a successful route to ZnO rod-like particles. In agreement with literature, it was found that the particles grew by directional aggregation of spherical subunits in the c-axis direction.

- By heating the reaction using a microwave oven, the same growth process was observed, with aggregation of the spherical particles along their c-axes. The reaction time was enhanced using microwave heating procedures, decreasing the total heating time by nearly three fold at the lowest power setting.

4.5 REFERENCES

1. T. Tsuchida, S. Kitajima, *Chem. Lett.*, 1990, 1769-1772
2. G.J. de A.A. Soler-Illia, M. Jobbagy, A.E. Regazzoni, M.A. Blesa, *Chem. Mater.*, 1999, **11**, 3140-3146
3. A. Kajiyama, T. Nakamura, *Colloid Surface A*, 2000, **163**, 301-307
4. Y.X. Huang, C.J. Guo, *Powder Technol.*, 1992, **72**, 101-104
5. M. Dixit, G.N. Subbanna, P.V. Kamath, *J. Mater. Chem.*, 1996, **6**, 1429-1432
6. B.M. Reddy, S.S. Madhavendra, E.P. Reddy, *Indian J. Chem. Technology*, 1994, **1**, 60-62
7. G.J. de A.A. Soler-Illia, M. Jobbagy, R.J. Candal, A.E. Regazzoni, M.A. Blesa, *J. Disper. Sci. Tech.*, 1998, **2-3**, 207-228
8. T. Tsuchida, S. Kitajima, *J. Mater. Sci.*, 1992, **27**, 2713-2718
9. M. Castellano, E. Matijevic, *Chem. Mater.*, 1989, **1**, 78-82
10. D. Klissurski, I. Uzunov, K. Kumbilieva, *Thermochimica Acta*, 1985, **93**, 485-488
11. E. Matijevic, *Chem. Mater.*, 1993, **3**, 412-426
12. E. Matijevic, *Faraday Discuss.*, 1991, **92**, 229-239
13. Chittofratti, E. Matijevic, *Colloids and Surfaces*, 1990, **48**, 65-78
14. H. Nishizawa, T. Tani, K. Matsuoka, *Comm. Am. Ceram. Soc.*, 1984, **67**, C98-C100
15. T. Trindade, J.D. Pedrosa de Jesus, P. O'Brien, *J. Mater. Chem.*, 1994, **4**, 1611-1617
16. M. Andres-Verges, A. Mifsud, C.J. Serna, *J. Chem. Soc. Faraday Trans.*, 1990, **86**, 959-963
17. K. Fujita, K. Matsuda, S. Mitsuzawa, *Bull. Chem. Soc. Jpn.*, 1992, **65**, 2270-2271
18. V. LaMer, R.H. Dinegar, *J. Am. Chem. Soc.*, 1950, **72,** 4847-4854
19. *Comprehensive Inorganic Chemistry Vol. 3*, J.C. Bailar, H.J. Emeléus, R. Nyholm, A.F. Trotman-Dickenson, Pergamon Press, Oxford, 1975
20. M. Ocaña, R. Rodriguez-Clemente, C.J. Serna, *Adv. Mater.*, 1995, **7**, 212-216

Chapter 5

Particle coating.

5.1 INTRODUCTION

In chapter 1 (section 1.2) the industrial applications of microparticulate inorganics were discussed. It can be useful to enhance properties of these microparticles, for example their conductivity, for applications in the electronics industry. Metal coating can increase the conductivity of such particles; however, if the particle uniformity is to be maintained, a uniform surface coating only is required. This can be accomplished by electroless deposition techniques.

The majority of studies on the coating of uniform inorganic particles have involved coating onto hematite. Matijevic and co-workers have prepared a number of examples including hematite coated with zirconium hydrous oxide,[1] yttrium oxide and basic carbonate[2] and silica.[3] There have also been a limited number of reports relating to metal coating of uniform particles. Polystyrene microspheres have been palladium[4] and gold[5] coated and hematite and magnetite spindle particles have been successfully silver coated.[6] In a previous study carried out in our laboratories, cubic PbS was successfully plated with tin, palladium and gold.[7] These gold coated PbS particles showed an improvement in conductivity when compared to the industrial standard of gold-coated polystyrene beads.

5.1.1 Theories for metal coating mechanisms.[8]

$$M^{z+} + ze^- \rightarrow M \qquad \text{equation 5.1}$$

A redox reaction is the basis of coating procedures. The methods by which the electrons are produced represent the characteristic differences between electrolytic and non-electrolytic processes. The term 'separation' is used in coating / plating industry to describe the movement of a metal from one medium to another to facilitate coating.

5.1.1.1 Electrolytic processes. During the electrolysis of a solution of metal salt, metal ions are reduced at the cathode to the metal. The cathode acts as the source of electrons. A direct current from an outside source provides the required number of electrons for the reaction.

5.1.1.2 Non-electrolytic processes. In this case, no outside source of electrons is necessary, the required electrons are produced by chemical reaction. The processes can be divided into three groups:

(i) Separation by reduction of metal ion and subsequent precipitation from solution. This may be achieved by exchange of ions or charge, that is, reaction of the immersed metal with the metallic ions in solution.

(ii) Separation by contact of the metal to be coated with an auxiliary metal can produce the necessary electrons.

(iii) Separation can be attained by addition of a reducing medium - this is sub-divided into separation on surfaces acting catalytically, called chemical separation and uncontrolled separation throughout the entire solution.

5.1.1.2.1 'Ion exchange' processes. In the so-called 'ion exchange' process, the metal salt in solution (M_2) is exchanged with an immersed metal (M_1), whereby the surface of the first metal is partly attacked and partly covered spontaneously by the second metal.

$$M_1 \rightarrow M_1^{z+} + ze^- \qquad \text{equation 5.2}$$

$$M_2^{z+} + ze^- \rightarrow M_2 \qquad \text{equation 5.3}$$

In this process, the base metal itself is the reducing medium. This is commonly referred to as "immersion plating", but it is not a specific term. Since the separation depends on the base metal itself, once the surface is covered the reaction stops and often

the immersion time is critical. The layer thickness is therefore limited and its strength and adhesion are rarely as good as that found by electroplating.

5.1.1.2.2 'Contact' processes. In this case, separation occurs when the conducting article to be coated comes in contact with a metal that has a lower reduction potential than the one that is to be separated. This contact forms a galvanic cell, whereby the auxiliary metal acts as an anode and the article to be coated acts as the cathode. The dissolved metal can then be separated onto it. This is akin to electrolytic coating except a reaction provides the electrons and not an outside source. Contact processes are rarely used and as such are of little importance.

5.1.1.2.3 Reducing processes. This process can provide continuous separation of thick layers of metal. The coatings are therefore only formed on certain catalytically active surfaces (autocatalytic separation). The necessary electrons are provided by a reducing medium (R^{n+}).

$$R^{n+} \rightarrow R^{(n+z)+} + ze^- \qquad \text{equation 5.4}$$

$$M^{z+} + ze^- \rightarrow M \qquad \text{equation 5.5}$$

As was previously mentioned, uncontrolled separation can also take place, whereby all the metal in solution is separated. An example of this is the reducing of silver in ammonia by formaldehyde. A silver mirror is formed, using up all the metal present.

5.1.2 Components of coating solutions.

Plating solutions usually contain a number of different components. Most importantly, the metal ions are present in the form of a metal salt. The solution may also contain a buffer or a complexing agent, to prevent precipitation of metal hydroxides for example. If the metal to be coated is of a lower reduction potential than that onto which

it is to be coated, the solution must also contain a reducing agent. The components of a coating solution are outlined below in Table 5.1.

Table 5.1 Principle components of coating solutions.

Component	Mode of Operation	Examples
Metal ions	To deliver the metal to be separated.	Metal chloride, sulphate, nitrate or acetate.
Reducing medium	To reduce the metal ion to the metal.	Sodium hypophosphite, formaldehyde.
Complexing agents	To form metal complexes – prevents concentration of metal ions from climbing, ppt of metal hydroxide or phosphite is delayed. Can also act as a buffer.	Pyrophosphate, ammonia, carbonic acids.
Buffers	Keep the pH constant.	Sodium salts of some complexing agents, TEA.

5.1.2.1 Reducing media. The plating of some metals takes place by simply following the electrochemical series.

$$(-0.76\ V)\ Zn < Sn < Ni < Cu < Pd < Au\ (+1.68\ V)^{9}$$

The reduction potential ($E^{0}_{red.}$) of a species must be lower, to replace something in solution. In other words, in order for a metal to coat onto another, its $E^{0}_{red.}$ must be higher than that already on the substrate. Following this, it is easy to explain how palladium (+0.83 V) can coat onto tin (-0.14V). However, the electrochemical series does not allow for example nickel or copper to coat onto a palladium layer. This deposition is facilitated by a reducing medium being present in the plating bath. There

are a number of different reducing media that can be used. A palladium seed layer initiates the oxidation of the reducing media, which is then followed by the reduction of the metal. Hypophosphite and formaldehyde, are the most common reducing media used for nickel and copper respectively.

5.1.3 Aims.

In this study electroless deposition techniques will be used to plate ZnO particles with tin, palladium, copper, nickel, silver and gold. Silica coating of ZnO needle-like particles will also be studied. The nature of these coatings will be examined using SEM, XRD and XRF.

5.2 RESULTS

In order to enhance the conductive properties of ZnO, for better use in electronic applications, metal coating of the particles must be carried out. Before a metal coating can be deposited, the surface of the particle must be sensitised and activated, by tin and palladium coatings respectively. Details of all the plating solutions and conditions can be found in Chapter 6 (section 6.3).

5.2.1 Tin and palladium coating.

Tin coating was achieved by stirring the ZnO particles at ambient temperature in a basic tin chloride solution. After one hour, the particles changed from white to a grey colour. The particles were then stirred for two hours at ambient temperature in an acidic palladium chloride solution. The previously grey particles now appeared brown in colour. The XRD patterns show a ZnO signal reduced in intensity and definition after each treatment (Figure 5.1).

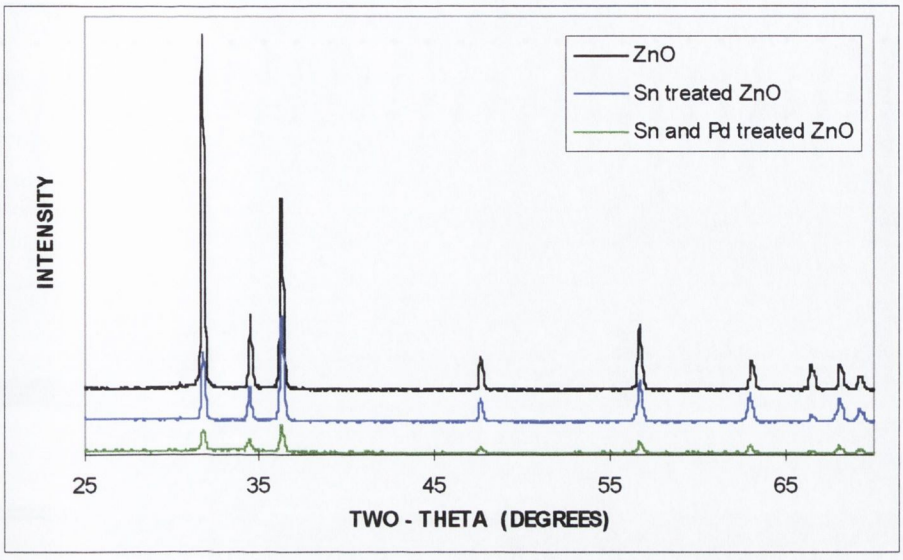

Figure 5.1 XRD patterns for ZnO needle-like particles, ZnO needle-like particles treated in a basic tin chloride solution (Sn-ZnO) and ZnO needle-like particles treated in a basic tin chloride solution followed by treatment in an acidic palladium chloride solution (Pd-Sn-ZnO).

Both the tin and palladium coated particles were also analysed by XRF and SEM. The XRF patterns shown below (Figure 5.2) represent ZnO, Sn treated ZnO (Sn-ZnO) and Pd and Sn treated ZnO (Pd-Sn-ZnO). The peaks due to Zn, O, Sn and Pd are marked. The carbon peak also present is due to the graphite coating on the sample, used to prevent charging. The peak at approximately 1.8 keV is a result of aluminium, from the stub onto which the sample is mounted.

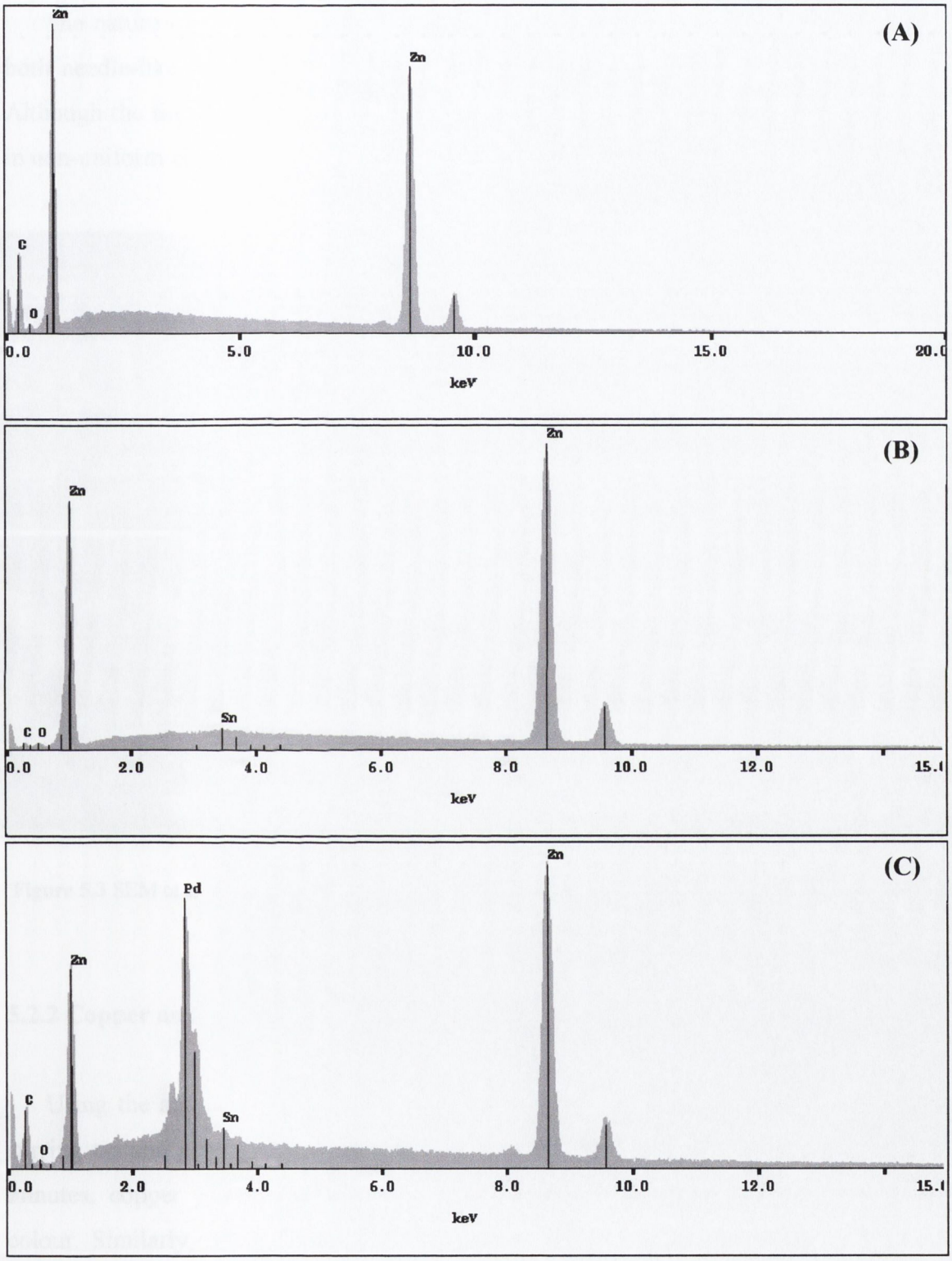

Figure 5.2 XRF spectra for (A) ZnO, (B) Sn treated ZnO and (C) Sn and Pd treated ZnO.

The nature of the coatings was investigated by SEM. Figure 5.3 shows images of both needle-like and star-like ZnO treated with tin and also with tin and palladium. Although the tin coating appears to be relatively uniform, the palladium coating forms in non-uniform clusters on the ZnO particle surface.

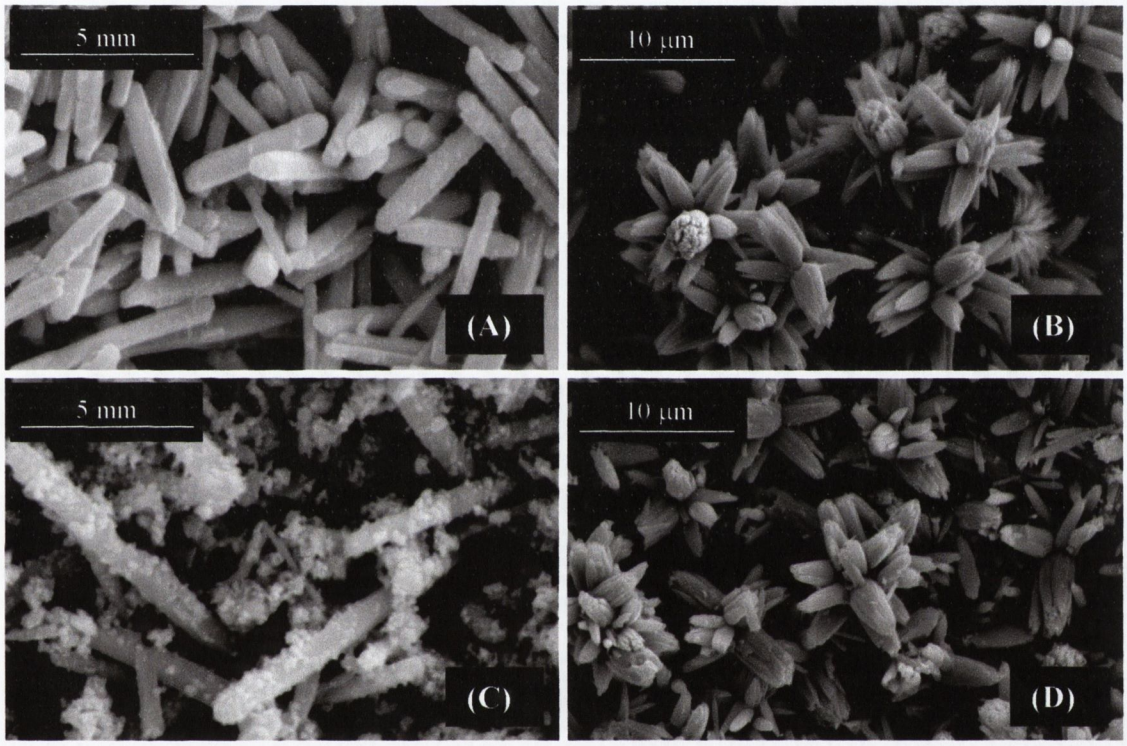

Figure 5.3 SEM of ZnO particles (A), (B) stirred for one hour in a tin chloride bath (C), (D) followed by four hours in acidic palladium chloride.

5.2.2 Copper and nickel coating.

Using the activating palladium layer, further metallic coatings can be applied. By stirring tin and palladium coated ZnO particles in a copper sulphate bath for circa 3 minutes, copper plating can be carried out. The particles now appear red-black in colour. Similarly, a nickel-plating solution can be prepared from nickel sulphate. By stirring tin- and palladium-coated particles in this solution, nickel coating can be carried out, resulting in green-black coloured particles. The nature of the copper and nickel

coatings was examined by XRD, XRF and SEM. The XRD patterns obtained can be seen below in Figures 5.4 and 5.5, overlaid with the pattern for Pd-Sn-ZnO. Peaks due to ZnO are still visible, however, the intensity of the signal and the crystallinity of the sample appears to have decreased after treatment in the copper- or nickel-plating solutions.

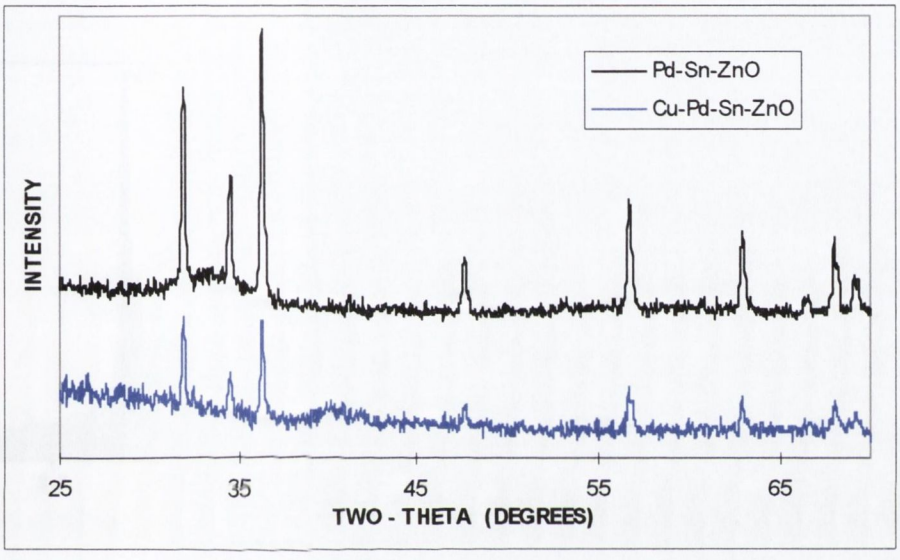

Figure 5.4 XRD patterns obtained for Pd-Sn-ZnO and copper-plated Pd-Sn-ZnO.

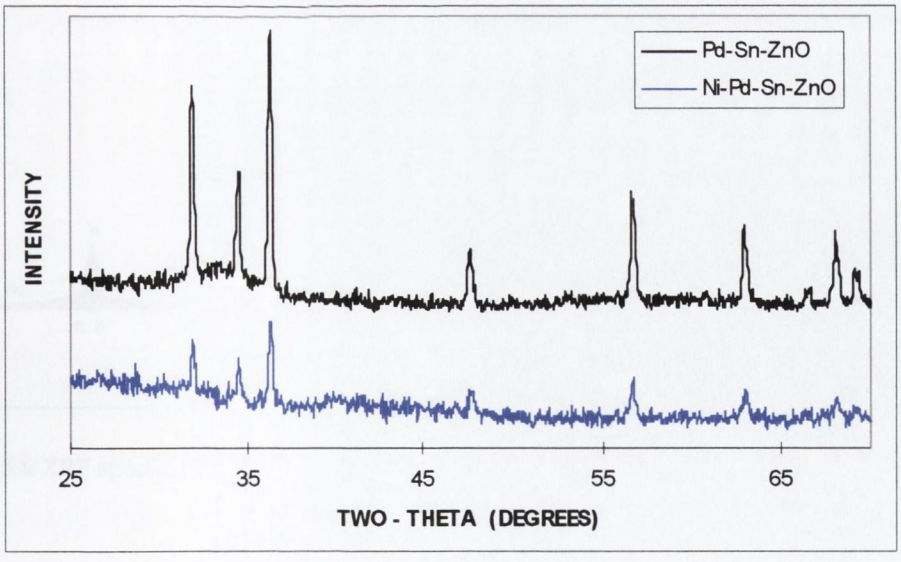

Figure 5.5 XRD patterns obtained for Pd-Sn-ZnO and nickel-plated Pd-Sn-ZnO.

The XRF spectra of nickel and copper coated samples can be seen in Figure 5.6. In addition to the peaks for Zn, O and Pd, peaks for Cu are also present in spectrum (A). The intensity of the Zn peaks has also decreased. In spectrum (B) peaks for Ni and P can be observed. The phosphorus peaks are a result of the sodium hypophosphite reducing agent used in the plating solution. This will be discussed in detail in section 5.3.2.

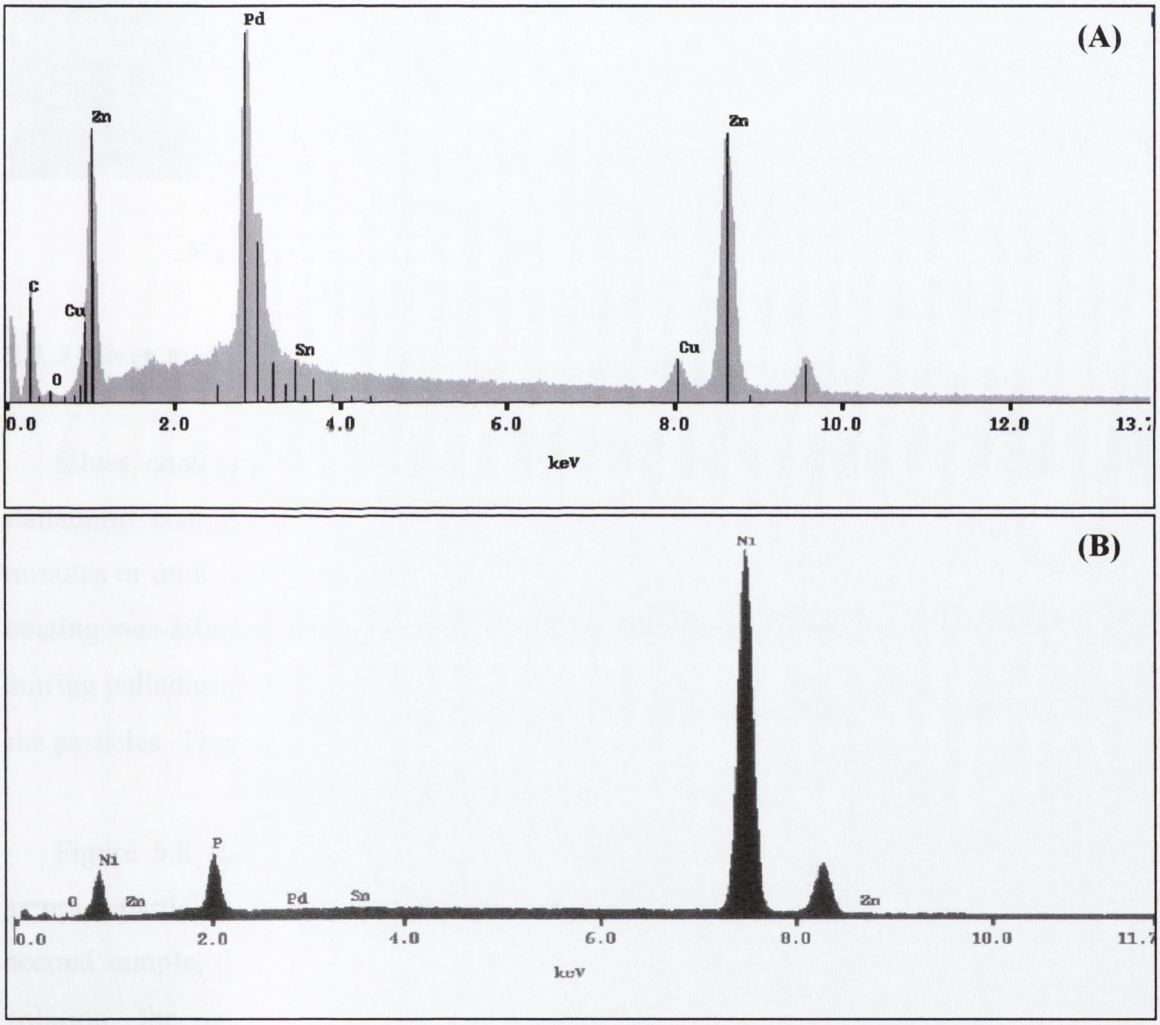

Figure 5.6 XRF spectrum for Pd-Sn-ZnO particles stirred in (A) a copper-plating solution and (B) a nickel-plating solution.

SEM shows that both the copper- and nickel-plating procedures are self-catalysed (autocatalytic), resulting in an aggregation of the ZnO particles. A sample of copper- and nickel-plated needle-like ZnO particles can be seen in Figure 5.7.

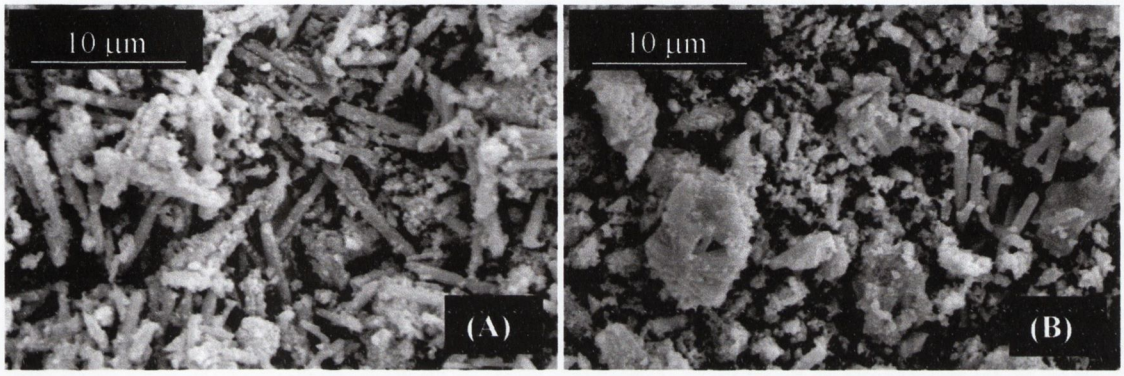

Figure 5.7 SEM of (A) Cu plated Pd-Sn-ZnO and (B) Ni plated Pd-Sn-ZnO.

5.2.3 Silver and gold coating.

Silver coating of ZnO particles was carried out using a silver nitrate solution. Palladium coated ZnO particles were stirred in the solution for approximately 10 minutes or until the colour of the particles had changed from brown to grey-black. Gold coating was attempted using a commercially available gold plating solution. However, stirring palladium coated ZnO particles in the solution at 90 °C resulted in dissolution of the particles. Therefore, no data is presented for gold-coated ZnO particles.

Figure 5.8 shows two XRD patterns obtained for silver coated ZnO. In the first sample, particles were stirred in the plating solution for 10 minutes, whereas in the second sample, the particles were plated for 30 minutes. After 10 minutes in the silver solution, the crystallinity and signal intensity of the ZnO peaks has decreased significantly. However, after 30 minutes, additional peaks are seen in the XRD pattern. These peaks are consistent with metallic Ag.

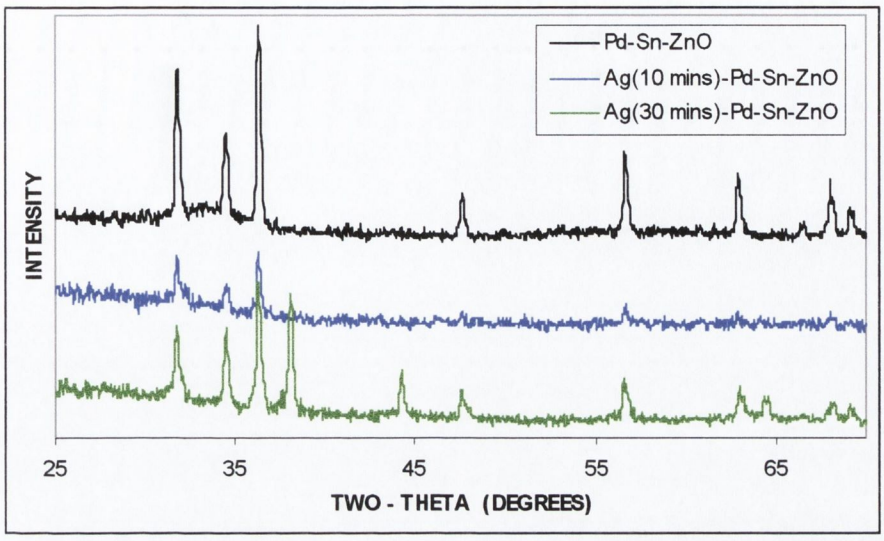

Figure 5.8 XRD patterns for palladium coated ZnO and for silver coated ZnO at two different deposition times.

The XRF spectra for Ag coated ZnO particles are similar at the two different deposition times, differing only slightly in the intensity of the Ag peaks. Figure 5.9 shows the XRF spectrum for Pd-Sn-ZnO after 10 minutes stirring at room temperature in a silver-plating solution.

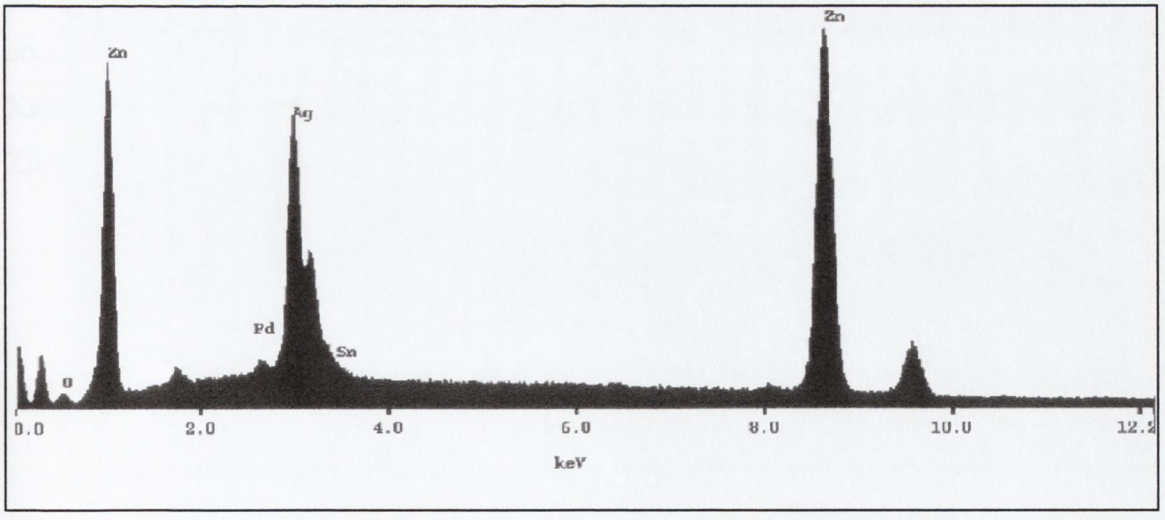

Figure 5.9 XRF spectrum for Pd-Sn-ZnO stirred for 10 minutes in a silver-plating solution.

Silver plating was carried out on both the needle-like and star-like ZnO particles. The coating is not uniform, evident from the SEM images that show aggregation of the particles after 10 minutes in the plating solution (Figure 5.10).

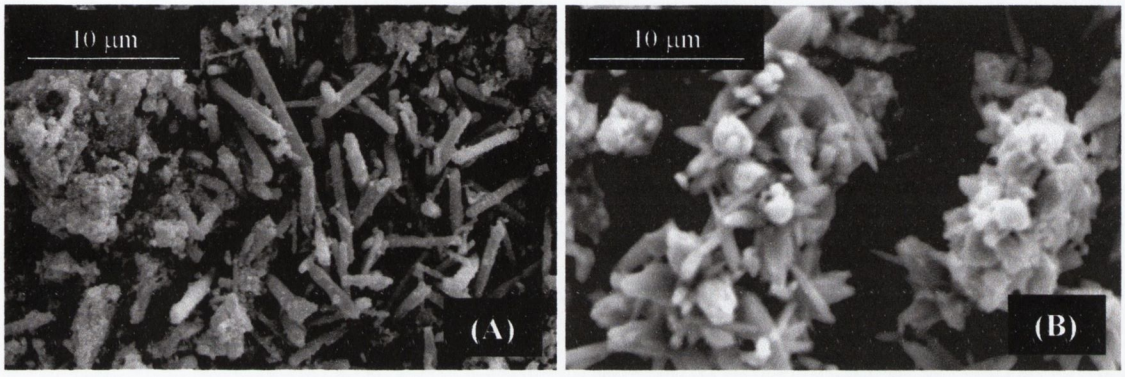

Figure 5.10 SEM of silver-plated (A) needle-like and (B) star-like ZnO particles.

5.2.4 Silica coating.

Ohmori and Matijevic[3] used an alcoholic tetraethyl orthosilicate (TEOS) solution to uniformly silica coat hematite particles. Using the optimised conditions reported, this method was applied to ZnO needle-like particles. After 4 hours stirring at 42 °C in the coating solution, the isolated particles were analysed by XRD, TEM and XRF. The XRD patterns before and after coating are shown in Figure 5.11. The signal intensity for ZnO is seen to decrease and become less crystalline.

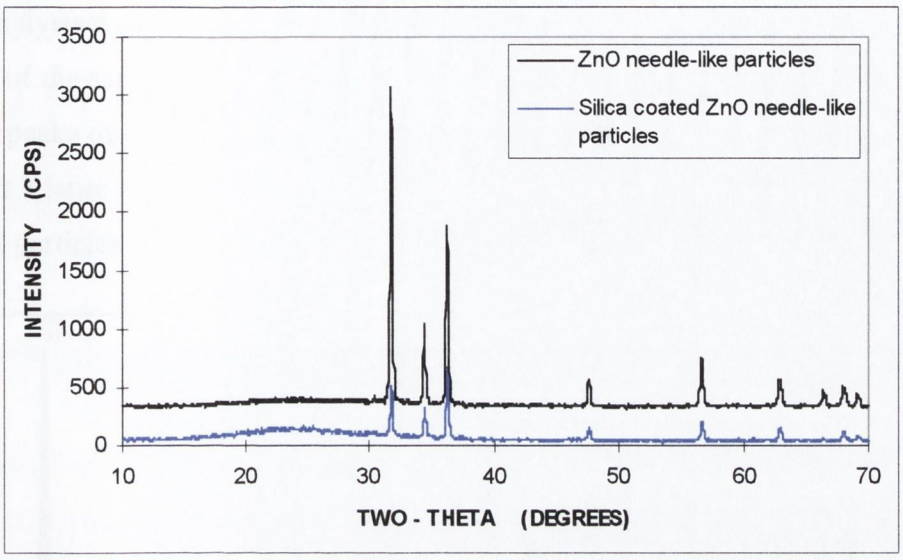

Figure 5.11 XRD patterns for ZnO needle-like particles and silica-coated ZnO needle-like particles.

TEM (Figure 5.12) shows that a uniform coating formed on the surface of the needle-like particles, approximately 15 nm wide. However, sphere-like particles, thought to be amorphous silica, are also present.

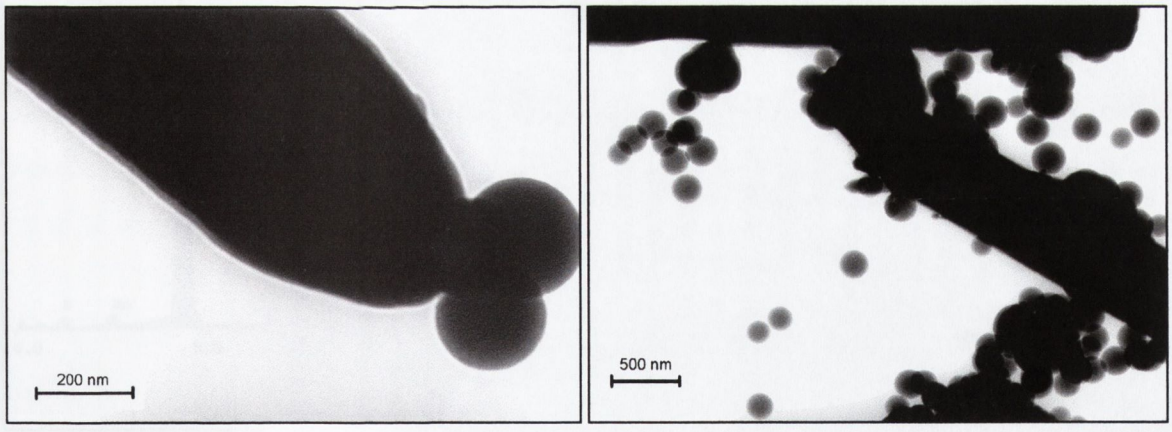

Figure 5.12 TEM images of silica coated ZnO needles and silica spheres.

XRF analysis was carried out on both the silica coated needle-like ZnO particles and on an area of the sample predominantly occupied by the spherical particles. Figure 5.13 (A) shows peaks due to ZnO as well as the presence of Si. Figure 5.13 (B) on the other hand shows a large peak for silicon and only a small amount of Zn, indicating that these sphere-like particles are silica.

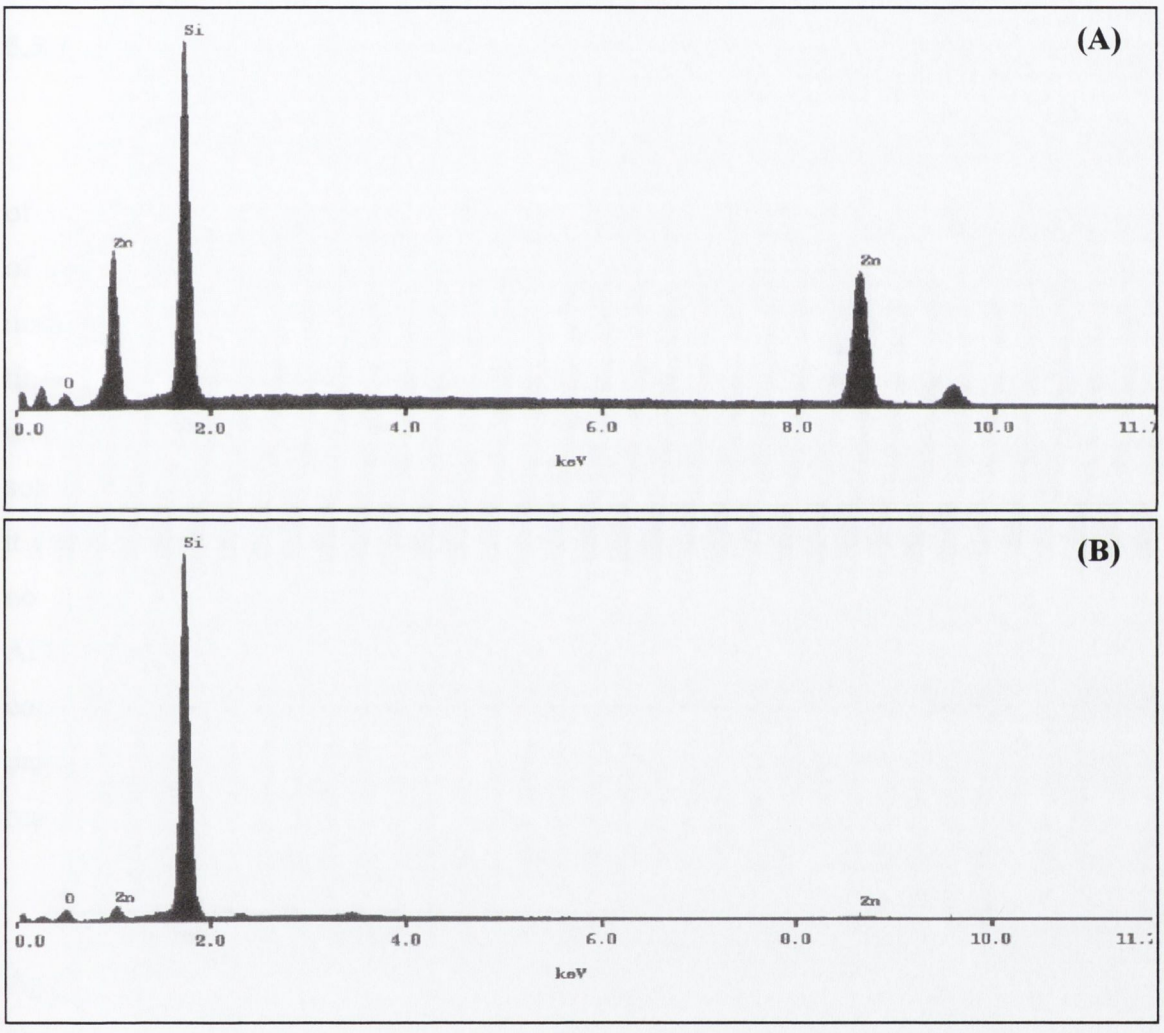

Figure 5.13 XRF spectra for (A) silica coated ZnO needles and (B) silica spheres, both shown above in Figure 5.12.

5.3 DISCUSSION

In order to enhance the conductivity of the uniform ZnO particles and hence make them more applicable to the electronics industry (see Chapter 1, section 1.2), metal coatings were applied to the needle-like and star-like particles.

5.3.1 Tin and palladium coating.

The surface of a particle must be sensitised and activated to facilitate the deposition of various metal coatings. This is usually done by tin and palladium coating the surface of the substrate.[8] The process by which tin electrolessly plates onto a substrate is poorly understood. It is most likely that the tin is deposited as a Sn^{2+} compound, for example a tin oxide. Tin (II) compounds are strong reducing agents. After one hour stirring at ambient temperature in an alkaline tin chloride bath, the sample colour and acid solubility has changed and the intensity of the XRD pattern has decreased significantly, it can therefore be concluded that coating has taken place. As SEM (Figure 5.3) shows no change in the ZnO particle morphology, it is assumed that the coating is uniform. Also as only a very small peak due to Sn can be seen by XRF (Figure 5.2 B), the coating is thought to be quite thin. No coating thickness estimation was made by particle sizing, as the size distributions were not narrow enough to allow a accurate result to be obtained.

Palladium coating was achieved using an acidified palladium chloride solution. Again no reducing agent was added, as the difference in reduction potential between tin and palladium is favourable for spontaneous separation of palladium from the solution to take place. The coating was examined by XRF, XRD and SEM. The XRF spectrum (Figure 5.2 C) showed a significant peak for Pd and also an Sn peak, indicating that not all of the Sn is exchanged with the Pd. The XRD pattern shows peaks for ZnO, however, the signal intensity is quite low and the sample crystallinity poor. SEM images (Figure 5.3) show a non-uniform deposition of Pd on the surface of the particle. As the

palladium layer is present simply to act as a reduction site for other metal cations, a uniform coating is not necessary. This is in agreement with what was observed by Shu *et al*[10] and Li *et al*[11] who saw non-uniform palladium coating onto stainless steel substrates and carbon nanotubes respectively, also over an Sn layer.

5.3.2 Copper and nickel plating.

Copper- and nickel-plating of various substrates have both previously been investigated in depth.[e.g. 12, 13] The mechanisms by which the coatings are formed are well understood.

The copper plating solution contains a reducing agent, formaldehyde, as its reduction potential is not sufficient to allow spontaneous coating onto palladium. Electroless deposition takes place on the surface of the particles, mainly in the vicinity of the palladium deposits, where they act as catalysts for reducing agents. The formaldehyde is adsorbed onto the Pd, where it then reduces the copper. As palladium a poor catalyst for formaldehyde reduction, the initial reaction is slow. However, as the copper begins to be deposited, the reaction accelerates. This is due to the fact that copper itself is a very active catalyst for formaldehyde reduction.[14] Therefore, the reaction is said to be autocatalytic. The reaction can be represented as such:

$$Cu^{2+} + 2\,CH_2O + 4\,OH^- \rightarrow Cu^0 + H_2 + 2\,HCOO^- + 2\,H_2O \qquad \text{equation 5.1}$$

The hydrogen produced in this reaction can be seen as the plating reaction occurs, bubbles form in the solution emanating from the particles being coated. Sodium potassium tartrate is also used in the solution to prevent precipitation of copper hydroxide. A large Cu peak is observed in the XRF (Figure 5.6A) and again the XRD signal intensity for ZnO is seen to be reduced (Figure 5.4). The autocatalytic nature of the reaction is evident by the particle aggregation seen by SEM (Figure 5.7 A). A

uniform coating of Cu is not formed, instead all the copper available in solution is used and the particles combine.

A similar reaction is observed for nickel coating. The reducing agent in this case is sodium hypophosphite, $NaH_2PO_2.H_2O$. Its potential in a pH 7 solution is –1.065 V, making it an extremely strong reducing agent. The palladium layer initiates oxidation of the hypophosphite, followed by nickel reduction.[15] In alkaline hypophosphite solutions, complexing agents must be added to the nickel-plating solutions, in order that the nickel ions don't precipitate as hydroxides or basic salts. The pyrophosphate ion is used for this purpose. This results in the formation of nickel-phosphorous layers and not pure nickel. The temperature at which the metal coating is laid down will determine the amount of phosphorus present, (2-3 wt % at 25 °C or 5 wt % P when coating is formed at 80 °C).[8] This phosphorus is seen along with the Ni by XRF (Figure 5.6 B). As this reaction is also autocatalytic, ZnO peaks are barely visible due to the particles being completely engulfed by the Ni. XRD however, still shows a weak signal for ZnO (Figure 5.5). The SEM further confirms the autocatalytic nature of the reaction, as the particles are not uniformly coated, instead they are thickly coated and aggregated by the nickel.

5.3.3 Silver and gold coating.

Should the final aim of the coating processes be to enhance the particle conductivity, a uniform metal coating of high conductivity must be achieved. Silver coating was carried out using a silver nitrate solution, with formaldehyde as the reducing agent. Figure 5.8 shows the XRD patterns obtained when silver coating was carried out at two different deposition times. At short times (10 minutes), as reduction in ZnO signal intensity was seen, with a loss of crystallinity. However, at longer deposition times (30 minutes), peaks were present which were consistent with metallic Ag. As this reaction is also thought to be autocatalytic, longer deposition times are not

desirable. The XRF spectrum (Figure 5.9) shows strong peaks for Ag. SEM suggests that particle aggregation took place and hence a uniform coating was not achieved.

Gold coating of ZnO particles was also attempted using a commercially available gold plating solution. No results were obtained for these experiments however, as the solubility of ZnO in the solution was too high. It is though that the solution is buffered using ammonium hydroxide, in which ZnO is soluble. As the tin and palladium coated particles also dissolved in this solution, it can be assumed that either pinholes exist in the tin coating or else the palladium treatment causes holes to form. Should the coating be completely uniform, with no holes, the Sn and Pd layers would protect the ZnO from the ammonium hydroxide solution. Another method, traditionally used for gold coating, is to employ a nickel seed layer.[16, 17] However, as a uniform nickel coating is not achieved, this method was not investigated.

5.3.4 Silica coating.

It was hoped that by forming a silica coating beneath the tin and palladium layers, the ZnO core would be protected from plating solutions and hence, gold coating could be achieved. To do this, a method reported by Ohmori and Matijevic[3] was investigated. By stirring the ZnO particles in a tetraethyl orthosilicate solution, a uniform silica coating can be produced. Using the optimised conditions reported, ZnO needle-like particles were coated.

TEM was used to examine the particles and a uniform coating approximately 20 nm thick can be seen on the needles at high magnification (Figure 5.12). However, alongside the coated needles, spherical particles also formed. The silica-coated particles were also examined by XRD, which showed a reduction in the signal intensity for the ZnO pattern, along with an amorphous background signal. XRF was carried out on both the coated needle-like particles and on an area predominantly composed of spherical particles. The needle-like particles show peaks for Zn and Si and the spherical particles

were confirmed to be most likely amorphous silica particles. Under certain conditions, (alterations in concentrations etc.), Ohmori and Matijevic[3] also observed these spherical silica particles. Therefore, the coating conditions must be optimised for each individual system.

Due to the formation of the silica spheres alongside the coated needle-like ZnO, these samples were not further treated with tin and palladium. Although the coating may have been successful, the desired uniform sample would not have been produced.

5.4 CONCLUSION

- Metal coating of the ZnO particles, star-like and needle-like, can be achieved by electroless deposition.
- A uniform tin coating can be obtained using an alkaline tin chloride bath. Palladium can subsequently be placed over the tin, forming a non-uniform coat on the surface of the particles.
- Additional layers, such as copper, nickel and silver can also be added over the activating palladium layer, however, each of these coating reactions are autocatalytic, resulting in particle aggregation.

5.5 REFERENCES

1. A. Garg, E. Matijevic, *J. Colloid Interface Sci.*, 1988, **126**, 243-250
2. B. Aiken, E. Matijevic, *J. Colloid Interface Sci.*, 1988, **126**, 645-649
3. M. Ohmori, E. Matijevic, *J. Colloid Interface Sci.*, 1992, **150**, 594-598
4. A. Dokoutchaev, J. T. James, S.C. Koene, S. Pathak, G.K.S. Prakash, M.E. Thompson, *Chem. Mater.*, 1999, **11**, 2389-2399

5. E. Matijevic, *European Patent*, No. 91107325.2
6. N. Dilsiz, R. Partch, E. Matijevic, E. Sancaktar, *J. Adhesion Sci. Technol.*, 1997, **11**, 1105-1118
7. Mark T. Armstrong, *Ph.D. Thesis*, University of Dublin, 1998
8. *Chemical (Electroless) Nickel-Plating*, G. G. Gawrilov, Portcullis Press Ltd., 1979
9. P.W. Atkins, *Physical Chemistry*, 5th Edt., Oxford University Press, Oxford, 1994
10. J.Shu, B.P.A. Grandjean, E. Ghali, S. Kaliaguine, *J. Electrochem. Soc.*, 1993, **140**, 3175-3180
11. Q. LI, S. FAN, W. HAN, C. SUN, W. LIANG, *Jpn. J. Appl. Phys.*, 1997, **36**, L501-L503
12. T. Ogura, *Langmuir*, 1990, **6**, 1709-1710
13. K. Hagiwara, J. Watanabe, H. Honma, *Plating and Surface Finishing*, 1997, **84**, 74-76
14. I. Ohno, *Mater. Sci. and Engineering*, 1991, **A146**, 33-49
15. N.V. Mandich, G.A. Krulik, *Trans. Inst. Metal Finish.*, 1992, **70**, 111-116
16. L.G. Bhatgadde, *Trans Metal Finish Assoc. India*, 1997, **6**, 229-233, and references therein
17. E.A. Parker, K.E. Langford, *Modern Electroplating*, Extract provided by Schlötter Ireland

Chapter 6

Experimental, materials and methods.

6.1 MATERIALS

6.1.1 ZnO preparation.

Zinc nitrate hexahydrate – $Zn(NO_3)_2.6H_2O$ (Aldrich 98%); zinc sulphate heptahydrate – $ZnSO_4.7H_2O$ (M&B 98%); zinc chloride – $ZnCl_2$ (BDH 97%); sodium hydroxide – NaOH (Wardle Chemicals Ltd. 96%); urea – $CO(NH_2)_2$ (BDH 99.5%); hexamethylenetetraamine – $(CH_2)_6N_4$ (Aldrich 99%); nitric acid – HNO_3 (Fisons 70 % w/w).

6.1.2 Titration analysis.

Ethylenediaminetetraacetic acid – $[CH_2.N(CH_2.COOH).CH_2COONa].2H_2O$ (BDH 98%); nitric acid - HNO_3 (Fisons 70% w/w); ammonia - NH_3 (BDH 35% solution); ammonium chloride - NH_4Cl (Merck 99.5%); solochrome black indicator.

6.1.3 Coating procedures.

Tin chloride dihydrate - $SnCl_2.2H_2O$ (BDH 97%); sodium potassium tartrate – $C_4H_4O_6NaK$ (BDH 99%); palladium chloride - $PdCl_2$ (Aldrich 99%); hydrochloric acid - HCl (BDH 37%); copper sulphate pentahydrate - $CuSO_4.5H_2O$ (Riedel-de Haën 99%); formaldehyde - HCHO (Hopkins and Williams 37% solution); nickel sulphate pentahydrate - $NiSO_4.5H_2O$ (TLS 93%); sodium hypophosphite – NaH_2PO_2 (BDH 98%); sodium pyrophosphate decahydrate – $Na_4P_2O_7.10H_2O$ (Aldrich 99%); triethanolamine – $C_6H_{15}NO_3$ (Merck 98%); silver nitrate solution, Ormex™ Au solution (Schlötter Ireland, 15.55 mg / 250 ml); citric acid; ammonia – NH_3 (BDH 35% solution); 2-propanol – C_3H_7OH (Aldrich +99%); tetraethyl orthosilicate – $Si(OC_2H_5)_4$ (Aldrich 98%).

All materials were used without further purification. Solutions were prepared with singly distilled water. All glassware was washed in both base (NaOH / MeOH) and acid (10% HNO_3) baths prior to use.

6.2 PREPARATION METHODS

6.2.1 Preparation of ZnO and $Zn(OH)_2$ by NaOH forced hydrolysis.

Sodium hydroxide (1 M, 150 ml) was added with stirring to aqueous zinc nitrate hexahydrate (0.04 M, 250 ml) in a round-bottomed flask. After addition of approximately 20 ml of NaOH, an initial white precipitate formed, which dissolved on the addition of the remainder of the base. After this point in the reaction, two different methods were investigated.

The first method involved heating the reaction mixture to reflux temperature (101 °C) over a silicon oil bath and holding the temperature constant (ageing) for given times. Approximately 10 to 15 minutes after mixing, when the temperature is approximately 55 – 60 °C, a second precipitate forms. This second precipitate was identified as star-like ZnO. After the ageing time has elapsed, the white solid is filtered hot through a 0.45 μm pore filter and dried in air to constant weight. The effect of ageing time and reactant concentration on the particles produced was investigated. Zinc sulphate heptahydrate (0.04 M) and zinc chloride (0.04 M) were also used, to see the effect of zinc counter-ion on the final particles produced.

In an alternative method, the reaction mixture was stirred for a given time at room temperature prior to heating. Similarly, after approximately 10 to 15 minutes, a second white precipitate formed. However, in this case the precipitate is identified as rhombic $Zn(OH)_2$. After the stirring time had elapsed, the mixture was then heated to reflux (101 °C) and aged at that temperature for a given time period. The hot solution was filtered through a Sartorius filter (0.45 μm pore size) and the white powder, now needle-

like ZnO, was dried in air to constant weight. The effect of both the stirring time and the heating time was investigated. The reactant concentrations and zinc counter-ion was also varied.

All particles were analysed using powder XRD, SEM and in some cases DSC and UV/vis. spectroscopy. Analysis techniques are described in detail in section 6.4 of this chapter.

6.2.2 Precipitation studies.

In order to determine the temperature at which ZnO becomes more stable with respect to $Zn(OH)_2$ in the reaction solution, the following reactions were carried out; $Zn(NO_3)_2.6H_2O$ (0.04 M, 50 ml) and NaOH (1 M, 30 ml) were added together at temperatures ranging between 20 and 70 °C. The white precipitate formed after mixing was filtered at turbidity and analysed using powder XRD.

6.2.3 Microwave preparation of ZnO using NaOH forced hydrolysis.

In similar experiments to those outlined in section 6.2.1, sodium hydroxide (1 M, 30 ml) was added to zinc nitrate hexahydrate (0.04 M, 50 ml) in a sealed Teflon® microwave digestion bomb. Solutions were heated in a Sanyo EM-S002 microwave oven at various power settings and for a range of times. Some samples were stirred for two hours prior to heating. After heating, the white powder that had formed was filtered hot using 0.45 μm pore size Sartorius filters.

The temperature of the solutions heated in the microwave oven were monitored using 8-level irreversible colour change temperature strips (Fisherbrand). The temperature probes were affixed to the outside of the Teflon® bombs. Calibration was

carried out at temperatures below 100 °C. The calibration data is reported in Chapter 3 (section 3.2.1).

6.2.3.1 Microwave experimental constraints. The microwave heated ZnO formation reactions were carried out in a Teflon® acid digestion bomb. Although these vessels are designed for use in microwave ovens, it is recommended that irradiation be carried out for no longer than twenty minutes.[1] As pressure builds up when heating aqueous solutions in these vessels, they are fitted with pressure release valves. It was found that heating at power settings above 450 W caused swelling of the bomb and resulted in rupturing of the valve. For these reasons, experimental conditions were varied only between one and fifteen minutes irradiation and 150 to 450 W power setting.

6.2.4 Study of particle growth mechanisms.

The growth of the ZnO and $Zn(OH)_2$ particles was studied for the NaOH hydrolysis of zinc nitrate solutions. Under conventional heating methods, using the experiments outlined in section 6.2.1, samples (approx. 30 ml) were removed at regular intervals using a pipette and filtered through Sartorius filters (0.45 μm pore size). The particles were then characterised by SEM and XRD and the filtrate was analysed by EDTA titration.

Growth studies using the microwave method (section 6.2.3) were carried out using separate experiments at each time period required, as samples could not be removed during the reaction. All particles were characterised using SEM and XRD and the filtrate was titrated to find the concentration of Zn^{2+} ions.

6.2.5 Preparation of ZnO by urea hydrolysis.

This was carried out according to the method used by Tsuchida and Kitajima.[2] Zinc sulphate heptahydrate (1×10^{-3} M, 250 ml) was added to urea (0.03 M, 250 ml) and the solution was heated at an approximate temperature ramp of 0.5 °C / min. to 95 °C. The temperature was then held constant for one to five hours after which the resulting white precipitate, which formed at approximately 90 °C, was filtered using Sartorius filters (0.45 μm pore size). The powder was then dried to constant weight in an oven (100°C).

6.2.6 Preparation of ZnO by treatment with HMT.

In an adaptation of the method used by Andres-Verges *et al*,[3] Zinc nitrate hexahydrate (0.05M, 250 ml) was added to hexamethylenetetraamine, HMT (0.05 M, 250 ml) and the pH adjusted to 5 using HNO_3 (1 M). The solution was then heated to reflux and aged for 30 minutes after turbidity. The white solid was filtered through a 0.45 μm Sartorius filter and dried in air. Removing samples at regular intervals during the reaction allowed the growth of these particles to be followed. Samples were removed by pipette.

In a similar experiment, the solutions (40 ml of each) were heated in a Teflon® bomb, using a Sanyo EM-S002 microwave oven. Power settings and heating times were varied.

6.3 PARTICLE COATING PROCEDURES

6.3.1 Sn Coating.

A tin plating solution was prepared from tin (II) chloride dihydrate (5 g), sodium hydroxide (7.5 g), sodium potassium tartrate (8.75 g) and distilled H_2O (500 ml). ZnO

particles (approximately 200 mg) were stirred in the solution for 1 hour at ambient temperature. This yielded a grey powder (ZnO particles were originally white in colour).

6.3.2 Pd Coating.

The palladium coating solution consisted of palladium (II) chloride - (2 % w/v in 10 % HCl, 2.5 ml) and distilled H_2O (300 ml). Tin coated ZnO particles (typically 50 mg) were stirred gently in the solution, at ambient temperature, for 2 hours. The particles were then filtered and washed using distilled water. The resultant particles were brown in colour.

6.3.3 Cu Coating.

The copper coating solution comprised of copper (II) sulphate pentahydrate (5 g), sodium hydroxide (7 g), sodium potassium tartrate (25 g), formaldehyde (37%, 10 ml) and distilled H_2O (950 ml). The ZnO particles, which had previously been coated with tin and palladium, were stirred vigorously in the solution for ca. 3 minutes at room temperature, then filtered and washed using distilled water. The resultant particles are red-black in colour. The reducing agent (formaldehyde) was added when the solution was ready for use.

6.3.4 Ni Coating.

The nickel coating solution contained nickel (II) sulphate pentahydrate (30 g), sodium hypophosphite (30 g), triethanolamine (100 ml), sodium pyrophosphate (60 g) and distilled H_2O (900 ml). The particles, which have been previously coated with both tin and palladium, were stirred vigorously for ca. 5 minutes at ambient temperature. The nickel-coated particles, which are black in colour, were filtered and washed with distilled water.

6.3.5 Ag coating.

ZnO particles, which were previously coated in tin and palladium, were stirred for ca. 10 minutes in a silver nitrate solution (0.01 M) to which a few drops of formaldehyde solution have been added. The coated ZnO particles were filtered and washed with distilled water. The resultant particles are charcoal grey in colour.

6.3.6 Au Coating.

The gold solution is prepared from a gold solution commercially available from Schlötter Ireland, Ormex™ 91 immersion solution (250 ml makes up 6250 ml of stock). The solution is then buffered to pH 5 using ammonia (50%, 0.88) and citric acid (1 M). A plating temperature of 90 °C is recommended by Schlötter Ireland.[4] Tin and palladium coated ZnO particles were stirred in the solution at this temperature.

6.3.7 Silica coating.

Approximately 40 mg of ZnO particles were stirred in a silica coating solution for 4 hours at 42°C. This method was adapted from that used by Ohmori and Matijevic.[5] The silica solution was prepared by adding tetraethyl orthosilicate (TEOS, 0.45 ml) to 2-propanol (475 ml), H_2O (20 ml) and NH_3 (13 ml). The TEOS was added when the coating solution was ready for use, as formation of silica beings immediately.

6.4 PARTICLE AND SOLUTION ANALYSIS.

6.4.1 Scanning electron microscopy (SEM).

Particle morphology was determined using a Hitachi S-3500N scanning electron microscopy (SEM). Samples for SEM were affixed to an aluminium stub using double-sided sticking tape, then coated with gold by sputtering.

6.4.2 Powder X-ray diffraction (XRD).

Crystal structure data was obtained using a Siemens Diffrac500 powder x-ray diffractometer (XRD). XRD samples were prepared in an acetone slurry and spread evenly on a glass slide. XRD was carried out using a copper filament and patterns matched to those in the JCPDS data library.

6.4.3 X-ray fluorescence (XRF).

Samples were analysed by XRF to determine their elemental composition. This was carried out using a PGT prism digital spectrometer XRF apparatus, connected to a Hitachi S-3500N SEM. Samples were attached to aluminium stubs and graphite coated.

6.4.4 Reflectance spectroscopy.

Band gap determinations were made using a Pye Unicam 8800 UV/vis. spectrometer fitted with reflectance apparatus. A $BaSO_4$ reference sample was used to determine total reflectance (A_0). Total absorption (A_T) was measured with a black standard provided. The following equation was used to calculate the percentage absorption of the sample (% A), where A_S is the measured sample absorption:

$$\% A = (A_S - A_0) / (A_T - A_0) * 100 \qquad \text{equation 6.1}$$

By plotting the percentage absorption (% A) against wavelength, an absorption spectrum can be obtained for a solid. The band edge of absorption can then be used to estimate the band gap of the solid. Pure $BaSO_4$ reference reflects 99 % light to 400 nm and 97 % from 400 to 300 nm.[6] Below 300 nm, $BaSO_4$ is not considered a reliable reference material. For this reason, ZnO spectra were recorded between 350 and 600 nm.

6.4.5 Particle sizing techniques.

Size distributions of samples were measured using an Olympus BX60 B201 light microscope using transmitted light connected to a Vantage CCD colour camera, MVD plug-in digitizer, running through a MAC 5300. Particles were suspended in distilled water and dispersed using ultrasonication for 15 minutes. A sample was then placed on a glass slide by pipette and the water allowed to evaporate. A number of slides were prepared for each sample. Ultrasonication was found to have no effect on the particle morphology. It was determined that by measuring approximately 150 particles, a representative size distribution was obtained.

Particle sizing was also kindly carried out in Enterprise Ireland by light scattering techniques using a Malvern Mastersizer 3. Samples were dispersed in water, using an ultrasonic bath and a few drops of calgon (sodium hexametaphosphate) were added. Enough of this dispersion was added to the Malvern Autodisperser to cause 6 to 7 % obscuration. This suspension was then passed through a sample cell and exposed to irradiation from a He-Ne laser (632.8 nm). Using a 44 diode array detector and reverse Fourier optics, a size distribution is obtained by taking 4000 sweeps over the array and signal averaging (Fourier transform). Calculations are carried out assuming perfectly spherical particles.

A comparison of both sizing methods, as applied to this study, is reported in Appendix IV.

6.4.6 Differential scanning calorimetry.

Differential scanning calorimetry (DSC) was carried out in Dublin Institute of Technology using a Rheometric Scientific DSC. Samples were heated between –50 and 300 °C at 10 °C / min in an aluminium pan and measured against a standard empty pan. By quench cooling the sample in the chamber using liquid nitrogen, a second scan could be obtained.

6.4.7 Raman spectroscopy.

Raman spectroscopy was carried out in the laboratories of Dublin Institute of Technology. Spectra were run on an ISA Dilor.Jobinyvon.Spex Labram Raman spectrometer. Samples were placed on a glass microscope slide and the desired sample area to be measured was isolated under the beam. The exciting 20 mW He-Ne laser (632.8 mm) was focussed using a 100X objective lens and focussing was confirmed using a CCD camera in imaging mode. A spectral resolution of 1.5 cm^{-1} per pixel was achieved using a grating of 1800 lines / mm.

6.4.8 Determination of zinc concentration.

The concentration of Zn^{2+} in solution was determined by EDTA titration. Fitrate taken from the reaction at various stages was neutralised by nitric acid (1 M), then buffered at pH 10 using an ammonia / ammonium chloride buffer, (4 % w/w ammonium hydrate, 1 % w/w ammonium chloride). These solutions were then titrated against EDTA using solochrome black indicator (red/blue colour change).

6.5 REFERENCES

1. Savillex Corporation, *Operational guidelines for acid digestion bomb*, 1997
2. T. Tsuchida, S. Kitajima, *Chem. Lett.*, 1990, 1769-1772
3. M. Andres-Verges, A. Mifsud, C.J. Serna, *J. Chem. Soc. Faraday Trans.*, 1990, **86**, 959-963
4. Schlötter Ireland Ltd., *Ormex™ 91 immersion plating solution data sheets*, 1999
5. M. Ohmori, E. Matijevic, *J. Colloid Interface Sci.*, 1992, **150**, 594-598
6. Pye Unicam, *Diffuse Reflectance accessory for PU8800 UV/vis. operational instructions*, 1978

Chapter 7

Conclusions and future work.

7.1 THESIS CONCLUSIONS

The aim of this thesis was to investigate the growth of uniform micron sized ZnO particles by hydrothermal methods and to compare conventional and microwave heating methods.

In Chapter 2, ZnO was prepared with two different morphologies, star-like and needle-like, by forced hydrolysis of zinc nitrate in the presence of hydroxide ions. The growth of star-like particles was clearly shown to be diffusional, with multiple nucleation events occurring. Growth of the particles continued until the $[Zn^{2+}]$ in solution had reduced to the level of solubility for ZnO. By altering the length of time for which the solution is heated at 101 °C, the size of the star-like particles could be altered, with increased ageing resulting in a broadening of the particle size distribution. With a doubling of the zinc nitrate solution concentration, the star-like particles underwent dendritic growth to form almost spherical particles. However, an increase in hydroxide ion concentration inhibited the precipitation of ZnO.

Needle-like ZnO particles formed from the decomposition of $Zn(OH)_2$ rhombic particles. The zinc hydroxide particles precipitated from a zinc nitrate aqueous solution in the presence of hydroxide ions, at room temperature and grew by diffusion until the solubility of $Zn(OH)_2$ in the reaction solution was reached. When this suspension was heated to 101 °C and held for up to 60 minutes, decomposition from $Zn(OH)_2$ to ZnO took place. From SEM and XRD data, it was shown that during the decomposition both $Zn(OH)_2$ and ZnO co-exist. EDTA titration reveals no increase in $[Zn^{2+}]$ in solution, therefore, the phase transformation is most likely via a solid state lattice rearrangement rather than by a dissolution-reprecipitation mechanism. Raman spectroscopy was used to distinguish between the decomposing $Zn(OH)_2$ particles and the growing ZnO particles in the samples during the decomposition reaction.

In Chapter 3, similar experiments were carried out on a smaller scale and using a microwave oven heat source. It was found that both star-like and needle-like particles could be produced using microwave heating and grew by the same mechanisms as those reported in Chapter 2. However, enhanced reaction times were observed in both cases. These faster growth rates are no doubt a product of more rapid heating using microwaves, however other mechanisms may also be at work.

Star-like particles of an equivalent size can be produced by microwave heating, with reaction times over 80 times shorter than those of conventional heating. This faster reaction rate may be related to a disruption by the microwave rotational energy of the aquation sheath surrounding the zinc ion. By at least partially denuding the zinc cation, reaction with the hydroxide anion can take place more readily.

The decomposition of $Zn(OH)_2$ rhombic particles to form needle-like ZnO occurs over 20 times faster using microwave heating when compared to conventional heating techniques. However, the uniformity of the needles is not comparable. Microwave heating results in the growth of highly disperse needle-like particles. This loss of uniformity is thought to be a result of the faster decomposition of $Zn(OH)_2$, preventing a controlled lattice rearrangement. In microwave heating, not only the solution is heated but also absorption of microwaves by ZnO and perhaps also by $Zn(OH)_2$, results in extremely high temperatures being reached inside the reaction vessel. This intensive heating of the particles themselves is the basis for the enhanced decomposition rates observed.

In Chapter 4, two alternative hydrothermal methods for ZnO microparticle preparation were investigated. The effect of ageing times and temperature on particles produced by urea hydrolysis of a dilute zinc sulphate solution was determined. With increasing ageing time, the average length of the rod-like particles increases, however the size distribution is seen to broaden. Also, it was observed that if the temperature at which the solution was aged was not held constant at 95 ± 2 °C but dropped to around

90 °C, a side product of amorphous zinc basic carbonate formed along side the rod-like ZnO particles.

The second method investigated was forced hydrolysis of zinc nitrate using HMT. Thermal decomposition of the Zn-HMT complex results in directional aggregation of ZnO spherical sub-units to form rod-like ZnO. By heating this reaction using a microwave oven the same growth mechanism took place, however the rate of formation was enhanced approximately 3-fold. This enhanced rate of reaction is attributed to faster heating and hence faster complex decomposition when microwave heating is used in place of conventional techniques.

In each of the routes to ZnO formation that were studied, a different growth mechanism is employed. By controlling the release of one or more of the reactants, the uniform nature of the particles can be determined. When star-like particles are produced, no control is exercised over the reaction and hence twinned particles result by a simple diffusional growth mechanism. Using the same reactants but forming a $Zn(OH)_2$ precursor, lends a certain amount of command over the reaction. The slow decomposition of $Zn(OH)_2$ to form ZnO results in an ordered crystallization and the formation of needle-like particles.

Alternatively, one reactant can be slowly released into the reaction mixture, as is the case with the two routes studied in Chapter 4. Urea decomposition controls the release of hydroxide ions into the solution, resulting in uniform growth of ZnO; however decomposition reactions can also give unwanted side products. With urea, the side product of decomposition is a carbonate ion and unless the ageing temperature is very precise, along with controlled growth of ZnO, a zinc carbonate may result. HMT was used in the last method, to form a complex with zinc ions in solution. Thermal decomposition of this complex then slowly releases zinc ions into the solution, thus controlling the reaction and ZnO particles form by directional aggregation of sub-units.

What can also be seen from this study, is the importance of the zinc counter-ion in determining the particle morphology. In all but the urea hydrolysis reaction, zinc nitrate was the source of zinc ions. The elongated hexagonal particles formed in each case had pointed ends making them needle-like in appearance (including the spines of the star-like particles). However, urea hydrolysis made use of zinc sulphate, resulting in similar particles, this time with flat ends and hence having a rod-like appearance. From the preliminary investigations carried out in Chapter 2, the same effect is observed by altering the zinc salt. It is suggested therefore that the nitrate ions adsorb preferentially onto surfaces of the growing particles and hinder growth in that direction, giving needles rather than rods.

Finally, Chapter 5 reported electroless deposition techniques for metal coating ZnO microparticles. This area was investigated, in order to improve the conductivity of the particles and hence, make them more applicable to the electronics industry. Following previous success by our laboratories in plating PbS cubic particles, similar coating procedures were employed for ZnO needle-like and star-like particles. Initial tin and palladium coatings are laid down to sensitise and activate the particle respectively. The tin covering appeared to be uniform, with no change in particle morphology observed after the coating procedure. The palladium coat, on the other hand, was not uniform, rather it formed in small clusters over the surface of the tin layer. These clusters were clearly visible under SEM. XRF data showed the presence of both tin and palladium, indicating that Pd deposition did not result in the complete depletion of the Sn coating.

A number of other metals were then investigated; copper, nickel and silver all being autocatalytic and hence forming non-uniform coatings and resulting in particle aggregation. Gold plating was also explored with less success, due to the nature of the commercial plating solution.

7.2 FUTURE WORK

The results reported throughout this thesis have answered some questions about the growth of ZnO microparticles, however, many more still need to be addressed. For the first time, the growth pattern of ZnO particles of two different morphologies has been studied by the forced hydrolysis method using hydroxide ions. Although these investigations clearly show the route by which star-like and needle-like ZnO particles form from zinc nitrate, some interesting preliminary results illustrate that the zinc salt used has a noticeable effect on the final particle morphology. This counter-ion effect merits further examination, studying in depth the growth pattern of ZnO particles from zinc sulphate and zinc chloride. Zeta potential measurements would help determine adsorbed species on the surface of growing particles, thought to be the reason behind the counter-ion effect.

The work carried out using a microwave oven is the first study into controlled particle growth by microwave heating. Again the growth of ZnO particles of both needle-like and star-like morphologies was investigated. Reasons for the enhanced growth rates observed were proposed, however, as this is a relatively new area of investigation, further consideration must be given to these processes. The interaction of all components of the reaction with microwave energy must be identified. Also, when fractional exposure is used to obtain lower power settings, the exact operating power of the microwave is somewhat doubtful. The true effect of changes in microwave power could only be recognized if a variable magnetron is used. Another problem encountered when using microwave heating is accurate recording of the temperature inside the reaction vessel. It is clear that the temperature registered outside the bomb is not precise and so a more efficient temperature probe must be used.

With the aim of applying these uniform particles to industrial or electronic uses, the coating of metals more conductive than tin and palladium must be achieved. The autocatalytic nature of nickel, copper and to a lesser extent silver negates the uniform

morphology and size of these microparticles. The most desirable coating would be gold but as coated ZnO particles dissolve in the commercially available plating solution, an alternative must be found. Once a uniform coating has been achieved, full characterisation in the way of coating thickness, compressibility and conductivity measurements must be performed. In this way, the particles could be compared to the industrial standards.

Appendix I

ZnO XRD data (zincite, 36-1451).

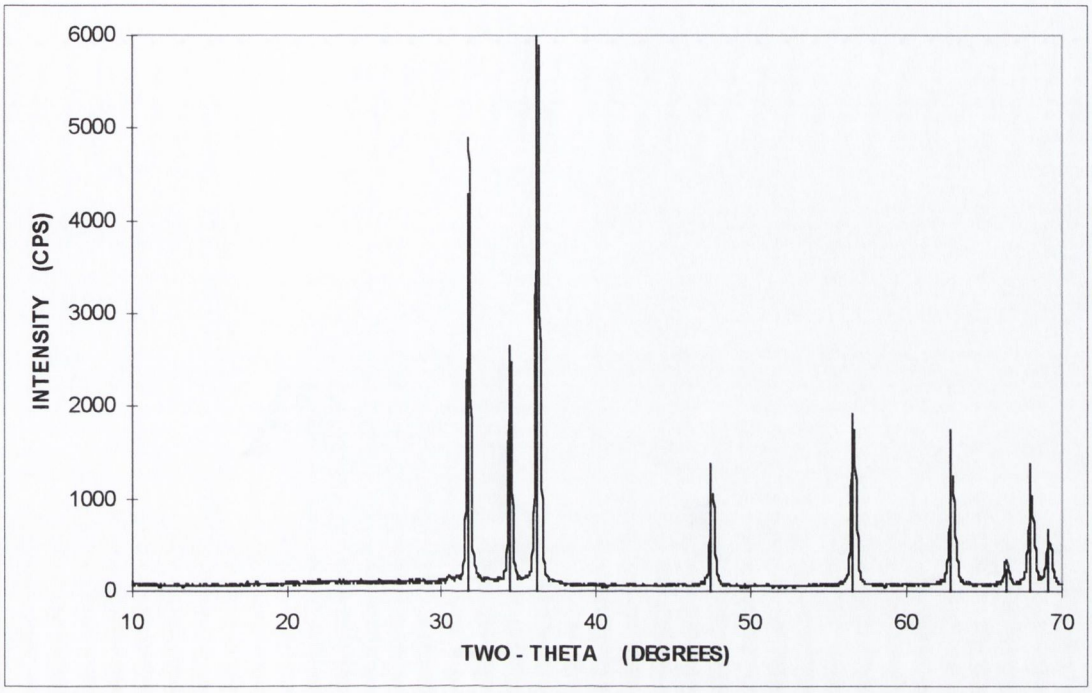

XRD pattern of sample prepared from $Zn(NO_3)_2.6H_2O$ (0.04 M) and NaOH (1 M), stirred at room temperature for two hours, followed by heating for five hours at 101 °C for 5 hours. (JCPDS library lines – zincite, 36-1451).

JCPDS Pattern 36-1541 ZnO, zincite

2 - Theta	Relative intensity	2 - Theta	Relative intensity	2 - Theta	Relative intensity
31.771	57	72.568	2	107.434	1
34.424	44	76.960	4	110.397	3
36.255	100	81.374	1	116.285	8
47.543	23	89.614	7	121.579	4
56.607	32	92.791	3	125.195	1
62.867	29	95.304	6	133.943	3
66.379	4	98.624	4	136.531	1
67.964	23	102.951	2	138.522	2
69.101	11	104.140	5	142.929	3

Appendix II

$Zn(OH)_2$ XRD data (wulfingite, 38-385).

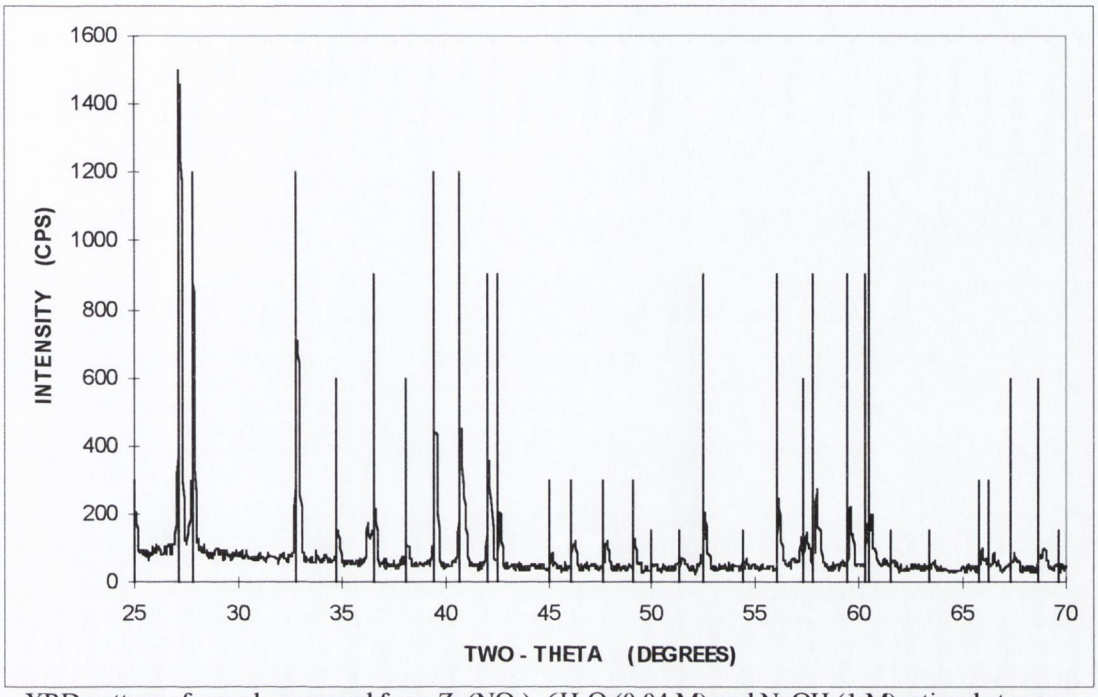

XRD pattern of sample prepared from $Zn(NO_3)_2.6H_2O$ (0.04 M) and NaOH (1 M), stirred at room temperature for two hours. (JCPDS library lines – $Zn(OH)_2$, wulfingite, 38-385).

JCPDS Pattern 38-385 $Zn(OH)_2$, wulfingite

2 - Theta	Relative Intensity	2 - Theta	Relative Intensity	2 - Theta	Relative Intensity
20.134	100	42.549	60	60.231	60
20.885	80	45.021	20	60.483	80
25.007	20	460113	20	61.518	10
27.167	100	47.683	20	63.360	10
27.752	80	49.052	20	65.783	20
32.817	80	49.961	10	66.236	20
34.757	40	51.316	10	67.270	20
36.238	20	52.439	60	68.651	40
36.527	60	54.378	10	69.574	10
38.086	40	55.985	60	70.313	10
39.421	80	57.295	40	71.682	40
40.704	80	57.802	60		
42.051	60	59.389	60		

Appendix III

$Zn_5(CO_3)_2(OH)_6$ XRD data (hydrozincite, 19-1458).

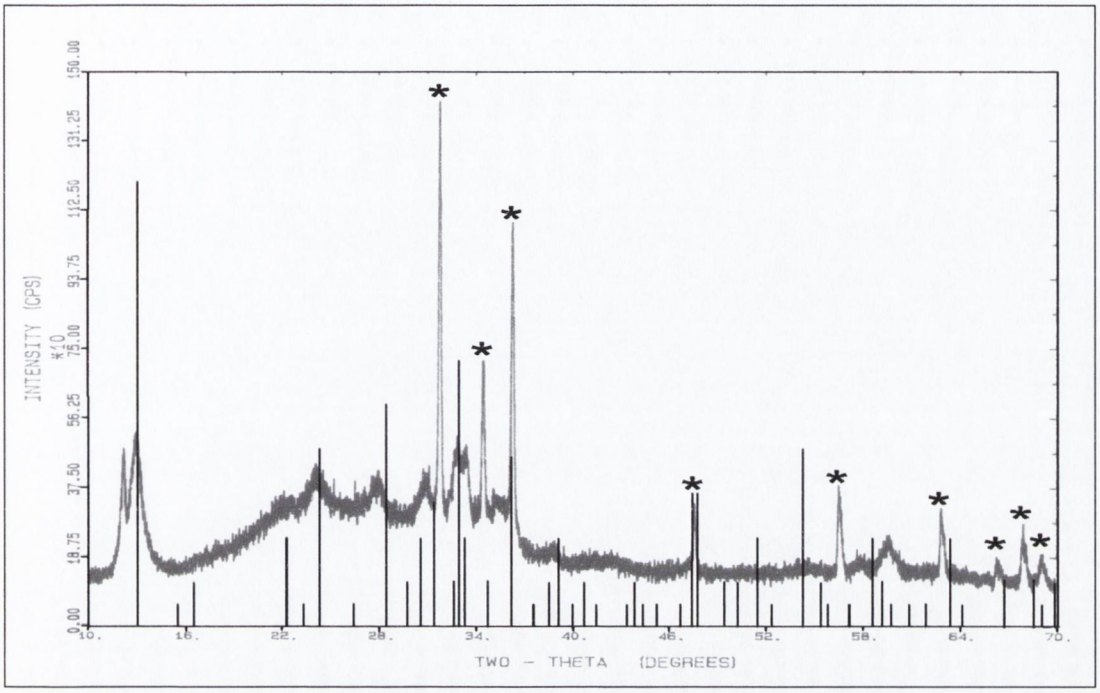

Sample prepared when $ZnSO_4.7H_2O$ (1 x 10^{-3} M) and $CO(NH_2)_2$ (0.03 M) are heated at 0.5 °C / min, then aged for three hours at 95 ± 5 °C.

(JCPDS library lines – hydrozincite, 19-1458, * – peaks due to zincite, 36-1541)

JCPDS Pattern 19-1458 $Zn_5(CO_3)_2(OH)_3$, hydrozincite

2 - theta	Relative intensity	2 - theta	Relative intensity	2 - theta	Relative intensity	2 - theta	Relative intensity
13.067	100	32.903	60	44.348	5	57.209	5
15.507	5	33.281	20	45.165	5	58.644	20
16.496	10	34.745	10	46.689	5	59.223	10
22.263	20	36.192	70	47.439	30	59.730	5
23.329	5	37.541	5	47.783	30	60.856	5
24.300	40	38.510	10	49.442	10	61.893	5
26.428	5	39.117	20	50.259	10	63.397	20
28.402	50	39.988	5	51.473	20	64.130	5
29.757	10	40.741	10	52.393	5	66.712	10
30.591	20	41.446	5	54.304	40	68.542	10
31.362	30	43.343	5	55.407	10	69.058	5
32.657	10	43.830	10	55.808	5	69.883	10

Appendix IV

Size distribution analysis.

SIZE DISTRIBUTION ANALYSIS.

In order to analyse the size distribution of particles, it is important to find a method that will give an accurate result. In this study, two methods were tested; light scattering and light microscopy.

Below are two size distributions calculated for the same sample, (A) by light scattering and (B) by light microscopy.

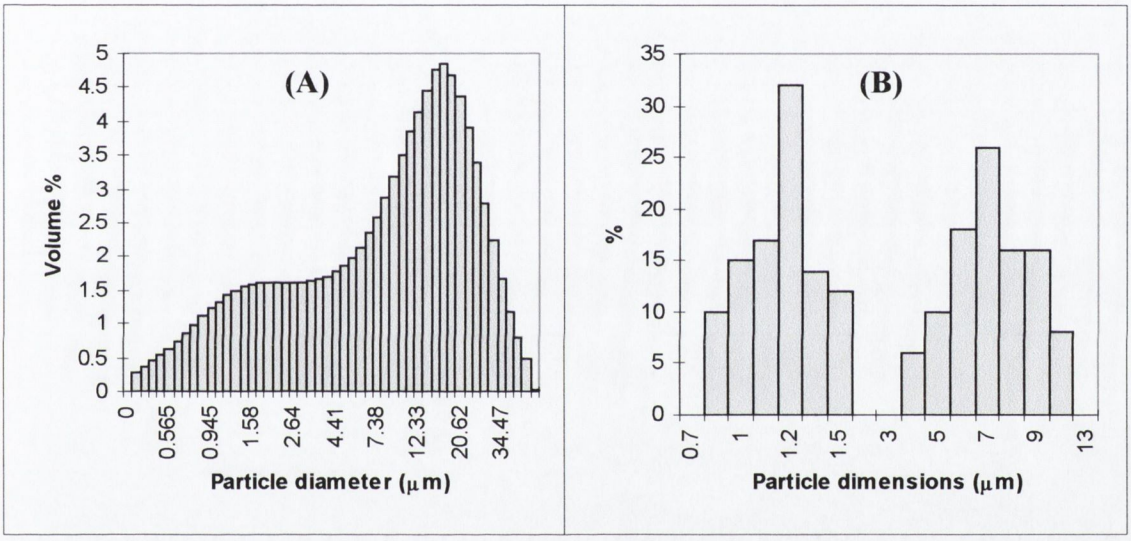

Light scattering was carried out in the laboratories of Enterprise Ireland. The calculations used to accumulate a distribution are based on spherical particles and hence for bimodal distributions, such as rod or needle-like particles, the sizes calculated are not expected to be accurate. It can be seen above that the sizes estimated by light scattering techniques are not reflective of the correct particle sizes as determined by microscopy. For this reason, light microscopy is used for the determination of particle sizes and the compilation of size distributions.

By measuring a number of particles, a size distribution can be produced. When using light microscopy however, it is important to analyse a representative population. In order to determine the amount of particle measurements necessary to give an accurate

result, a number of distributions were produced. It was found that when approximately 100 particles are measured, a representative distribution is obtained. However, for the particle distributions quoted, at least 150 particles were measured in all cases.